ERJ open research
THE BEST IN OPEN ACCESS BASIC, TRANSLATIONAL & CLINICAL RESPIRATORY RESEARCH

Early View

Original article

Alveolar macrophage transcriptomic profiling in COPD shows major lipid metabolism changes

Wataru Fujii, Theodore S. Kapellos, Kevin Baßler, Kristian Händler, Lisa Holsten, Rainer Knoll, Stefanie Warnat-Herresthal, Marie Oestreich, Emily R. Hinkley, Jan Hasenauer, Carmen Pizarro, Christoph Thiele, Anna C. Aschenbrenner, Thomas Ulas, Dirk Skowasch, Joachim L. Schultze

Please cite this article as: Fujii W, Kapellos TS, Baßler K, *et al*. Alveolar macrophage transcriptomic profiling in COPD shows major lipid metabolism changes. *ERJ Open Res* 2021; in press (https://doi.org/10.1183/23120541.00915-2020).

Alveolar macrophage transcriptomic profiling in COPD shows major lipid metabolism changes

Wataru Fujii[1,*], Theodore S. Kapellos[1,*], Kevin Baßler[1,*], Kristian Händler[2], Lisa Holsten[1], Rainer Knoll[1], Stefanie Warnat-Herresthal[1], Marie Oestreich[1], Emily R. Hinkley[2], Jan Hasenauer[6], Carmen Pizarro[3], Christoph Thiele[4], Anna C. Aschenbrenner[1,5], Thomas Ulas[1], Dirk Skowasch[3,#,] Joachim L. Schultze[1,2,#,†]

1 Genomics and Immunoregulation, Life & Medical Sciences (LIMES) Institute, University of Bonn, 53115 Bonn, Germany

2 Platform for Single Cell Genomics and Epigenomics (PRECISE), German Center for Neurodegenerative Diseases and the University of Bonn, 53115 Bonn, Germany

3 Department of Internal Medicine II, University Hospital Bonn, Section of Pneumology, 53115 Bonn, Germany

4 Membrane Biochemistry, Life & Medical Sciences (LIMES) Institute, University of Bonn, 53115 Bonn, Germany

5 Department of Internal Medicine and Radboud Center for Infectious Diseases (RCI), Radboud University Medical Center, Nijmegen 6525, The Netherlands

6 Interdisciplinary Research Unit Mathematics and Life Sciences, Department of Mathematics and Natural Sciences, University of Bonn, 53115 Bonn, Germany

* Authors contributed equally

shared last authorship

† Corresponding author: e-mail: j.schultze@uni-bonn.de; tel: +49 228 73 62787

ONLINE DATA SUPPLEMENT

This article has an online data supplement.

TAKE HOME MESSAGE

AMs from COPD patients undergo GOLD grade-specific transcriptional reprogramming and acquire a complex activation profile. Among the observed changes are gene programs involved in lipid metabolism which translate into alterations in the AM lipidome. A better understanding of the crosstalk between the AM transcriptome and lipidome adds to the understanding of COPD pathogenesis and aids in the design of novel immunotherapeutic strategies.

ABSTRACT

Background: Immune cells play a major role in the pathogenesis of chronic obstructive pulmonary disease (COPD). Albeit established changes in distribution and cellular functions of major immune cells, such as alveolar macrophages (AMs) and neutrophils, their transcriptional reprogramming and contribution to the pathophysiology of COPD are still not fully understood.

Aim and methods: To determine changes in transcriptional reprogramming and lipid metabolism in the major immune cell type within the bronchoalveolar lavage fluid, we analyzed whole transcriptomes and lipidomes of sorted $CD45^{+}Lin^{-}HLA\text{-}DR^{+}CD66b^{-}$ $Autofluorescence^{hi}$ AMs from control and COPD patients.

Results: We observed global transcriptional reprogramming featuring a spectrum of activation states, including pro- and anti-inflammatory signatures. We further detected significant changes between COPD patients and controls in genes involved in lipid metabolism, such as fatty acid biosynthesis in GOLD2 patients. Based on these findings, assessment of a total of 202 lipid species in sorted AMs revealed changes of cholesteryl esters, monoacylglycerols and phospholipids in a disease grade-dependent manner.

Conclusions: Transcriptome and lipidome profiling of COPD AMs revealed GOLD grade-dependent changes, such as in cholesterol metabolism and interferon alpha and gamma responses.

INTRODUCTION

Chronic obstructive pulmonary disease (COPD) is characterised by progressive airflow obstruction, inflammation in the airways, and systemic comorbidities, such as cardiovascular diseases and diabetes [1]. It is a leading cause of morbidity and mortality worldwide [2], and induces a substantial and increasing economic and social burden [3, 4]. Current guidelines for COPD patient classification use the Global Initiative for Chronic Obstructive Lung Disease (GOLD) criteria on the basis of spirometry-estimated severity of airflow limitation and range from mild (GOLD grade 1) to very severe (GOLD grade 4) disease [5]. Cigarette smoking is the leading environmental risk factor for COPD, yet even for heavy smokers, fewer than 50% develop COPD during their lifetime, indicating that the disease initiates from a complex interaction between environment and genome. Some genetic factors, e.g. deficiency of alpha-1 antitrypsin (4) or single nucleotide polymorphisms in MMP12 (5) have been associated with the risk to develop COPD.

Innate immune cells are key players in protecting the lung from airway infections and their impairment plays a major role in COPD pathogenesis and exacerbation episodes [1, 8, 9]. Although changes in cellular distribution and functions within the alveolar space have been described in COPD before [10], these findings are far from being complete. Furthermore, the advent of omics technologies even extending to metabolomics [11], as well as a better understanding of cell type classification requires revisiting these aspects of innate immune cell biology of the alveolar space, both in healthy individuals and COPD patients. Alveolar macrophages (AMs) are described to be the most abundant cells in humans [12]. Under physiological conditions, AMs are the major cell type on the luminal surface of the alveolar space and are major regulators of the initiation and resolution of inflammation [13, 14] and

surfactant metabolism [15]. AMs catabolize pulmonary surfactants, which are composed of phospholipids and proteins and humans lacking functional AMs develop pulmonary proteinosis [16].

Recent reports have shown that in respiratory diseases, such as asthma, COPD and pneumonia a lipidomic remodeling of the bronchoalveolar lavage fluid (BALF) is observed, with changes in the levels of cholesterol, sphingomyelins, phospholipids and fatty acids being the most prominent [17–19]. In particular, the role of sphingolipids and cholesterol metabolism are believed to play a role in the pathogenesis of COPD [20, 21]. Nevertheless, changes of the lipid metabolism within AMs in COPD patients have not been addressed so far.

In this study, we hypothesized that transcriptional changes leading to altered lipid metabolism occur in a disease grade-dependent manner. Using multi-colour flow cytometry (MCFC), we defined AMs as the major cell type in COPD patients for which we provide clear evidence of global transcriptional reprogramming, which differed between GOLD grade 2 and GOLD grade 3/4 COPD patients. Among the major alterations in the AM transcriptome of COPD patients, we identified genes associated with lipid metabolism, which was linked to significant changes in several lipid species by lipidomics analysis.

METHODS

Human specimens

Human studies were approved by the ethics committees of the University of Bonn and University hospital Bonn (local ethics vote 076/16). All patients provided written informed consent according to the Declaration of Helsinki before specimens were collected. Patients with COPD were diagnosed and stratified according to the guidelines of the global initiative for chronic obstructive lung disease (GOLD) [5]. Eligible patients were aged 18 years or older and were either current, past or non-smokers (Table E1). Age-matched individuals suffering from chronic idiopathic cough, demonstrating an exquisitely sensitive cough reflex without underlying pathology [22], served as control donors. Patients with other pulmonary diseases (termed other (Fig. 1A)) were diagnosed as asthma, ACO, bronchiectasis, cancer, fibrosis, pneumonia and sarcoidosis (Table E2), but were excluded from further evaluation within this study.

Bronchoscopy procedure

Bronchoscopy was performed as a part of the diagnostic workup by two bronchoscopists through oral access and with light conscious sedation and was performed in the middle lobe or, if not accessible, the lingular lobe. Warmed saline (6 syringes of 20 ml each) was instilled into the airways to enable BALF recovery.

BALF processing

Human BALF was obtained from all patients included in the study (control, COPD, other) through bronchoscopy. BALF specimens were washed with PBS, suspended with 0.02% EDTA-2Na and washed again for final re-suspension with 2% FCS/1 mM EDTA. $CD45^{+}Lin^{-}HLA\text{-}DR^{+}CD66^{-}Autofluorescence^{+}$ AMs were sorted using a FACS

Aria III cell sorter (BD Biosciences, USA).

Cell counting

Total cell counts were determined with (1:5) Trypan Blue exclusion (Sigma-Aldrich) under an optical microscope. BALF cells were diluted 1:10 in the Trypan Blue solution and counted in a Neubauer haemocytometer.

Flow cytometry/FACS

Single-cell suspensions were stained with Live/Dead yellow fluorescent dye (ThermoFisher, USA) for 15 min at room temperature and were washed with PBS at 300xg for 5 min at 4^{o}C. They were then re-suspended in 100 ul PBS and blocked with 5 ul human FcR blocking reagent (Miltenyi, Germany) for 15 min on ice and were subsequently stained with the listed anti-human antibodies (Table E4) in buffer containing PBS, 2% FCS, 1 mM EDTA for 30 min on ice. Cells were spinned at 300xg for 5 min at 4^{o}C and re-suspended in buffer containing PBS, 2% FCS, 1 mM EDTA for analysis. Data acquisition was performed on a FACS Aria III cell sorter (BD Biosciences, USA). Analysis was performed with FlowJo v.10 software (Tree Star, USA).

Cytospin preparation

Cytospins were obtained by centrifuging $2x10^{5}$ cells in 200 ul PBS on microscope slides at 20% power for 5 min. Excess buffer was carefully discarded and slides were air dried for 3 min followed by fixation with 100% methanol for 5 min at 4^{o}C. The slides were subsequently washed with PBS and stained with 1:20 Giemsa solution (Sigma, USA) for 25 min at room temperature. A final rinsing step with H_2O and air

drying before mounting followed. Cell morphology was examined by microscopic evaluation of stained cells using an Axio Lab A1 microscope (Zeiss, Germany).

RNA extraction and library preparation

Total RNA was isolated from human AMs with the miRNeasy Micro kit (Qiagen, Germany) according to the manufacturer's protocol. cDNA libraries were prepared from 5 ng total RNA with the SMART-seq2 protocol [23] and were tagmented with the Nextera XT kit (Illumina, USA). Library size selection was carried out with AMPure beads (Beckman-Coulter, USA). Libraries were sequenced for SR 75 cycles on a NextSeq500 system (Illumina) using High Output v2 chemistry. Base call files were converted to fastq format and demultiplexed using bcl2fastq v2.20.

Data pre-processing and RNA sequencing analysis

The 75 bp single-end reads were aligned to the human reference transcriptome hg38 from UCSC by kallisto v0.44.0 using default parameters. Data were imported into DESeq2 (v.1.10.1; [24]) using the TXimport (v1.2.0, [25]) package. DESeq2 was used for the calculation of normalized counts for each transcript using default parameters. All normalized transcripts with a maximum over all group means lower than 10 were excluded resulting in 33,032 present transcripts. Unwanted or hidden sources of variation, such as batch, sex and smoking status were removed using the sva package [26]. The normalized rlog transformed expression values were adjusted according to the five surrogate variables identified by sva using the function removeBatchEffect from the limma package [27]. DE genes were defined by a p-value cut-off of 0.05 and an adjusted p-value (IHW) < 0.5 (independent hypothesis weighting).

Gene set enrichment analysis (GSEA)

GSEA [28] was performed on all present genes of the dataset using the gene ontology set of biological processes. Information of gene ontology was obtained from the biological process gene set “c5.bp.v7.0.symbols.gmt”, downloaded from the Molecular Signatures Database (MSigDB). All present genes were used as background (universe).

Linear support vector regression

Linear support vector regression [29] was employed to characterize the relative contribution of 28 different activation signatures derived from [30] to the control and COPD patients (1,000 permutations).

Filtering for TFs, epigenome, surfaceome and secretome

All present transcripts were filtered and sorted by their variance in the dataset. The 20 most variable genes of each category were selected and visualized in heatmaps. TF lists were extracted from [31], the epigenome gene list was derived from the literature, surface and secretome markers were extracted from the Human Protein Atlas [32, 33].

Construction of co-expressed network analysis – automated (CoCena²)

CoCena² was performed to elucidate similarities and differences within the gene expression patterns of the three different patient groups. Pearson correlation was calculated on the 6,000 most variable genes within the dataset using the R package Hmisc (v4.3-0; [34]). Data were filtered for significant (p-value < 0.05, Bonferroni

correction $p<0.05$) and positive (r-value > 0) correlation values. The Group Fold Change (GFC) was calculated for each gene and each condition on the inverse logarithmic count data using the R package gtools (v3.8.2; Unbiased clustering was performed using the R package igraph (v1.2.4.1; [35]). The clustering algorithm "cluster_louvain" was selected as it achieves the highest modularity score. Clusters with less than 35 genes are not shown. Network generation was performed with the R package igraph. The network information was imported to and exported from Cytoscape using the R package RCy3 (v2.6.2; [36]).

Biological function-related bioinformatic analysis of network modules

GSEA was performed on the patient group-related modules identified by CoCena[2] using the R package ClusterProfiler (v3.12.0; [37]). Information of hallmark genes was obtained from the hallmark gene set "h.all.v6.1.symbols.gmt", downloaded from the Molecular Signatures Database (MSigDB). All genes present in the network were used as background (universe).

Lipidomics

Sorted AMs ($5x10^4$) pelleted and frozen at -80°C until analysis. Extraction mix (Chloroform 1:5 methanol-containing internal standards was spiked to the pellets before sonication. Samples were treated with chloroform and 1% acetic acid, the lower phase was transferred after centrifugation, and let evaporate in the vacuum concentrator (45°C for 10 min). After addition of spray buffer and sonication, samples were analyzed separately with a Thermo Q Exactive Plus spectrometer equipped with the HESI II ion source for shotgun lipidomics.

Lipidomics analysis

LipidXplorer software was used for analysis using custom mfql files to identify sample lipids and internal standards. Absolute amounts were calculated using the internal standard intensities followed by normalization on the sum of all measured lipid species per sample. %mol values were averaged for each patient group, log2-transformed and then used for fold change calculations. CoCena[2] was used to find patient group-specific co-regulated lipid species using Pearson correlation and clustering using the “cluster_louvain” algorithm.

Statistics

A two-tailed Welch’s unpaired t test was used to analyze data from two groups. Equality of population variance was assessed with the F-test statistic for two independent groups. A non-parametric Wilcoxon test was used to perform a pairwise comparison between patient groups for all enriched macrophage activation signatures in Fig. 3F. For more than two groups, normality and homoscedasticity were first assessed using the Shapiro-Wilk and Levene tests in R (v3.6.1). A non-parametrical Kruskal-Wallis test with Dunn’s multiple correction post hoc was used in Fig. E3 because the data did not follow a normal distribution. Statistical significance was inferred when $p<0.05$.

For a full list of the methods an Online Supplement is provided.

RESULTS

Macrophages are the most abundant cell type in the alveolar space in COPD

We first evaluated the cell type distribution in the BALF to ensure that AMs are the most abundant cell type in control and COPD samples, the latter of which an enrichment of neutrophils had been postulated [38]. We performed MCFC integrating marker to determine all major immune cell types expected within the alveolar space [39]. Individuals with chronic coughing served as controls (Table E1). Only BALF samples of the highest quality following quality criteria established previously for the processing of BALF [40], such as recovery rate higher than 30% and absence or minimal blood/mucus contamination were included in the study (Fig. 1a). Out of 177 screened BALF samples in the clinic, 72 were derived from COPD patients, 44 from control individuals, while patients suffering from asthma, asthma-COPD overlap, bronchiectasis, cancer, fibrosis, pneumonia or sarcoidosis were excluded (Table E2). Sixty-nine patients (36 COPD and 33 controls) finally qualified for further analysis (Table E3).

We stained for markers of the myeloid cell compartment (Fig. 1b; Table E5), whereas lymphocytes were labelled with antibodies against CD3, CD19 and CD56 (Fig. 1b). Our data show that AM numbers undergo a non-significant increase in COPD patients, whereas we could detect a statistically significant upregulation ($p<0.05$) in the neutrophil numbers of GOLD3/4 grade patients compared to controls (Fig. 1c). Eosinophil and monocyte numbers varied widely within groups and reached no significance, whilst mast cells were found to be significantly higher ($p<0.05$) in GOLD3/4 compared to GOLD2 COPD patients (Fig. 1c).

Table E3. Clinical characteristics of control and COPD patients

	Flow cytometry		RNA-sequencing		Lipidomics	
	Control (n=29)	COPD (n=30)	Control (n=6)	COPD (n=9)	Control (n=7)	COPD (n=8)
Sex	11M 18F	21M 9F	5M 1F	8M 1F	4M 3F	5M 3F
Age (years)	56 ± 11	65 ± 9	53 ± 9	64 ± 9	51 ± 15	59 ± 7
GOLD grade	-	17GOLD2, 10GOLD3, 3GOLD4	-	5GOLD2, 2GOLD3, 2GOLD4	-	4GOLD2, 4GOLD3, 0GOLD4
GOLD group	-	0A, 16B, 14D	-	1A, 6B, 2D	-	0A, 3B, 5D
FEV1/FVC	86 ± 11	GOLD2: 63 ± 6 GOLD3: 59 ± 8 GOLD4: 66 ± 1	81 ± 4	GOLD2: 67 ± 3 GOLD3: 66 ± 1 GOLD4: 52 ± 1	81 ± 6	GOLD2: 67 ± 1 GOLD3: 61 ± 11
FEV1%	95 ± 13	GOLD2: 65 ± 9 GOLD3: 40 ± 6 GOLD4: 32 ± 9	94 ± 20	GOLD2: 68 ± 7 GOLD3: 48 ± 1 GOLD4: 28 ± 1	99 ± 15	GOLD2: 71 ± 11 GOLD3: 37 ± 7
Smoking history	5S, 7ex-S, 17NS	GOLD2: 7S, 10ex-S, 0NS GOLD3: 1S, 9ex-S, 0NS GOLD4: 0S, 3ex-S, 0NS	0S, 2ex-S, 4NS	GOLD2: 2S, 2ex-S, 1NS GOLD3: 2S, 0ex-S, 0NS GOLD4: 1S, 1ex-S, 0NS	0S, 2ex-S, 5NS	GOLD2: 2S, 2ex-S, 0NS GOLD3: 1S, 3ex-S, 0NS
Packyears	29 ± 20	58 ± 40	2 ± 3	51 ± 38	4 ± 9	69 ± 33
LAMA	1Y 28N	26Y 4N	0Y 6N	7Y 2N	0Y 7N	8Y 0N
LABA	4Y 25N	26Y 4N	0Y 6N	7Y 2N	0Y 7N	8Y 0N
ICS	4Y 25N	8Y 22N	0Y 6N	1Y 8N	0Y 7N	3Y 5N
Death	0Y 29N	3Y 1N/A 26N	0Y 6N	0Y 9N	0Y 7N	0Y 8N
Hospitalizations	0Y 29N	12Y 1N/A 17N	0Y 6N	3Y 6N	0Y 7N	2Y 6N
Exacerbations	0Y 29N	18Y 1N/A 11N	0Y 6N	6Y 3N	0Y 7N	4Y 4N

Lymphoid cells were of much lower frequency and using a second panel for lymphoid cell markers (Fig. S1a; Table E5), we observed that only innate lymphoid cells (ILCs) were statistically significantly ($p<0.05$) changed in all COPD samples (Fig. S1b-c), with a similar trend when taking GOLD grades into account (Fig. S1b). Within ILCs, ILC1s were the only significantly increased ($p<0.05$) ILC population in COPD patients (Fig. S1d). Cell type classification was also confirmed on sorted cells by Giemsa staining of cytospins (Fig. 1d). Collectively, AMs are the most abundant cell type in BALF, which was then our focus for subsequent transcriptome and lipidome analyses.

Transcriptional changes in AMs within the alveolar space of COPD patients

To elucidate molecular changes of AMs as the most prevalent cells within the alveolar space, we sorted $CD45^{+}Lin^{-}HLA\text{-}DR^{+}CD66b^{-}Autofluoreschence^{hi}$ AMs from the BALF of 9 COPD and 6 control patients and generated whole transcriptomes by RNA sequencing (Fig. 2a). Principal component analysis (PCA) of all present genes (Fig. 2b) and hierarchical clustering of the 25% most variable genes within the dataset (Fig. S2a) revealed a clear disease grade-dependent structure within the data suggesting significant differences between COPD GOLD2, GOLD3/4, and control samples.

Next, we calculated differentially expressed (DE) genes between GOLD2 or GOLD3/4 COPD and control patients, respectively. There were 563 DE genes (229 up, 334 down, $p<0.05$, $FC>1.5$) between GOLD2 and control, 1,456 (618 up, 838 down, $p<0.05$, $FC>1.5$) between GOLD3/4 and control, and 1,147 (572 up, 575 down, $p<0.05$, $FC>1.5$) between GOLD2 and GOLD3/4 COPD patients (Fig. 2c), which we visualised in Volcano plots for all pairwise comparisons (Fig. 2d).

We first assessed overall transcriptional changes. We provide information for

the top 20 altered transcription factors (TFs), epigenetic modulators, cell surface molecules (surfaceome) and soluble mediators as micro-environmental interactors (Fig. S2b-e). Upregulated TFs included *ETS2* in COPD patients consistent with its function as a biomarker for loss of lung function [41] (Fig. S2b). Consistent with the reported dysregulation of histone deacetylase (HDAC) and sirtuin epigenetic signalling in AMs from COPD patients [42–45], the expression of histone modifying enzymes *HDAC9* and *SETD1A* was downregulated in GOLD3/4 COPD (Fig. S2c). Regarding the surfaceome of the AMs, we measured decreased antigen presentation molecules (*HLA-DQA2* and *CD1B)* [46, 47] and *CCR2* expression in GOLD3/4 COPD patients (Fig. S2d). Notably, expression of the ligand chemokine to CCR2, *CCL2*, was elevated in the secretome-associated gene set of GOLD3/4 COPD patients, similar to other members of the CC family of chemokines, including *CCL8* and *CCL20* (Fig. S2d), highlighting the role of chemokines in COPD pathophysiology [48]. Finally, we detected the downregulation of *MMP7* and *MMP9* in GOLD3/4 COPD patients, with *MMP12* being expressed significantly higher only in GOLD2 COPD patients (Fig. S2e), in agreement with the role of metalloproteinases in the progression of COPD [49–52].

Activation state analysis indicates changes in lipid metabolism

We have previously reported that macrophage activation follows a multi-dimensional model of cell activation [30]. However, for AMs in COPD, it has been proposed that AMs in COPD follow a dual polarization model with deviation towards an anti-inflammatory phenotype [47, 49, 53, 54] with no hints on alterations in lipid metabolism. To analyse how the observed transcriptional changes in COPD AMs related to our multi-dimensional model of activation states, we performed linear

support vector regression utilizing our previous human macrophages activation spectrum model based on 29 conditions [30] (Fig. 3a). Our activation spectrum model could be grouped into 9 major activation programs (c1-9) and were used here as the bait to deconvolute the AM transcriptomes from COPD and control patients. The COPD and control transcriptomes were enriched in a spectrum of activation signatures ranging from pro-inflammatory to anti-inflammatory, as well as those extracted from fatty acid-stimulated macrophages (c5 module signature) that show deviations in lipid metabolism. AMs from GOLD2 COPD patients exhibited significantly lower enrichment ($p<0.05$) of the c4 module signature (P3C/PGE_2, P3C and PGE_2 stimulation) compared to GOLD3/4 COPD and control patients and c8 module signatures (TNF-α/P3C, TNF-α and P3C stimulation) in comparison with GOLD3/4 COPD patients (Fig. 3a). In addition, COPD GOLD2 AMs showed a higher enrichment ($p<0.05$) of the c5 module signatures (LA, LiA, OA, PA, and SA stimulation) compared to AMs from control patients (Fig. 3a).

Based on these results indicating potential changes in lipid metabolism associated-genes, we next performed gene set enrichment analysis (GSEA) for either GOLD2 or GOLD3/4 COPD patients compared to controls (Fig. 3b-c). Lipid-related gene sets, such as fatty acid catabolic process, fatty acid oxidation and regulation of cholesterol biosynthetic process were enriched in AMs from GOLD2 COPD patients (Fig. 3b). AMs from GOLD3/4 COPD patients presented with enrichment in cholesterol and lipid storage compared to controls (Fig. 3c).

To highlight the genes that are involved in the lipid-associated phenotype of COPD AMs, we visualised the 20 most variable genes for the gene ontology term “fatty acid metabolism” of the c5 module from Fig. 3a (Fig. 3d) and “fatty acid catabolic process” from Fig. 3b (Fig. 3e). Several genes which are involved in

cholesterol homeostasis were dysregulated in COPD patients. For example, enzymes involved in fatty acid metabolism, such as *ACAT2*, *FAAH*, *MLCYD* and *ACOX2* or enzymes that synthesize diacylglycerols (*LPIN3*) were expressed higher in GOLD2 COPD patients. On the contrary, the acyltransferase *CRAT* and the triglyceride synthesis enzyme *LPIN2* were overexpressed in GOLD3/4 COPD patients. Fatty acid synthase *FASN* and the anti-inflammatory TF *ATF3* [55, 56] were both downregulated in COPD patients irrespective of GOLD grade (Fig. 3d-e). These findings strongly support that AMs do not follow a simple polarization model, but rather display a multi-activation phenotype with a shift towards lipid activation signatures.

Co-expression analysis reveals changes in cholesterol homeostasis in COPD

Co-expression network analysis is an alternative to statistical methods describing changes in transcriptome data, such as the calculation of differentially expressed genes based on a set fold change and p-value [57]. To further investigate active gene programs in AMs, we performed gene co-expression analysis using CoCena^2 (construction of co-expression network analysis – automated) (Fig. 4a). The clustering of the genes within the constructed network led to the identification of groups of transcriptionally similarly regulated genes within the dataset. The mean GFC of these gene modules in GOLD2, GOLD3/4 COPD and control patients were visualised in a heatmap (Fig. 4b). We detected 11 modules, three of which demonstrated GOLD grade-associated average expression; for instance, modules 7 and 8 had a higher GFC in GOLD2 COPD patients, modules 3 and 4 were GOLD3/4-related, whilst modules 9, 10 and 11 had a higher GFC in AMs from control patients.

Next, GSEA was applied to concatenated modules per disease group (control: 1,

2, 6, 9, 10, 11, GOLD2: 5, 7, 8, GOLD3/4: 3, 4) to link the co-expressed genes to biological processes (Fig. 4c). While genes of control patients were enriched in apical junctions, genes from the modules enriched in AMs derived from GOLD2 patients suggested changes in cholesterol homeostasis in addition to the findings based on statistical analysis (Fig. 3). However, GSEA of modules enriched in AMs derived from GOLD3/4 patients were not revealing any enrichment of terms related to lipid metabolism, but rather terms associated with cell cycle and the secretion of pro-inflammatory cytokines.

The co-expression of genes associated with cholesterol homeostasis were not previously described to be altered in AMs of COPD patients. Therefore, we investigated the GOLD2-associated modules in more detail and identified genes involved in sterol biosynthesis (*DHCR7*, *SQLE*), cholesterol transportation to cells (*LDLR*) and fatty acid metabolism (*FADS2*) (Fig. 4d). In contrast, genes of the interferon response (*CXCL10*, *IFIT3*, *IFITM1*, *IFITM3*, *OAS1*, *RSAD2*, and *ISG15*) (Fig.4e) and genes involved in the G2M checkpoint including the proliferation marker *MKI67*, cyclin-dependent kinases (*CDK1*) and DNA replication machinery (*TOP2A*, *CENPA*) (Fig.4f) were highly expressed in GOLD3/4 AMs.

In summary, AMs derived from the BALF of COPD patients show numerous transcriptional changes that suggest broad reprogramming including genes involved in lipid metabolism with different functionalities that follow GOLD grade-specific patterns.

Lipidome analysis of AMs reveals GOLD-specific changes in COPD

The AMs are the major cell type in the alveolar space being involved in lipid metabolism, e.g. of the surfactant [58]. Performing a transcriptome analysis of AMs

derived from COPD and control patients using two different mathematical approaches identified reprogramming of lipid metabolism. To elucidate whether the changes we observed in these cells' transcriptomes in COPD is associated with changes in their lipidome, $CD45^{+}Lin^{-}HLA\text{-}DR^{+}CD66b^{-}Autofluoreschence^{hi}$ AMs were sorted from the BALF of 8 COPD and 7 control patients and were used for mass spectrometry-based lipidomics (Fig. 5a). Seventeen different lipid classes including a total of 202 lipid species were quantified. Glycerophospholipids, especially the phosphatidylcholines (PC), alongside phosphatidylethanolamines (PE), phosphatidylinositols (PI) and phosphatidylserines (PS), the sphingolipids (ceramides (Cer) and sphingomyelins (SM)) and the monoacylglycerols (MAG) constituted the major lipid mass of AMs (Fig. 5b). Comparison of the AM lipidome of COPD with that of control patients indicated most prominent changes in the cholesterol ester (CE) and MAG classes (Fig. 5b) and quantification of the mean GFC revealed disease severity-specific changes in the analysed lipid classes (Fig. 5c). In accordance with the predicted change in cholesterol metabolism, AMs from GOLD2 COPD patients exhibited an upregulation of CE, but also downregulation of hexosylceramides (HexCer). In contrast, AMs from GOLD3/4 COPD patients showed an increase in MAG and diacylglycerols (DAG) and a decrease in the PC class. GOLD grade-specific patterns were reflected as well on the single lipid species level, revealing the diverse changes within each lipid class (Fig. 5d-e), all in all prompting us to investigate this in greater detail.

For this purpose, we determined lipid-lipid level correlations using the CoCena[2] pipeline. We identified nine different modules encompassing similarly regulated lipid species across the disease groups (Fig. 5f). Modules 1, 2 and 3 showed enriched

lipid species in GOLD2, whereas module 8 encompassed lipid species specifically enriched in GOLD3/4 COPD patients (Fig. 5f).

A closer look at the GOLD2-specific modules revealed enrichment for many unsaturated PC (e.g. PC(32:2, 36:3, 38:4, 38:5, 40:4) and CE (CE(16:1, 18:0, 18:1, 18:2, 18:3, 20:4)), as well as a few SM (e.g. SM(18:0, 22:1, 24:0 ,24:2)), lysophosphatidylcholines (LPC) (e.g. LPC(20:4, 22:5, 22:6)) and Cer, such as Cer(d18:1/24:0) or (d18:1/24:1) (Fig. 5g). On the other hand, distinct lipid species were correlated in the module specific for GOLD3/4 AMs, which showed an accumulation of neutral lipids, such as saturated MAG (MAG(16:0, 18:0)) and DAG (DAG(32:0, 34:0, 36:0)) (Fig. 5h). Taken together, AMs from COPD patients display changes in their lipidome, which, in addition to their transcriptome, are GOLD grade-associated and could constitute a hallmark in the pathogenesis of COPD.

DISCUSSION

Chronic inflammatory diseases such as COPD are associated with functional and transcriptional alterations of immune cells involved in the pathophysiological processes and disturbances of organ-related homeostatic functions, e.g., surfactant biology in the lung. Here we focused on the most abundant immune cell type in the alveolar space, namely the alveolar macrophage to determine transcriptional changes particularly in those genes associated with lipid metabolism. By defining the AM transcriptomes, we observed numerous GOLD grade-specific changes in COPD patients. Evident changes in gene expression related to lipid homeostasis were further evaluated by lipidome profiling of AMs, which demonstrated that prominent lipid changes correlate with disease severity.

We focused on AMs, the most prevalent immune cell in the alveolar space of COPD patients and investigated their transcriptomes. Previously, AMs were shown to convert to an anti-inflammatory phenotype in COPD smokers based on the simple paradigm of M1,M2 polarization [47, 49, 54]. Additionally, a recent article found that some of those cells may carry a dual M1,M2 pattern in severe COPD [53]. However, we have previously demonstrated that macrophages follow a multi-dimensional model of activation [30]. Comparison of these various activation signatures with the transcriptome of AMs from COPD patients revealed that these cells can be better described by various activation signatures (including PGE_2 (c4, c8) and lipid (c5) signatures). To further explore the overall transcriptional changes in AMs derived from COPD patients, we provide the data for further easy inspection at FASTGenomics.org. Here we focused on the changes related to lipid metabolism.

AMs maintain lung function by supporting the air-liquid interface on the alveolar surface, which, when compromised, results in augmented surface tension and

pulmonary proteinosis [16]. It has been shown that lipid homeostasis in COPD is perturbed in both humans [21] and cigarette smoke-induced mouse models [59]. In addition, decreased BALF levels of cholesterol, SM and phospholipids correlate with loss in lung function in COPD patients [17]. Our analysis shows that AMs from GOLD2 COPD patients are enriched in PC and cholesterol esters, and express higher levels of lysosomal lipase *LIPA*, which suggests that in mild severity stages, AMs may contribute to the decrease in surfactant lipids in the alveolar space by increasing their surfactant catabolism rate. In contrast, in more severe stages, AMs are characterised by the enrichment in saturated MAG and DAG, which indicates a degradation defect is very likely due to the accumulation of glycerolipids.

Recently, lipidome analysis of perturbed macrophages showed that changes in lipid composition correlate with functional responses [60]. AMs exhibit a foam-like phenotype with augmented TGF-β secretion in response to silica dust and cholesterol uptake [61]. Other findings were changes in cholesterol biology. Here one could postulate that the balance between cholesterol synthesis and the liver X receptor (LXR) pathway acts as a rheostat that controls AM inflammatory responses. In GOLD2 patients, cholesterol synthesis was upregulated and LXR signaling was repressed. In contrast, in GOLD3/4 COPD patients, cholesterol synthesis was downregulated which would be consistent with the upregulation of the LXR pathway and the induction of lipogenesis [62]. This switch could have implications in AM biology in COPD, as LXR activation confers anti-viral protection [63] and inflammation resolution [64].

In addition, the observed heightened levels of CE and SM in AMs from GOLD2 COPD patients may be responsible for the dysregulation of AM functionalities, such as efferocytosis of apoptotic cells as shown before in rats exposed to cigarette

smoke [65]. Dampened PI levels curtail viral infections in mice via TLR pathway inhibition [66]. Our data provide the enriched interferon responses as additional mechanistic insight in AMs from GOLD3/4 patients.

As with every exploratory study, some of the limitations of our study need to be mentioned. First, the control cohort consisted of patients suffering from chronic idiopathic cough, which might be regarded as a potential confounder given the presence of lipid laden macrophages in human BALF samples [67]. However, the assessment of these patients demonstrated that they suffered from an exquisitely sensitive cough reflex without any underlying lung pathology. On average, the control group was also younger than the COPD group and too small to thoroughly investigate differences between smokers and non-smokers in COPD and control patients. To alleviate any confounding age, smoking status effects in our transcriptome analysis, we computationally removed technical and unknown variance before downstream analysis. We suggest that any effect of age or smoking on high-dimensional data, including lipidomics might be indeed interesting questions for future studies.

Taken together, although the numbers of AMs are not significantly changed in the alveolar space in COPD, we conclude that they undergo transcriptional reprogramming that leads to GOLD grade-dependent changes in lipid metabolism. Elucidation of the concomitant alterations in the transcriptome and lipidome of alveolar macrophages aids the understanding of their role in COPD and provides druggable molecular pathways, such as cholesterol metabolism and interferon alpha and gamma responses.

ACKNOWLEDGMENTS

We thank Dr. Tamás Varga, German Center for Neurodegenerative Diseases (DZNE) for the helpful discussion.

SUPPORT STATEMENT

Wataru Fujii was supported by a fellowship of the Alexander von Humboldt Foundation (JPN-1186019-HFST-P). This work was further supported by the German Research Foundation (Deutsche Forschungsgemeinschaft, SCHU 950,9-1, 639379 & under Germany's Excellence Strategy – EXC2151 – 390873048 & EXC2047) and Sparse2Big, a pilot project within the Helmholtz Association Information & Data Science Incubator. Jan Hasenauer was supported by the Hausdorff Center of Mathematics (EXC 2047) and Immunosensation2 (EXC 2151).

AUTHOR CONTRIBUTIONS

WF, TSK and KB collected samples and performed experiments. KH carried out RNA sequencing. CT carried out mass spectrometry for lipidomics. WF, TSK, TU, LH, RK, SWH, MO, JH and ACA analyzed data. CP and DS recruited patients. DS and JLS designed study. WF, TSK, and JLS wrote the manuscript with input from all authors. All authors were involved in discussing the results of the study.

CONFLICT OF INTEREST DECLARATION

The authors declare no conflicts of interest.

REFERENCES

1. Decramer M, Janssens W, Miravitlles M. Chronic obstructive pulmonary disease. *Lancet* Lancet Publishing Group; 2012. p. 1341–1351.
2. Lozano R, Naghavi M, Foreman K, Lim S, Shibuya K, Aboyans V, Abraham J, Adair T, Aggarwal R, Ahn SY, AlMazroa MA, Alvarado M, Anderson HR, Anderson LM, Andrews KG, Atkinson C, Baddour LM, Barker-Collo S, Bartels DH, Bell ML, Benjamin EJ, Bennett D, Bhalla K, Bikbov B, Bin Abdulhak A, Birbeck G, Blyth F, Bolliger I, Boufous S, Bucello C, et al. Global and regional mortality from 235 causes of death for 20 age groups in 1990 and 2010: A systematic analysis for the Global Burden of Disease Study 2010. *Lancet* Lancet Publishing Group; 2012; 380: 2095–2128.
3. Vos T, Flaxman AD, Naghavi M, Lozano R, Michaud C, Ezzati M, Shibuya K, Salomon JA, Abdalla S, Aboyans V, Abraham J, Ackerman I, Aggarwal R, Ahn SY, Ali MK, Almazroa MA, Alvarado M, Anderson HR, Anderson LM, Andrews KG, Atkinson C, Baddour LM, Bahalim AN, Barker-Collo S, Barrero LH, Bartels DH, Basáñez MG, Baxter A, Bell ML, Benjamin EJ, et al. Years lived with disability (YLDs) for 1160 sequelae of 289 diseases and injuries 1990-2010: A systematic analysis for the Global Burden of Disease Study 2010. *Lancet* Lancet Publishing Group; 2012; 380: 2163–2196.
4. Rennard SI, Vestbo J. COPD: the dangerous underestimate of 15%. *Lancet (London, England)* [Internet] 2006 [cited 2019 Dec 21]; 367: 1216–1219Available from: http://www.ncbi.nlm.nih.gov/pubmed/16631861.
5. Global Initiative for Chronic Obstructive Lung Disease (GOLD) [Internet]. [cited 2021 Jan 24].Available from: https://goldcopd.org/wp-content/uploads/2020/11/GOLD-REPORT-2021-v1.1-25Nov20_WMV.pdf.

6. Stoller JK, Aboussouan LS. α1-antitrypsin deficiency. *Lancet* 2005. p. 2225–2236.

7. Hunninghake GM, Cho MH, Tesfaigzi Y, Soto-Quiros ME, Avila L, Lasky-Su J, Stidley C, Melén E, Söderhäll C, Hallberg J, Kull I, Kere J, Svartengren M, Pershagen G, Wickman M, Lange C, Demeo DL, Hersh CP, Klanderman BJ, Raby BA, Sparrow D, Shapiro SD, Silverman EK, Litonjua AA, Weiss ST, Celedón JC. MMP12, lung function, and COPD in high-risk populations. *N. Engl. J. Med.* Massachussetts Medical Society; 2009; 361: 2599–2608.

8. Taylor AE, Finney-Hayward TK, Quint JK, Thomas CMR, Tudhope SJ, Wedzicha JA, Barnes PJ, Donnelly LE. Defective macrophage phagocytosis of bacteria in COPD. *Eur. Respir. J.* 2010; 35: 1039–1047.

9. Berenson CS, Wrona CT, Grove LJ, Maloney J, Garlipp MA, Wallace PK, Stewart CC, Sethi S. Impaired alveolar macrophage response to Haemophilus antigens in chronic obstructive lung disease. *Am. J. Respir. Crit. Care Med.* 2006; 174: 31–40.

10. Ni L, Dong C. Roles of myeloid and lymphoid cells in the pathogenesis of chronic obstructive pulmonary disease. Front. Immunol. Frontiers Media S.A.; 2018.

11. Kan M, Shumyatcher M, Himes BE. Using omics approaches to understand pulmonary diseases [Internet]. Respir. Res. BioMed Central Ltd.; 2017 [cited 2020 Aug 17].Available from: /pmc/articles/PMC5543452/?report=abstract.

12. Yu Y-RA, Hotten DF, Malakhau Y, Volker E, Ghio AJ, Noble PW, Kraft M, Hollingsworth JW, Gunn MD, Tighe RM. Flow Cytometric Analysis of Myeloid Cells in Human Blood, Bronchoalveolar Lavage, and Lung Tissues. *Am. J. Respir. Cell Mol. Biol.* [Internet] 2016 [cited 2017 Jun 20]; 54: 13–24Available

from: http://www.atsjournals.org/doi/10.1165/rcmb.2015-0146OC.

13. Iwasaki A, Foxman EF, Molony RD. Early local immune defences in the respiratory tract. Nat. Rev. Immunol. Nature Publishing Group; 2017. p. 7–20.
14. Watanabe S, Alexander M, Misharin A V., Budinger GRS. The role of macrophages in the resolution of inflammation. J. Clin. Invest. American Society for Clinical Investigation; 2019. p. 2619–2628.
15. Agassandian M, Mallampalli RK. Surfactant phospholipid metabolism. Biochim. Biophys. Acta - Mol. Cell Biol. Lipids 2013. p. 612–625.
16. Suzuki T, Trapnell BC. Pulmonary Alveolar Proteinosis Syndrome. Clin. Chest Med. W.B. Saunders; 2016. p. 431–440.
17. Agudelo CW, Kumley BK, Area-Gomez E, Xu Y, Dabo AJ, Geraghty P, Campos M, Foronjy R, GarciaArcos I. Decreased surfactant lipids correlate with lung function in chronic obstructive pulmonary disease (COPD). *PLoS One* Public Library of Science; 2020; 15.
18. Kang YP, Lee WJ, Hong JY, Lee SB, Park JH, Kim D, Park S, Park CS, Park SW, Kwon SW. Novel approach for analysis of bronchoalveolar lavage fluid (BALF) using HPLC-QTOF-MS-based lipidomics: Lipid levels in asthmatics and corticosteroid-treated asthmatic patients. *J. Proteome Res.* [Internet] American Chemical Society; 2014 [cited 2020 Nov 28]; 13: 3919–3929Available from: https://pubmed.ncbi.nlm.nih.gov/25040188/.
19. Zheng Y, Ning P, Luo Q, He Y, Yu X, Liu X, Chen Y, Wang X, Kang Y, Gao Z. Inflammatory responses relate to distinct bronchoalveolar lavage lipidome in community-acquired pneumonia patients: A pilot study. *Respir. Res.* [Internet] BioMed Central Ltd.; 2019 [cited 2020 Nov 28]; 20Available from: https://pubmed.ncbi.nlm.nih.gov/31046764/.

20. Kikuchi T, Sugiura H, Koarai A, Ichikawa T, Minakata Y, Matsunaga K, Nakanishi M, Hirano T, Akamatsu K, Yanagisawa S, Furukawa K, Kawabata H, Ichinose M. Increase of 27-hydroxycholesterol in the airways of patients with COPD: Possible role of 27-hydroxycholesterol in tissue fibrosis. *Chest* [Internet] American College of Chest Physicians; 2012 [cited 2020 Nov 28]; 142: 329–337Available from: https://pubmed.ncbi.nlm.nih.gov/22281802/.

21. Telenga ED, Hoffmann RF, Ruben t'Kindt, Hoonhorst SJM, Willemse BWM, van Oosterhout AJM, Heijink IH, van den Berge M, Jorge L, Sandra P, Postma DS, Sandra K, ten Hacken NHT. Untargeted lipidomic analysis in chronic obstructive pulmonary disease. Uncovering sphingolipids. *Am. J. Respir. Crit. Care Med.* [Internet] American Thoracic Society; 2014 [cited 2020 Feb 8]; 190: 155–164Available from: http://www.ncbi.nlm.nih.gov/pubmed/24871890.

22. Haque RA, Usmani OS, Barnes PJ. Chronic idiopathic cough: a discrete clinical entity? *Chest* [Internet] American College of Chest Physicians; 2005 [cited 2020 Mar 30]; 127: 1710–1713Available from: http://www.ncbi.nlm.nih.gov/pubmed/15888850.

23. Picelli S, Björklund ÅK, Faridani OR, Sagasser S, Winberg G, Sandberg R. Smart-seq2 for sensitive full-length transcriptome profiling in single cells. *Nat. Methods* [Internet] 2013 [cited 2017 Jun 20]; 10: 1096–1098Available from: http://www.nature.com/doifinder/10.1038/nmeth.2639.

24. Love MI, Huber W, Anders S. Moderated estimation of fold change and dispersion for RNA-seq data with DESeq2. *Genome Biol.* [Internet] 2014 [cited 2018 Feb 14]; 15: 550Available from: http://www.ncbi.nlm.nih.gov/pubmed/25516281.

25. Soneson C, Love MI, Robinson MD. Differential analyses for RNA-seq:

transcript-level estimates improve gene-level inferences. *F1000Research* [Internet] 2015 [cited 2018 Jul 23]; 4: 1521Available from: https://f1000research.com/articles/4-1521/v2.

26. Leek JT, Johnson WE, Parker HS, Jaffe AE, Storey JD. The SVA package for removing batch effects and other unwanted variation in high-throughput experiments. *Bioinformatics* 2012; 28: 882–883.

27. Ritchie ME, Phipson B, Wu D, Hu Y, Law CW, Shi W, Smyth GK. Limma powers differential expression analyses for RNA-sequencing and microarray studies. *Nucleic Acids Res.* Oxford University Press; 2015; 43: e47.

28. Subramanian A, Tamayo P, Mootha VK, Mukherjee S, Ebert BL, Gillette MA, Paulovich A, Pomeroy SL, Golub TR, Lander ES, Mesirov JP. Gene set enrichment analysis: a knowledge-based approach for interpreting genome-wide expression profiles. *Proc. Natl. Acad. Sci. U. S. A.* [Internet] 2005 [cited 2018 Nov 12]; 102: 15545–15550Available from: http://www.pnas.org/cgi/doi/10.1073/pnas.0506580102.

29. Newman AM, Liu CL, Green MR, Gentles AJ, Feng W, Xu Y, Hoang CD, Diehn M, Alizadeh AA. Robust enumeration of cell subsets from tissue expression profiles. *Nat. Methods* [Internet] 2015 [cited 2018 May 23]; 12: 453–457Available from: http://www.nature.com/articles/nmeth.3337.

30. Xue J, Schmidt SV, Sander J, Draffehn A, Krebs W, Quester I, De Nardo D, Gohel TD, Emde M, Schmidleithner L, Ganesan H, Nino-Castro A, Mallmann MR, Labzin L, Theis H, Kraut M, Beyer M, Latz E, Freeman TC, Ulas T, Schultze JL. Transcriptome-Based Network Analysis Reveals a Spectrum Model of Human Macrophage Activation. *Immunity* [Internet] 2014 [cited 2017 Jun 16]; 40: 274–288Available from:

http://www.ncbi.nlm.nih.gov/pubmed/24530056.

31. Fulton DL, Sundararajan S, Badis G, Hughes TR, Wasserman WW, Roach JC, Sladek R. TFCat: the curated catalog of mouse and human transcription factors. *Genome Biol.* [Internet] 2009 [cited 2018 May 26]; 10: R29Available from: http://genomebiology.biomedcentral.com/articles/10.1186/gb-2009-10-3-r29.

32. The Human Protein Atlas - surfaceome [Internet]. [cited 2020 Jan 23].Available from: https://www.proteinatlas.org/search/protein_class:Predicted+membrane+proteins+AND+NOT+protein_class:Predicted+secreted+proteins.

33. The Human Protein Atas - secretome [Internet]. [cited 2020 Jan 23].Available from: https://www.proteinatlas.org/search/protein_class:Predicted+secreted+proteins+AND+NOT+protein_class:Predicted+membrane+proteins.

34. Harrell Jr FE, with contributions from Charles Dupont, many others. Hmisc: Harrell Miscellaneous [Internet]. 2019.Available from: https://cran.r-project.org/package=Hmisc.

35. Csardi G, Nepusz T. The igraph software package for complex network research. *InterJournal* [Internet] 2006; Complex Systems: 1695Available from: http://igraph.org.

36. Gustavsen JA, Pai S, Isserlin R, Demchak B, Pico AR. RCy3: Network biology using Cytoscape from within R. *F1000Research* [Internet] 2019 [cited 2020 Jan 22]; 8: 1774Available from: https://f1000research.com/articles/8-1774/v3.

37. Yu G, Wang L-G, Han Y, He Q-Y. clusterProfiler: an R Package for Comparing Biological Themes Among Gene Clusters. *Omi. A J. Integr. Biol.* [Internet]

Mary Ann Liebert, Inc. 140 Huguenot Street, 3rd Floor New Rochelle, NY 10801 USA ; 2012 [cited 2019 Aug 1]; 16: 284–287Available from: http://www.liebertpub.com/doi/10.1089/omi.2011.0118.

38. Lee H, Um S-J, Kim YS, Kim DK, Jang AS, Choi HS, Kim YH, Kim TE, Yoo KH, Jung K-S. Association of the Neutrophil-to-Lymphocyte Ratio with Lung Function and Exacerbations in Patients with Chronic Obstructive Pulmonary Disease. Loukides S, editor. *PLoS One* [Internet] 2016 [cited 2019 Dec 30]; 11: e0156511Available from: https://dx.plos.org/10.1371/journal.pone.0156511.

39. Tricas L, Echeverría A, Blanco MA, Menéndez M, Belda J. Flow cytometry counting of bronchoalveolar lavage leukocytes with a new profile of monoclonal antibodies combination. *Cytometry B. Clin. Cytom.* [Internet] 2012 [cited 2019 Dec 21]; 82: 61–66Available from: http://www.ncbi.nlm.nih.gov/pubmed/22076931.

40. Meyer KC, Raghu G, Baughman RP, Brown KK, Costabel U, Du Bois RM, Drent M, Haslam PL, Kim DS, Nagai S, Rottoli P, Saltini C, Selman M, Strange C, Wood B. An official American Thoracic Society clinical practice guideline: The clinical utility of bronchoalveolar lavage cellular analysis in interstitial lung disease. Am. J. Respir. Crit. Care Med. 2012. p. 1004–1014.

41. Savarimuthu Francis SM, Larsen JE, Pavey SJ, Duhig EE, Clarke BE, Bowman R V., Hayward NK, Fong KM, Yang IA. Genes and gene ontologies common to airflow obstruction and emphysema in the lungs of patients with COPD. *PLoS One* [Internet] PLoS One; 2011 [cited 2020 Jul 31]; 6Available from: https://pubmed.ncbi.nlm.nih.gov/21423603/.

42. Yang S-R, Chida AS, Bauter MR, Shafiq N, Seweryniak K, Maggirwar SB, Kilty I, Rahman I. Cigarette smoke induces proinflammatory cytokine release by

activation of NF-kappaB and posttranslational modifications of histone deacetylase in macrophages. *Am. J. Physiol. Lung Cell. Mol. Physiol.* [Internet] 2006 [cited 2017 Jun 16]; 291: L46-57Available from: http://www.ncbi.nlm.nih.gov/pubmed/16473865.

43. Trocme C, Deffert C, Cachat J, Donati Y, Tissot C, Papacatzis S, Braunersreuther V, Pache J-C, Krause K-H, Holmdahl R, Barazzone-Argiroffo C, Carnesecchi S. Macrophage-specific NOX2 contributes to the development of lung emphysema through modulation of SIRT1/MMP-9 pathways. *J. Pathol.* [Internet] 2015 [cited 2017 Jul 12]; 235: 65–78Available from: http://doi.wiley.com/10.1002/path.4423.

44. Mercado N, Thimmulappa R, Thomas CMR, Fenwick PS, Chana KK, Donnelly LE, Biswal S, Ito K, Barnes PJ. Decreased histone deacetylase 2 impairs Nrf2 activation by oxidative stress. *Biochem. Biophys. Res. Commun.* [Internet] 2011 [cited 2020 Jan 1]; 406: 292–298Available from: http://www.ncbi.nlm.nih.gov/pubmed/21320471.

45. Ito K, Lim S, Caramori G, Chung KF, Barnes PJ, Adcock IM. Cigarette smoking reduces histone deacetylase 2 expression, enhances cytokine expression, and inhibits glucocorticoid actions in alveolar macrophages. *FASEB J.* [Internet] 2001 [cited 2017 Jun 17]; 15: 1110–1112Available from: http://www.ncbi.nlm.nih.gov/pubmed/11292684.

46. Pons AR, Noguera A, Blanquer D, Sauleda J, Pons J, Agustí AGN. Phenotypic characterisation of alveolar macrophages and peripheral blood monocytes in COPD. *Eur. Respir. J.* [Internet] 2005 [cited 2017 Jun 20]; 25: 647–652Available from: http://www.ncbi.nlm.nih.gov/pubmed/15802338.

47. Hodge S, Matthews G, Mukaro V, Ahern J, Shivam A, Hodge G, Holmes M,

Jersmann H, Reynolds PN. Cigarette smoke-induced changes to alveolar macrophage phenotype and function are improved by treatment with procysteine. *Am. J. Respir. Cell Mol. Biol.* [Internet] 2011 [cited 2017 Jun 18]; 44: 673–681Available from: http://www.atsjournals.org/doi/abs/10.1165/rcmb.2009-0459OC.

48. Henrot P, Prevel R, Berger P, Dupin I. Chemokines in COPD: From implication to therapeutic use [Internet]. Int. J. Mol. Sci. MDPI AG; 2019 [cited 2020 Aug 1].Available from: https://pubmed.ncbi.nlm.nih.gov/31174392/.

49. Shaykhiev R, Krause A, Salit J, Strulovici-Barel Y, Harvey B-G, O'Connor TP, Crystal RG. Smoking-dependent reprogramming of alveolar macrophage polarization: implication for pathogenesis of chronic obstructive pulmonary disease. *J. Immunol.* [Internet] 2009 [cited 2017 Jun 16]; 183: 2867–2883Available from: http://www.jimmunol.org/cgi/doi/10.4049/jimmunol.0900473.

50. Woodruff PG, Koth LL, Yang YH, Rodriguez MW, Favoreto S, Dolganov GM, Paquet AC, Erle DJ. A distinctive alveolar macrophage activation state induced by cigarette smoking. *Am. J. Respir. Crit. Care Med.* [Internet] 2005 [cited 2017 Jun 18]; 172: 1383–1392Available from: http://www.atsjournals.org/doi/abs/10.1164/rccm.200505-686OC.

51. Finlay GA, O'Driscoll LR, Russell KJ, D'Arcy EM, Masterson JB, FitzGerald MX, O'Connor CM. Matrix metalloproteinase expression and production by alveolar macrophages in emphysema. *Am. J. Respir. Crit. Care Med.* [Internet] 1997 [cited 2017 Jun 18]; 156: 240–247Available from: http://www.ncbi.nlm.nih.gov/pubmed/9230755.

52. Wallace AM, Sandford AJ, English JC, Burkett KM, Li H, Finley RJ, M?ller NL,

Coxson HO, Par? PD, Abboud RT. Matrix Metalloproteinase Expression by Human Alveolar Macrophages in Relation to Emphysema. *COPD J. Chronic Obstr. Pulm. Dis.* [Internet] 2008 [cited 2017 Jun 18]; 5: 13–23Available from: http://www.ncbi.nlm.nih.gov/pubmed/18259971.

53. Bazzan E, Turato G, Tinè M, Radu CM, Balestro E, Rigobello C, Biondini D, Schiavon M, Lunardi F, Baraldo S, Rea F, Simioni P, Calabrese F, Saetta M, Cosio MG. Dual polarization of human alveolar macrophages progressively increases with smoking and COPD severity. *Respir. Res.* [Internet] 2017 [cited 2018 Jun 3]; 18: 40Available from: http://respiratory-research.biomedcentral.com/articles/10.1186/s12931-017-0522-0.

54. Eapen MS, Hansbro PM, McAlinden K, Kim RY, Ward C, Hackett TL, Walters EH, Sohal SS. Abnormal M1/M2 macrophage phenotype profiles in the small airway wall and lumen in smokers and chronic obstructive pulmonary disease (COPD). *Sci. Rep.* Nature Publishing Group; 2017; 7.

55. Labzin LI, Schmidt S V, Masters SL, Beyer M, Krebs W, Klee K, Stahl R, Lütjohann D, Schultze JL, Latz E, De Nardo D. ATF3 Is a Key Regulator of Macrophage IFN Responses. *J. Immunol.* [Internet] The American Association of Immunologists; 2015 [cited 2020 Feb 20]; 195: 4446–4455Available from: http://www.ncbi.nlm.nih.gov/pubmed/26416280.

56. De Nardo D, Labzin LI, Kono H, Seki R, Schmidt S V, Beyer M, Xu D, Zimmer S, Lahrmann C, Schildberg FA, Vogelhuber J, Kraut M, Ulas T, Kerksiek A, Krebs W, Bode N, Grebe A, Fitzgerald ML, Hernandez NJ, Williams BRG, Knolle P, Kneilling M, Röcken M, Lütjohann D, Wright SD, Schultze JL, Latz E. High-density lipoprotein mediates anti-inflammatory reprogramming of macrophages via the transcriptional regulator ATF3. *Nat. Immunol.* [Internet]

2014 [cited 2020 Feb 20]; 15: 152–160Available from: http://www.ncbi.nlm.nih.gov/pubmed/24317040.

57. van Dam S, Võsa U, van der Graaf A, Franke L, de Magalhães JP. Gene co-expression analysis for functional classification and gene-disease predictions. *Brief. Bioinform.* [Internet] NLM (Medline); 2018 [cited 2020 Aug 17]; 19: 575–592Available from: http://pcwww.liv.ac.uk/$aging/.

58. Trapnell BC, Nakata K, Bonella F, Campo I, Griese M, Hamilton J, Wang T, Morgan C, Cottin V, McCarthy C. Pulmonary alveolar proteinosis [Internet]. Nat. Rev. Dis. Prim. Nature Publishing Group; 2019 [cited 2020 Aug 17].Available from: https://pubmed.ncbi.nlm.nih.gov/30846703/.

59. Morissette MC, Shen P, Thayaparan D, Stämpfli MR. Disruption of pulmonary lipid homeostasis drives cigarette smoke-induced lung inflammation in mice. *Eur. Respir. J.* [Internet] 2015 [cited 2019 Dec 21]; 46: 1451–1460Available from: http://www.ncbi.nlm.nih.gov/pubmed/26113683.

60. Köberlin MS, Snijder B, Heinz LX, Baumann CL, Fauster A, Vladimer GI, Gavin A-C, Superti-Furga G. A Conserved Circular Network of Coregulated Lipids Modulates Innate Immune Responses. *Cell* [Internet] Cell Press; 2015 [cited 2020 Feb 8]; 162: 170–183Available from: http://www.ncbi.nlm.nih.gov/pubmed/26095250.

61. Hou X, Summer R, Chen Z, Tian Y, Ma J, Cui J, Hao X, Guo L, Xu H, Wang H, Liu H. Lipid Uptake by Alveolar Macrophages Drives Fibrotic Responses to Silica Dust. *Sci. Rep.* [Internet] Nature Publishing Group; 2019 [cited 2020 Aug 2]; 9Available from: https://pubmed.ncbi.nlm.nih.gov/30674959/.

62. Muse ED, Yu S, Edillor CR, Tao J, Spann NJ, Troutman TD, Seidman JS, Henke A, Roland JT, Ozeki KA, Thompson BM, McDonald JG, Bahadorani J,

Tsimikas S, Grossman TR, Tremblay MS, Glass CK. Cell-specific discrimination of desmosterol and desmosterol mimetics confers selective regulation of LXR and SREBP in macrophages. *Proc. Natl. Acad. Sci. U. S. A.* [Internet] National Academy of Sciences; 2018 [cited 2020 Nov 29]; 115: E4680–E4689Available from: https://pubmed.ncbi.nlm.nih.gov/29632203/.

63. Zeng J, Wu Y, Liao Q, Li L, Chen X, Chen X. Liver X receptors agonists impede hepatitis C virus infection in an Idol-dependent manner. *Antiviral Res.* [Internet] Antiviral Res; 2012 [cited 2020 Nov 29]; 95: 245–256Available from: https://pubmed.ncbi.nlm.nih.gov/22713431/.

64. Körner A, Zhou E, Müller C, Mohammed Y, Herceg S, Bracher F, Rensen PCN, Wang Y, Mirakaj V, Giera M. Inhibition of Δ24-dehydrocholesterol reductase activates pro-resolving lipid mediator biosynthesis and inflammation resolution. *Proc. Natl. Acad. Sci. U. S. A.* [Internet] National Academy of Sciences; 2019 [cited 2020 Nov 28]; 116: 20623–20634Available from: https://pubmed.ncbi.nlm.nih.gov/31548397/.

65. Petrusca DN, Gu Y, Adamowicz JJ, Rush NI, Hubbard WC, Smith PA, Berdyshev E V., Birukov KG, Lee C-H, Tuder RM, Twigg HL, Vandivier RW, Petrache I. Sphingolipid-mediated Inhibition of Apoptotic Cell Clearance by Alveolar Macrophages. *J. Biol. Chem.* [Internet] 2010 [cited 2017 Jul 30]; 285: 40322–40332Available from: http://www.ncbi.nlm.nih.gov/pubmed/20956540.

66. Voelker DR, Numata M. Phospholipid regulation of innate immunity and respiratory viral infection. *J. Biol. Chem.* [Internet] American Society for Biochemistry and Molecular Biology Inc.; 2019 [cited 2020 Aug 2]; 294: 4282–4289Available from: https://pubmed.ncbi.nlm.nih.gov/30733339/.

67. Palomo B, Belda J, Arias M, Pandiella CJR, Paniagua P, Rebollo M, Casan P.

Lipid laden macrophages in patients with chronic cough. *Eur. Respir. J.* 2011; 38.

FIGURE LEGENDS

Fig. 1 - Identification of lymphoid immune populations in the BALF of COPD and control patients. Schema of the pipeline for collection and processing of human bronchoalveolar lavage fluid samples. Of 177 BALF samples, 69 satisfied the quality criteria (>30% recovery rate and no blood and/or mucus contamination and were included in the study for multiple colour flow cytometry, transcriptomics and/or lipidomics. Sixty-one patients suffering from asthma, ACO, bronchiectasis, cancer, fibrosis, pneumonia or sarcoidosis were excluded from the study (a). Representative multi-colour flow cytometry analysis of the myeloid compartment of a control patient (b). Absolute numbers of myeloid immune cells in the BALF of control, GOLD2 and GOLD3/4 COPD patients calculated with traditional gating. Data are from 8-29 patients per group except for mast cells GOLD3/4 (n=2) and re represented as mean ± SD (c). Data are represented as mean ± SEM and were analysed with an unpaired two-tailed student t-test, * $p<0.05$. Giemsa staining of cytospins for sorted BALF myeloid cell types (d). Black bars indicate 10 um.

Fig. 2 – Whole transcriptome analysis of AMs reveals lipidomic dysregulation in COPD patients. Schematic representation of the bioinformatics workflow and methods used for the transcriptome analysis of 15 RNA-seq samples from GOLD2, GOLD3/4 COPD and control patients (a). PCA of all 33,032 present transcripts (b). Distribution and amount of DE genes (c). Volcano plots of the comparisons GOLD2 vs control, GOLD3/4 vs control and GOLD2 vs GOLD3/4. Upregulated genes are marked in red, downregulated genes in blue. Fold change cut-off was set to 1.5, adjusted p-value cut-off was set to 0.05 (d).

Fig. 3 – Overlay of human macrophage activation states in AMs from COPD patients show lipid term enrichment. 29 macrophage activation signatures from [30] were used as input to identify the relative fraction of these activation signatures in COPD and control patients. Grouping of activation signatures in 9 clusters was used as proposed in [30]. Data were statistically analysed with the non-parametrical Wilcoxon test, * < 0.05 (a). GSEA using the gene ontology (GO) database filtered for “fat” and “lipid” as reference signatures. Normalized enrichment scores (NES) and enrichment p-values for the 5 most enriched GO terms for the comparison GOLD2 COPD vs control (b) and GOLD3/4 COPD vs control patients (c). Heatmap of the mean expression of the 20 most variable genes filtered by the GO term fatty acid metabolism (d) and fatty acid catabolic process (e).

Fig. 4 – Co-expression network analysis uncovers lipid metabolism-associated functions for AMs in COPD. Schematic representation of the bioinformatics workflow for co-expression network analysis of the 6,000 most variable genes in the dataset by CoCena^2 (a). CoCena^2 cluster-condition heatmap (b). Significant enrichment (q-value < 0.1) of hallmark genes within patient groups. Patient group modules consist of the respective cluster-condition heatmap modules (c). CoCena^2 network with GOLD2-associated genes within the hallmark term “Cholesterol homeostasis” marked by black edging and coloured according to their cluster name. Each node represents one gene in the network and each edge represents a co-expression. The expression levels are presented in more detail in the following heatmap (d). CoCena^2 network with GOLD3/4-associated genes within the hallmark term “Interferon alpha response” marked by black edging and coloured according to their cluster name. Each node

represents one gene in the network and each edge represents a co-expression. The expression levels are presented in more detail in the following heatmap (e). Genes enriched within the hallmark term “G2M checkpoint” marked by black edging and coloured according to their cluster name. Each node represents one gene in the network and each edge represents a co-expression. The expression levels are presented in more detail in the following heatmap (f).

Fig. 5 – Quantitative lipidomics of AMs of COPD patients describe disease severity. Schematic representation of the analysis workflow for analysis of the 202 lipid species assessed by lipidomics of AMs from BALF of 11 COPD and 4 control patients (a). Mean mol% per patient group for lipid class sums of lipid species normalized to total identified lipid content (b). Hierarchical clustering of average $\log_2$ fold changes (FC) of mol% of lipid class sums (c). Average $\log_2$ FC of mol% for single lipid species per lipid class for GOLD2 vs control (d) or GOLD3/4 vs control (e). Bubble size indicates p-value. CoCena[2] cluster-condition heatmap (f). Hierarchical clustering of the average lipid abundance for lipid species encompassed in the GOLD2-specific modules 2 and 3 (g) and GOLD3/4-specific module 8 (h). CE, cholesteryl ester; Cer, ceramide; CL, cardiolipin; DAG, diacylglycerol; DiHexCer, dihexosylceramide; HexCer, hexosylceramide; LPC-O, ether-lysophosphatidylcholine; LPC, lysophosphatidylcholine; MAG, monoacylglycerol; PC-O, ether-phosphatidylcholine; PC, phosphatidylcholine; PE-O, ether-phosphatidylethanolamine; PE, phosphatidylethanolamine; PI, phosphatidylinositol

Figure 1

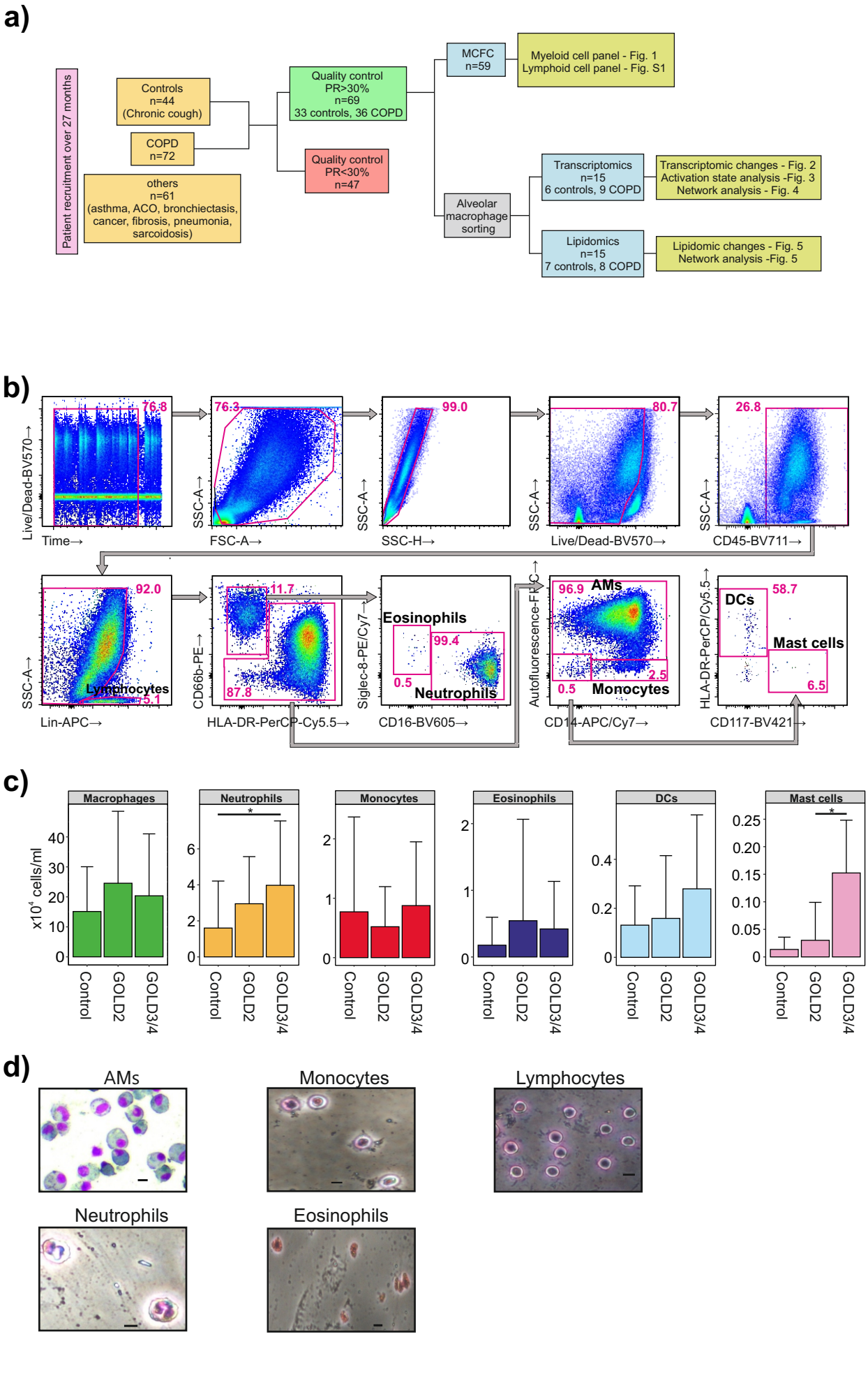
a)
Patient recruitment over 27 months
Controls n=44 (Chronic cough)
COPD n=72
others n=61 (asthma, ACO, bronchiectasis, cancer, fibrosis, pneumonia, sarcoidosis)
Quality control PR>30% n=69 33 controls, 36 COPD
Quality control PR<30% n=47
MCFC n=59
Myeloid cell panel - Fig. 1
Lymphoid cell panel - Fig. S1
Alveolar macrophage sorting
Transcriptomics n=15 6 controls, 9 COPD
Transcriptomic changes - Fig. 2
Activation state analysis -Fig. 3
Network analysis - Fig. 4
Lipidomics n=15 7 controls, 8 COPD
Lipidomic changes - Fig. 5
Network analysis -Fig. 5
b)
Live/Dead-BV570→
Time→
76.8
SSC-A→
FSC-A→
76.3
SSC-H→
99.0
Live/Dead-BV570→
80.7
CD45-BV711→
26.8
Lin-APC→
92.0
Lymphocytes
5.1
CD66b-PE→
HLA-DR-PerCP-Cy5.5→
11.7
87.8
Siglec-8-PE/Cy7→
CD16-BV605→
Eosinophils
99.4
0.5
Neutrophils
Autofluorescence-FITC→
CD14-APC/Cy7→
96.9
AMs
0.5
Monocytes
2.5
HLA-DR-PerCP/Cy5.5→
CD117-BV421→
DCs
58.7
Mast cells
6.5
c)
Macrophages
Neutrophils
Monocytes
Eosinophils
DCs
Mast cells
x10⁴ cells/ml
Control
GOLD2
GOLD3/4
d)
AMs
Monocytes
Lymphocytes
Neutrophils
Eosinophils

Figure 2

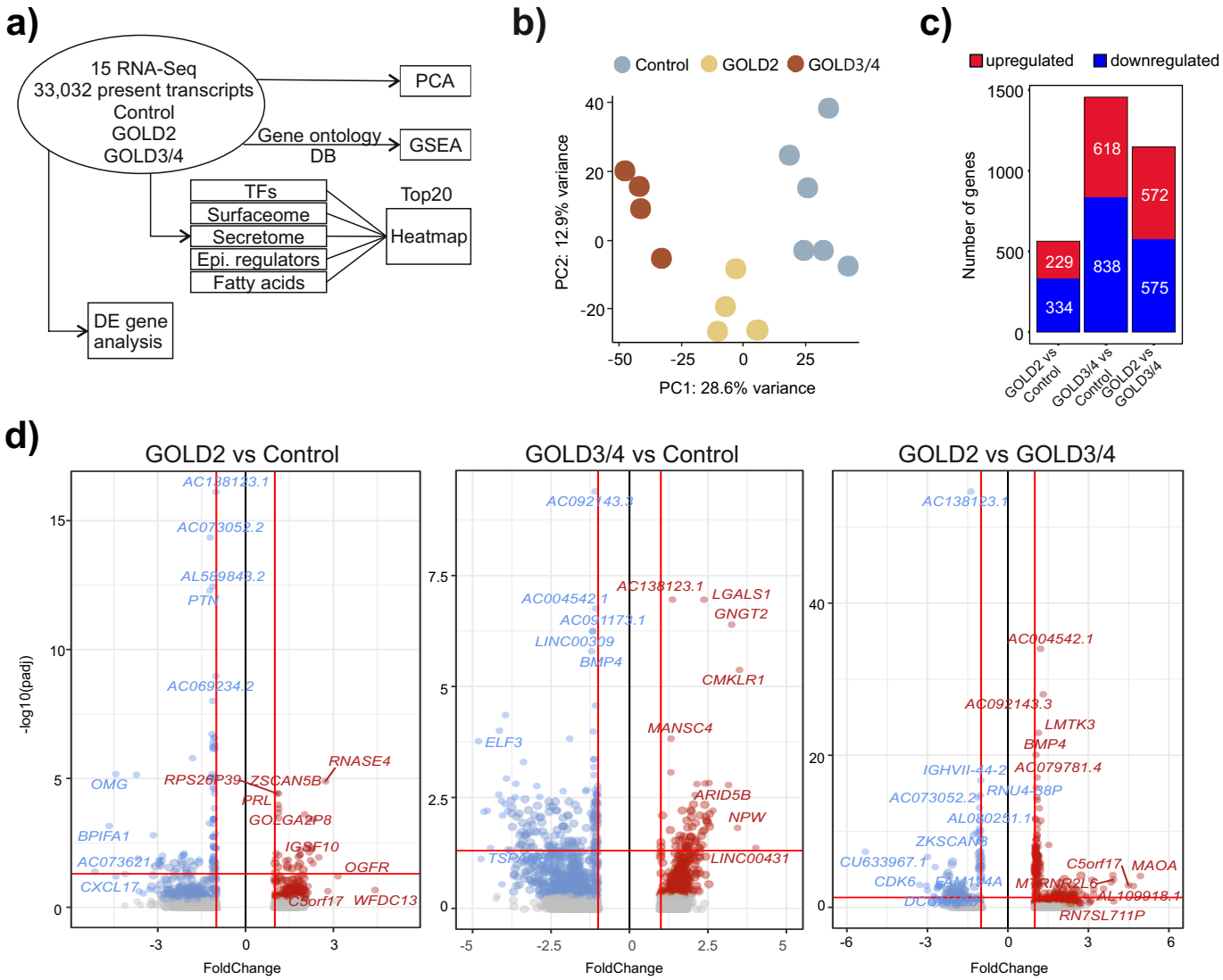
a)
15 RNA-Seq
33,032 present transcripts
Control
GOLD2
GOLD3/4
PCA
Gene ontology
DB
GSEA
TFs
Surfaceome
Secretome
Epi. regulators
Fatty acids
Top20
Heatmap
DE gene
analysis
b)
Control
GOLD2
GOLD3/4
PC2: 12.9% variance
PC1: 28.6% variance
c)
upregulated
downregulated
Number of genes
229
334
618
838
572
575
GOLD2 vs Control
GOLD3/4 vs Control
GOLD2 vs GOLD3/4
d)
GOLD2 vs Control
GOLD3/4 vs Control
GOLD2 vs GOLD3/4
-log10(padj)
FoldChange
AC138123.1
AC073052.2
AL589843.2
PTN
AC069234.2
OMG
RPS26P39
ZSCAN5B
RNASE4
PRL
GOLGA2P8
BPIFA1
AC073621.4
IGSF10
OGFR
CXCL17
C5orf17
WFDC13
AC092143.3
AC004542.1
LGALS1
GNGT2
AC091173.1
LINC00309
BMP4
CMKLR1
MANSC4
ELF3
ARID5B
NPW
TSPAN6
LINC00431
LMTK3
IGHVII-44-2
AC079781.4
RNU4-38P
AC073052.2
AL080251.1
ZKSCAN8
CU633967.1
C5orf17
MAOA
CDK6
FAM124A
MTRNR2L6
AL109918.1
RN7SL711P

Figure 3

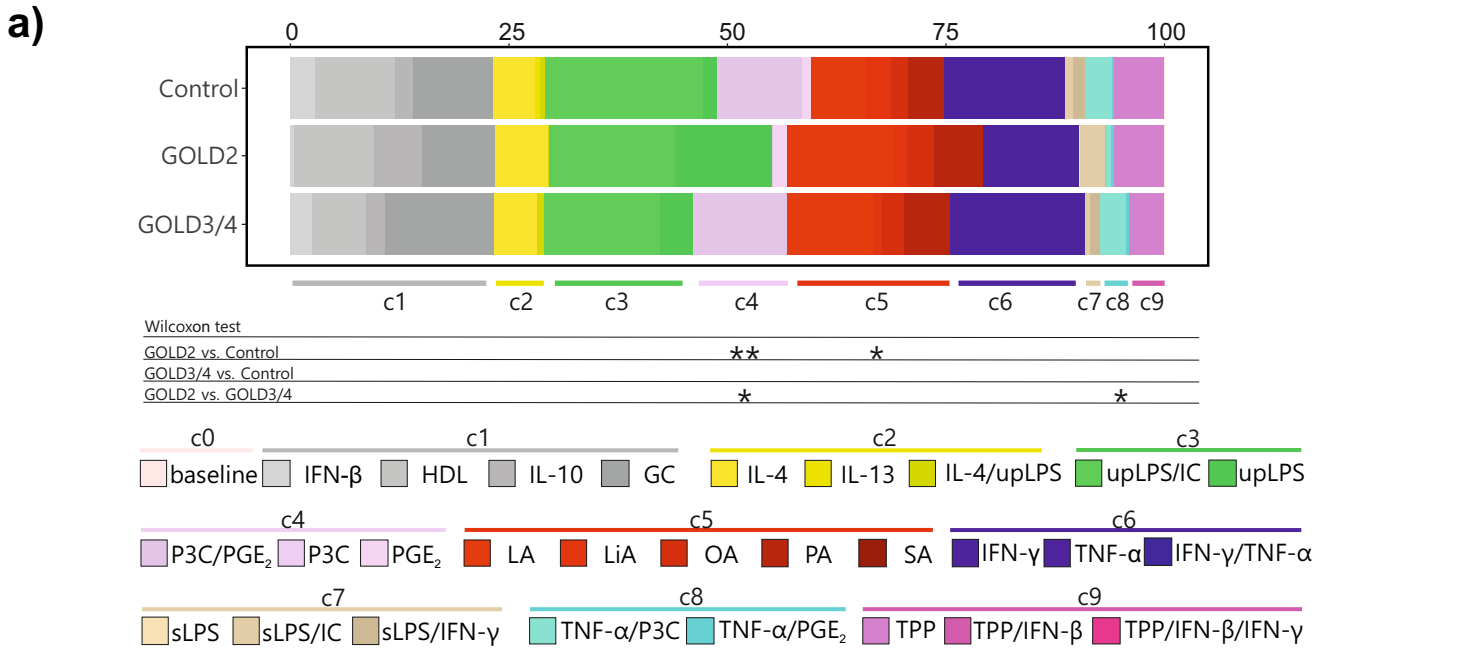
a)
0
25
50
75
100
Control
GOLD2
GOLD3/4
c1
c2
c3
c4
c5
c6
c7
c8
c9
Wilcoxon test
GOLD2 vs. Control
GOLD3/4 vs. Control
GOLD2 vs. GOLD3/4
**
*
*
*
c0
baseline
c1
IFN-β
HDL
IL-10
GC
c2
IL-4
IL-13
IL-4/upLPS
c3
upLPS/IC
upLPS
c4
P3C/PGE2
P3C
PGE2
c5
LA
LiA
OA
PA
SA
c6
IFN-γ
TNF-α
IFN-γ/TNF-α
c7
sLPS
sLPS/IC
sLPS/IFN-γ
c8
TNF-α/P3C
TNF-α/PGE2
c9
TPP
TPP/IFN-β
TPP/IFN-β/IFN-γ

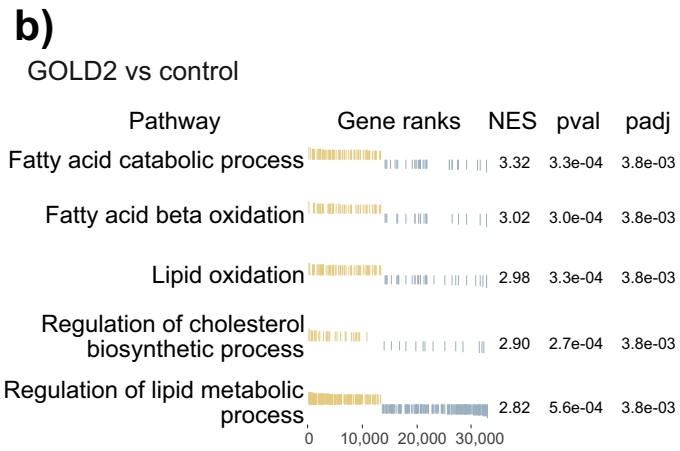
b)
GOLD2 vs control
Pathway
Gene ranks
NES
pval
padj
Fatty acid catabolic process
3.32
3.3e-04
3.8e-03
Fatty acid beta oxidation
3.02
3.0e-04
3.8e-03
Lipid oxidation
2.98
3.3e-04
3.8e-03
Regulation of cholesterol biosynthetic process
2.90
2.7e-04
3.8e-03
Regulation of lipid metabolic process
2.82
5.6e-04
3.8e-03
0
10,000
20,000
30,000

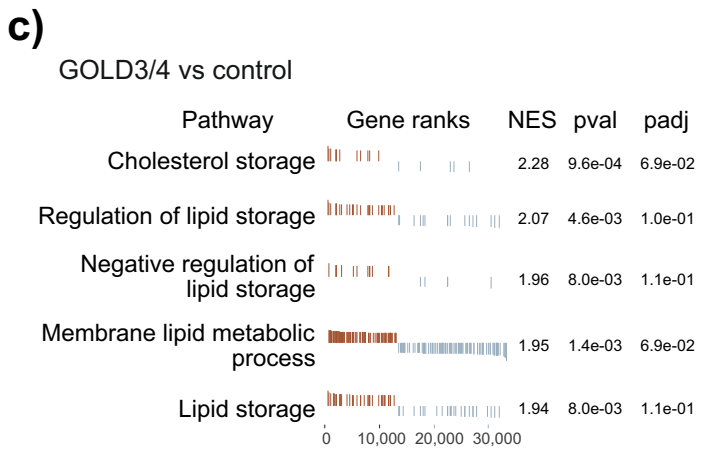
c)
GOLD3/4 vs control
Pathway
Gene ranks
NES
pval
padj
Cholesterol storage
2.28
9.6e-04
6.9e-02
Regulation of lipid storage
2.07
4.6e-03
1.0e-01
Negative regulation of lipid storage
1.96
8.0e-03
1.1e-01
Membrane lipid metabolic process
1.95
1.4e-03
6.9e-02
Lipid storage
1.94
8.0e-03
1.1e-01
0
10,000
20,000
30,000

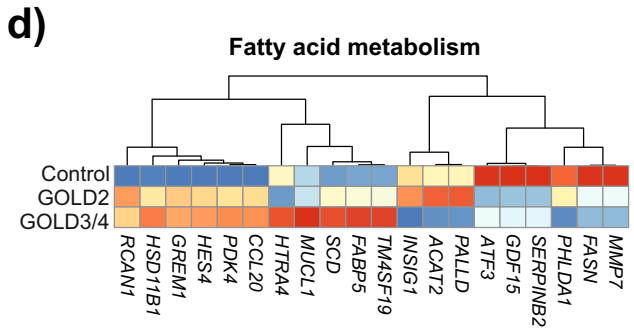
d)
Fatty acid metabolism
Control
GOLD2
GOLD3/4
RCAN1
HSD11B1
GREM1
HES4
PDK4
CCL20
HTRA4
MUCL1
SCD
FABP5
TM4SF19
INSIG1
ACAT2
PALLD
ATF3
GDF15
SERPINB2
PHLDA1
FASN
MMP7

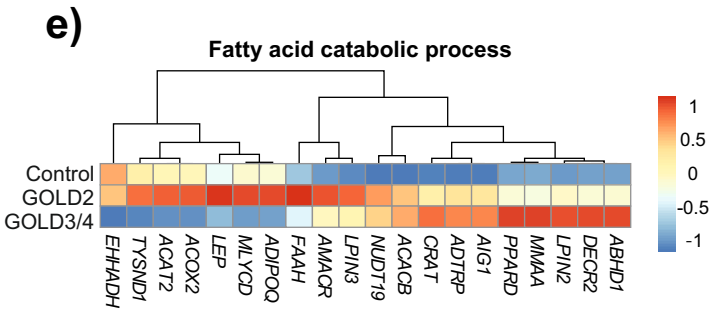
e)
Fatty acid catabolic process
Control
GOLD2
GOLD3/4
EHHADH
TYSND1
ACAT2
ACOX2
LEP
MLYCD
ADIPOQ
FAAH
AMACR
LPIN3
NUDT19
ACACB
CRAT
ADTRP
AIG1
PPARD
MMAA
LPIN2
DECR2
ABHD1
1
0.5
0
-0.5
-1

Figure 4

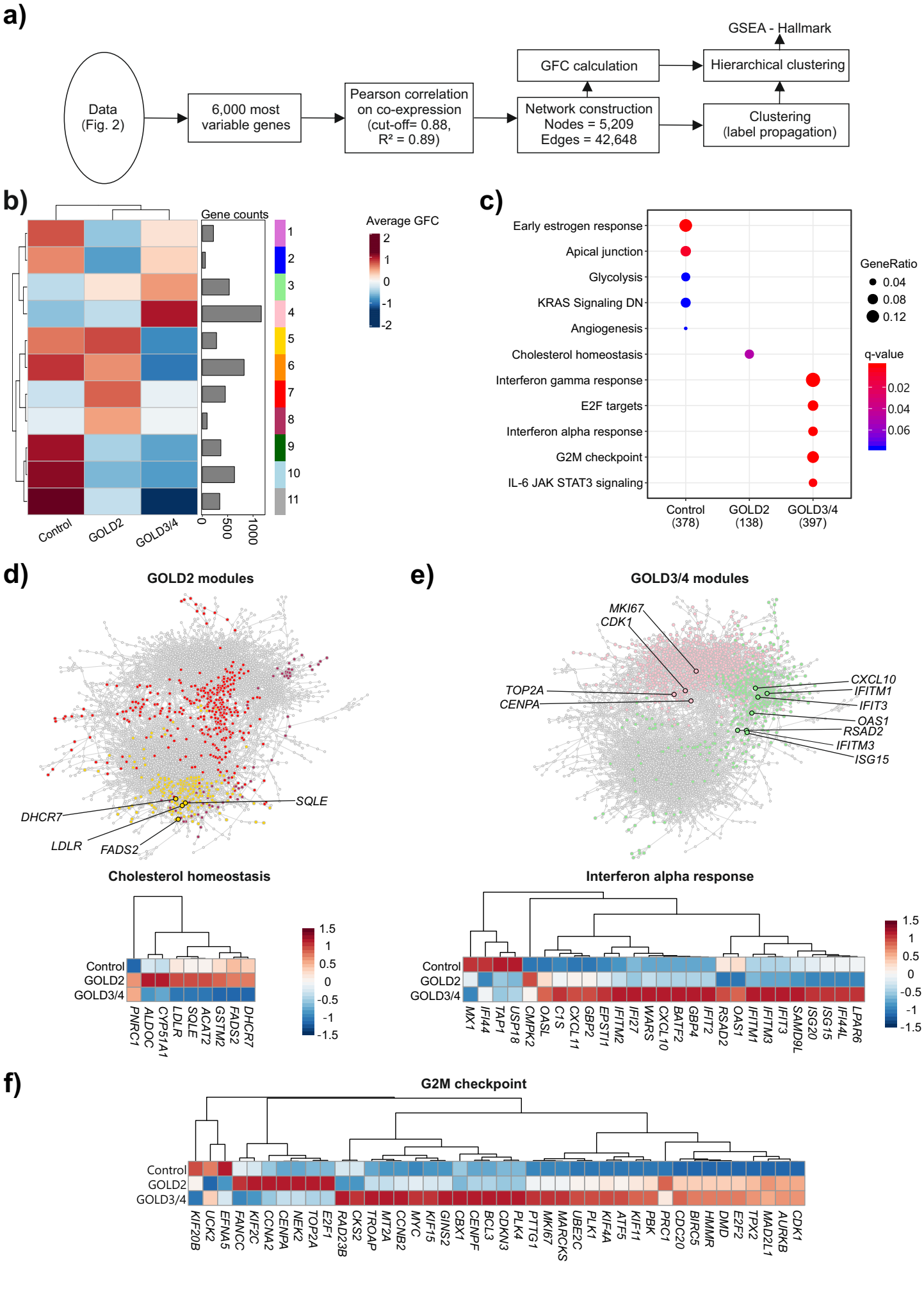
a)
Data (Fig. 2)
6,000 most variable genes
Pearson correlation on co-expression (cut-off= 0.88, R² = 0.89)
Network construction Nodes = 5,209 Edges = 42,648
GFC calculation
Clustering (label propagation)
Hierarchical clustering
GSEA - Hallmark
b)
Gene counts
Average GFC
Control
GOLD2
GOLD3/4
c)
Early estrogen response
Apical junction
Glycolysis
KRAS Signaling DN
Angiogenesis
Cholesterol homeostasis
Interferon gamma response
E2F targets
Interferon alpha response
G2M checkpoint
IL-6 JAK STAT3 signaling
GeneRatio
q-value
Control (378)
GOLD2 (138)
GOLD3/4 (397)
d)
GOLD2 modules
DHCR7
SQLE
LDLR
FADS2
Cholesterol homeostasis
PNRC1 ALDOC CYP51A1 LDLR SQLE ACAT2 GSTM2 FADS2 DHCR7
e)
GOLD3/4 modules
MKI67
CDK1
TOP2A
CENPA
CXCL10
IFITM1
IFIT3
OAS1
RSAD2
IFITM3
ISG15
Interferon alpha response
MX1 IFI44 TAP1 USP18 CMPK2 OASL C1S CXCL11 GBP2 EPSTI1 IFI27 IFITM2 WARS CXCL10 BATF2 GBP4 IFIT2 RSAD2 OAS1 IFITM1 IFITM3 IFIT3 SAMD9L ISG20 ISG15 IFI44L LPAR6
f)
G2M checkpoint
KIF20B UCK2 EFNA5 FANCC KIF2C CCNA2 CENPA NEK2 TOP2A E2F1 RAD23B CKS2 TROAP MT2A CCNB2 MYC KIF15 GINS2 CBX1 CENPF BCL3 CDKN3 PLK4 PTTG1 MKI67 MARCKS UBE2C PLK1 KIF4A ATF5 KIF11 PBK PRC1 CDC20 BIRC5 HMMR DMD E2F2 TPX2 MAD2L1 AURKB CDK1

Figure 5

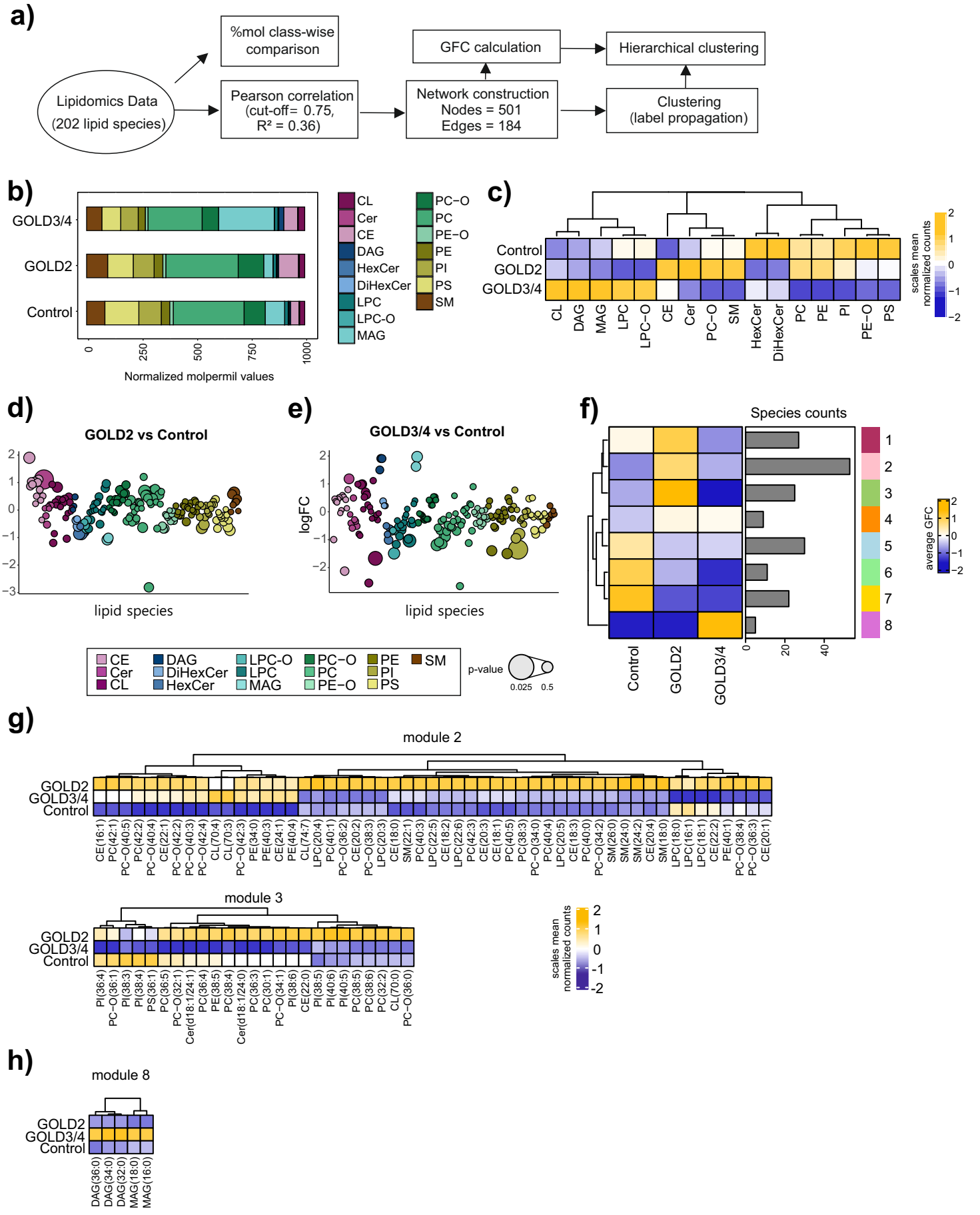
a)
Lipidomics Data
(202 lipid species)
%mol class-wise comparison
Pearson correlation
(cut-off= 0.75,
R² = 0.36)
Network construction
Nodes = 501
Edges = 184
GFC calculation
Hierarchical clustering
Clustering
(label propagation)
b)
GOLD3/4
GOLD2
Control
0
250
500
750
1000
Normalized molpermil values
CL
Cer
CE
DAG
HexCer
DiHexCer
LPC
LPC-O
MAG
PC-O
PC
PE-O
PE
PI
PS
SM
c)
Control
GOLD2
GOLD3/4
CL
DAG
MAG
LPC
LPC−O
CE
Cer
PC−O
SM
HexCer
DiHexCer
PC
PE
PI
PE−O
PS
scales mean normalized counts
d)
GOLD2 vs Control
logFC
lipid species
e)
GOLD3/4 vs Control
logFC
lipid species
p-value
0.025
0.5
f)
Species counts
Control
GOLD2
GOLD3/4
average GFC
g)
module 2
GOLD2
GOLD3/4
Control
CE(16:1)
PC(42:1)
PC−O(40:5)
PC(42:2)
PC−O(40:4)
CE(22:1)
PC−O(42:2)
PC−O(40:3)
PC−O(42:4)
CL(70:4)
CL(70:3)
PC−O(42:3)
PE(34:0)
PE(40:3)
CE(24:1)
PE(40:4)
CL(74:7)
LPC(20:4)
PC(40:1)
PC−O(36:2)
CE(20:2)
PC−O(38:3)
LPC(20:3)
CE(18:0)
SM(22:1)
PC(40:3)
LPC(22:5)
CE(18:2)
LPC(22:6)
PC(42:3)
CE(20:3)
CE(18:1)
PC(40:5)
PC(38:3)
PC−O(34:0)
PC(40:4)
LPC(20:5)
CE(18:3)
PC(40:0)
PC−O(34:2)
SM(26:0)
SM(24:0)
SM(24:2)
CE(20:4)
SM(18:0)
LPC(18:0)
LPC(16:1)
LPC(18:1)
CE(22:2)
PE(40:1)
PC−O(38:4)
PC−O(36:3)
CE(20:1)
module 3
GOLD2
GOLD3/4
Control
PI(36:4)
PC−O(36:1)
PI(38:3)
PI(38:4)
PS(36:1)
PC(36:5)
PC−O(32:1)
Cer(d18:1/24:1)
PC(36:4)
PE(38:5)
PC(38:4)
Cer(d18:1/24:0)
PC(36:3)
PC(30:1)
PC−O(34:1)
PI(38:6)
CE(22:0)
PI(38:5)
PI(40:6)
PI(40:5)
PC(38:5)
PC(38:6)
PC(32:2)
CL(70:0)
PC−O(36:0)
scales mean normalized counts
h)
module 8
GOLD2
GOLD3/4
Control
DAG(36:0)
DAG(34:0)
DAG(32:0)
MAG(18:0)
MAG(16:0)

Alveolar macrophage transcriptomic profiling in COPD shows major lipid metabolism changes

Wataru Fujii, Theodore S. Kapellos, Kevin Baßler, Kristian Händler, Lisa Holsten, Rainer Knoll, Stefanie Warnat-Herresthal, Marie Oestreich, Emily R. Hinkley, Jan Hasenauer[6], Carmen Pizarro, Christoph Thiele, Anna C. Aschenbrenner, Thomas Ulas, Dirk Skowasch, Joachim L. Schultze

ONLINE DATA SUPPLEMENT

METHODS

Human specimens

Human studies were approved by the ethics committees of the University of Bonn and University hospital Bonn (local ethics vote 076/16). All patients provided written informed consent according to the Declaration of Helsinki before specimens were collected. They were recruited as part of an exploratory observational clinical cohort study consecutively over a period of 27 months from the Department of Pneumology. Patients were categorized as either control (see definition below), COPD, or other diseases (see also Fig. 1A). Patients with COPD were diagnosed and stratified according to the guidelines of the global initiative for chronic obstructive lung disease (GOLD) [1]. Eligible patients were aged 18 years or older and were either current, past or non-smokers (Table E1). Current smokers had smoked in the last 3 months, ex-smokers had not smoked in the last 3 months prior the bronchoscopy and never smokers had not smoked more than 100 cigarettes in their lifetime and did not smoke at the time of recruitment. Age-matched individuals suffering from chronic idiopathic cough, demonstrating an exquisitely sensitive cough reflex without underlying pathology [2], served as control donors. A diagnostic algorithm that considered medical history (including drugs, e.g. ACE inhibitor and indications of heart burn), physical examination, echocardiography, chest X-ray, lung function, including methacholine challenge, presentation at an HNO doctor, blood test (including exclusion of eosinophilia), FeNO (excluding >50 ppb), computer tomography of the chest and finally bronchoscopy [3] was worked up to enroll the control group. Exclusion criteria included hypoxemia despite oxygen supplementation (O_2 saturation<90%), hypercapnia, increased risk of bleeding, unstable cardiac disease, and COPD exacerbations within

the 4 weeks prior to recruitment. Patients with other pulmonary diseases (termed other (Fig. 1A)) were diagnosed as asthma, ACO, bronchiectasis, cancer, fibrosis, pneumonia and sarcoidosis (Table E2), but were excluded from further evaluation within this study.

Bronchoscopy procedure

Bronchoscopy was performed as a part of the diagnostic workup by two bronchoscopists through oral access and with light conscious sedation. All participants received supplemental oxygen by nasal cannula. After a general inspection, BAL was performed in the middle lobe or, if not accessible, the lingular lobe. Warmed saline (6 syringes of 20 ml each) was instilled into the airways to enable BALF recovery. After each instillation, the aliquot was immediately recovered by gentle hand suction into a syringe.

BALF processing

Human BALF was obtained from all patients included in the study (control, COPD, other) through bronchoscopy. Within this report, only BALF samples of the highest quality following quality criteria established previously for the processing of BALF [4], such as recovery rate higher than 30% and absence or minimal blood/mucus contamination, from control and COPD patients were used further. BALF specimens were washed with PBS, suspended with 0.02% EDTA-2Na and washed again for final re-suspension with 2% FCS/1 mM EDTA. $CD45^{+}Lin^{-}HLA\text{-}DR^{+}CD66^{-}Autofluorescence^{+}$ AMs were sorted using a FACS Aria III cell sorter (BD Biosciences, USA).

Cell counting and decision making

Total cell counts were determined with (1:5) Trypan Blue exclusion (Sigma-Aldrich) under an optical microscope. BALF cells (10ul) were diluted 1:10 in the Trypan Blue solution and counted in a Neubauer haemocytometer. Due to material limitations, we prioritized flow cytometry-based immunophenotyping of total $CD45^+$ cells. If sufficient material was available, we also sorted alveolar macrophages from the remaining cells for RNA sequencing and lipidomics. For some patients, the absolute numbers of alveolar macrophages were not sufficient for both approaches (transcriptomics and lipidomics) and we therefore proceeded to either RNA sequencing or lipidomics (Table E3).

Flow cytometry/FACS

Single-cell suspensions were stained with Live/Dead yellow fluorescent dye (ThermoFisher, USA) for 15 min at room temperature and were washed with PBS at 300xg for 5 min at 4^oC. They were then re-suspended in 100 ul PBS and blocked with 5 ul human FcR blocking reagent (Miltenyi, Germany) for 15 min on ice and were subsequently stained with the listed anti-human antibodies (Table E4) in buffer containing PBS, 2% FCS, 1 mM EDTA for 30 min on ice. After an initial interim analysis of the first 36 samples, we identified a non-annotated cell population, which we identified as $Fc\varepsilon RI^+$ mast cells. All further samples from control and COPD patients (n=23) were also interrogated for the presence of mast cells in the BALF. Cells were spinned at 300xg for 5 min at 4^oC and re-suspended in buffer containing PBS, 2% FCS, 1 mM EDTA for analysis. Data acquisition was performed on a FACS Aria III cell sorter

(BD Biosciences, USA). Analysis was performed with FlowJo v.10 software (Tree Star, USA).

Cytospin preparation

Cytospins were obtained by centrifuging $2x10^5$ cells in 200 ul PBS on microscope slides at 20% power for 5 min. Excess buffer was carefully discarded and slides were air dried for 3 min followed by fixation with 100% methanol for 5 min at 4^oC. The slides were subsequently washed with PBS and stained with 1:20 Giemsa solution (Sigma, USA) for 25 min at room temperature. A final rinsing step with H_2O and air drying before mounting followed. Cell morphology was examined by microscopic evaluation of stained cells using an Axio Lab A1 microscope (Zeiss, Germany).

RNA extraction and library preparation

Total RNA was isolated from human AMs with the miRNeasy Micro kit (Qiagen, Germany) according to the manufacturer's protocol and RNA concentration and integrity was determined using the High Sensitivity RNA assay on a TapeStation 4200 system (Agilent, USA). All samples had RIN>7 and therefore no exclusions were made for poor RNA quality. cDNA libraries were prepared from 5 ng total RNA with the SMART-seq2 protocol [5] and were tagmented with the Nextera XT kit (Illumina, USA). Library size selection was carried out with AMPure beads (Beckman-Coulter, USA) and library size distribution was measured with the High Sensitivity D5000 assay on a TapeStation 4200 System (Agilent, USA). Library concentration was determined using the HS dsDNA assay on a Qubit. Libraries were sequenced for SR 75 cycles on a NextSeq500 system

(Illumina) using High Output v2 chemistry. Base call files were converted to fastq format and demultiplexed using bcl2fastq v2.20.

Data pre-processing and RNA sequencing analysis

The 75 bp single-end reads were aligned to the human reference transcriptome hg38 from UCSC by kallisto v0.44.0 using default parameters. Data were imported into DESeq2 (v.1.10.1; [6]) using the TXimport (v1.2.0, [7]) package. DESeq2 was used for the calculation of normalized counts for each transcript using default parameters. All normalized transcripts with a maximum over all group means lower than 10 were excluded resulting in 33,032 present transcripts. Unwanted or hidden sources of variation, such as batch, sex and smoking status were removed using the sva package [8]. Briefly, the SVA package models the provided gene expression tables to identify and construct surrogate variables which adjust for technical artifacts (batches), as well as variation of unknown sources. Subsequently, the user can assess these variables and test how each of the undesired factors is corrected by the algorithm. The normalized rlog transformed expression values were adjusted according to the five surrogate variables identified by sva using the function removeBatchEffect from the limma package [9]. DE genes were defined by a p-value cut-off of 0.05 and an adjusted p-value (IHW) < 0.5 (independent hypothesis weighting). All present transcripts were used as input for principal component analysis. Pearson Correlation Coefficient Matrix (PCCM) and the top 25% most variable transcripts within the dataset were selected and visualized as heatmaps.

Gene set enrichment analysis (GSEA)

To test for functional enrichment between COPD (GOLD2 and GOLD3/4, respectively) and control patients, we performed GSEA [10] on all present genes of the dataset using the gene ontology set of biological processes. Information of gene ontology was obtained from the biological process gene set “c5.bp.v7.0.symbols.gmt”, downloaded from the Molecular Signatures Database (MSigDB). All present genes were used as background (universe). Lipid-related genes were extracted upon filtering gene ontology terms for the keywords “fat” and “lipid”. Data were FDR-corrected.

Linear support vector regression

Linear support vector regression [11] was employed to characterize the relative contribution of 28 different activation signatures derived from [12] to the control and COPD patients. Our normalized gene expression table was utilized as input mixture file and the published activation signatures in [12] were used to compute the relative activation signatures within bulk control and COPD samples (1,000 permutations). The union of the c5 module genes (Fig. 3A) was used as a fatty acid signature and the 20 most variable genes were visualized in a heatmap.

Filtering for TFs, epigenome, surfaceome and secretome

All present transcripts were filtered and sorted by their variance in the dataset. The 20 most variable genes of each category were selected and visualized in heatmaps. TF lists were extracted from [13], the epigenome gene list was derived from the literature, surface and secretome markers were extracted from the Human Protein Atlas [14, 15].

Construction of co-expressed network analysis – automated (CoCena²)

To elucidate similarities and differences within the gene expression patterns of the three different patient groups -control, GOLD2 and GOLD3/4 COPD- CoCena² was performed. Pearson correlation was calculated on the 6,000 most variable genes within the dataset using the R package Hmisc (v4.3-0; [16]). Data were filtered for significant (p-value < 0.05, Bonferroni correction p<0.05) and positive (r-value > 0) correlation values. A Pearson correlation coefficient cutoff of 0.88 was applied as this yields a scale-free network (R^2 = 0.89) with 5,209 nodes and 42,648 edges. The Group Fold Change (GFC) was calculated for each gene and each condition on the inverse logarithmic count data using the R package gtools (v3.8.2; [17]). In brief, the mean expression of each gene for each patient group versus the overall mean expression of the gene was calculated. Unbiased clustering was performed using the R package igraph (v1.2.4.1; [18]). Five different clustering algorithms, namely “cluster_label_prop”, “cluster_fast_greedy”, “cluster_louvain”, “cluster_infomap” and “cluster_walktrep”, were tested and “cluster_louvain” was selected as it achieves the highest modularity score. The mean GFC for each cluster and condition was visualized in the cluster-condition heatmap using the R package ComplexHeatmap (v2.0.0; [19]). Clusters with less than 35 genes are not shown. Hierarchical clustering was performed on genes and cluster modules using the Euclidean clustering distance and the complete-linkage clustering method. Network generation was performed with the R package igraph. The network information was imported to and exported from Cytoscape using the R package RCy3 (v2.6.2; [20]). In Cytoscape, the prefuse force-directed layout was applied to the network. Network visualization was performed using the R packages ggnetwork (v0.5.1,

[21]) and ggplot2 (v3.2.1; [22]).

Biological function-related bioinformatic analysis of network modules

GSEA was performed on the patient group-related modules identified by CoCena² using the R package ClusterProfiler (v3.12.0; [23]). The *compareCluster* function was used to determine significant enrichment (q-value < 0.1 using the Benjamini-Hochberg method) of hallmark gene sets of biological processes. Information of hallmark genes was obtained from the hallmark gene set “h.all.v6.1.symbols.gmt”, downloaded from the Molecular Signatures Database (MSigDB). All genes present in the network were used as background (universe). Interesting hallmark terms for each patient group were selected and the mean gene expression of all genes within the selected term was visualized in heatmaps using the R package pheatmap (v1.0.12; [24]). The gene expression values were scaled over the three groups. Hierarchical clustering was performed on the genes using the Euclidean clustering distance and the complete clustering method. Enriched genes were highlighted on the CoCena^2 network.

Lipidomics

Sorted AMs ($5x10^4$) were washed with PBS, suspended with 150 mM ammonium acetate (Merck, Germany) and transferred into a glass tube. After centrifugation at 300xg for 10 min with low brake, supernatants were discarded, and the pellets were frozen at -80°C until analysis. Extraction mix (Chloroform 1:5 methanol-containing internal standards: 210 pmol PE(31:1), 396 pmol PC(31:1), 98 pmol PS(31:1), 84 pmol PI(34:0) , 56 pmol PA(31:1), 51 pmol PG (28:0), 28 pmol CL(56:0), 39 pmol LPA (17:0),

35 pmol LPC(17:1), 38 pmol LPE (17:1), 32 pmol Cer(17:0), 99 pmol SM(17:0),55 pmol GlcCer(12:0), 14 pmol GM3 (18:0-D3), 359 pmol TG(47:1), 111 pmol CE(17:1), 64 pmol DG(31:1), 103 pmol MG(17:1), 724 pmol Chol(d6), 45 pmol Car(15:0)) was spiked to the pellets before 2 min sonication and centrifugation at 20,000xg for 2 min. Chloroform and 1% acetic acid were added and the samples were spun at 20,000xg for 2 min. The lower phase was transferred and let evaporate in the vacuum concentrator (45°C for 10 min). Spray buffer (8/5/1 2-propanol/methanol/water, 10 mM ammonium acetate) was added, the samples were sonicated for 5 min and analyzed separately by infusing them at 10 ul/min into a Thermo Q Exactive Plus spectrometer equipped with the HESI II ion source for shotgun lipidomics. MS1 spectra (res. 280,000) were recorded in 100 m/z windows from 200 – 1,200 m/z (pos.) and 200 – 1,700 m/z (neg.) followed by recording of MS/MS spectra (res. 70,000) by data independent acquisition in 1 m/z windows from 200 – 1,200 (pos.) and 200 – 1,700 (neg.) m/z.

Lipidomics analysis

Raw files were converted to .mzml format and imported into the LipidXplorer software for analysis using custom mfql files to identify sample lipids and internal standards. Raw data were filtered during import into LipidXplorer by global thresholding in MS1 and MS2 to remove small stochastic noise peaks. For identification, mass errors were limited to 6 ppm in MS1 and 0.005 Th in MS2. The average mass error over all identifications in MS1 was 1.76 ppm. For a valid identification, all species must show both an identification of the unfragmented peak in MS1 and at least one specific fragment in MS2. Consistency of analysis was checked by determination of the coefficient of

variation of the intensities of the spiked internal standards within one sample series and was found to be 11.7%. Despite the low number of cells, total identified lipids in samples were 5.5-15-fold over the background blank. Further, species pattern within lipid classes were checked for consistency with expectations. We found the very characteristic pattern of dominating saturated PC (but not PC-O) and saturated DAG species (32:0, 34:0) characteristic for the lung tissue, originating from lung surfactant secretion. PE and PI showed the expected dominating PUFA-containing PE(38:4) and PI(38:4). The pattern of CE showed a stronger signal for CE(18:1) than CE(18:2), ruling out major contamination with blood, in which CE(18:2) is about 3-fold more abundant than CE(18:1). Lipid species showing signals above the blank in min. 70% of the samples were included in the analysis. For further data processing, absolute amounts were calculated using the internal standard intensities followed by normalization on the sum of all measured lipid species per sample. %mol values were averaged for each patient group, log2-transformed and then used for fold change calculations. To find patient group-specific co-regulated lipid species, CoCena[2] was used as for the transcriptome analysis. Pearson correlation was calculated on all lipid species. Data were filtered for significant (p-value < 0.05, Bonferroni correction $p<0.05$) and positive (r-value > 0) correlation values leading to the construction of a correlation network with 501 nodes and 184 edges (Pearson correlation coefficient cut-off of 0.75). The GFC was calculated for each lipid species and each condition and clustering performed using the "cluster_louvain" algorithm. Mean GFCs for each cluster and condition are visualized in the cluster-condition heatmap. Hierarchical clustering was performed on lipid species and cluster modules using the Euclidean clustering distance and the complete-linkage

clustering method. Network generation was performed with the R package igraph.

Statistics

A two-tailed Welch's unpaired t test was used to analyze data from two groups. Equality of population variance was assessed with the F-test statistic for two independent groups. A non-parametric Wilcoxon test was used to perform a pairwise comparison between patient groups for all enriched macrophage activation signatures in Fig. 3F. For more than two groups, normality and homoscedasticity were first assessed using the Shapiro-Wilk and Levene tests in R (v3.6.1). A non-parametrical Kruskal-Wallis test with Dunn's multiple correction post hoc was used in Fig. E3 because the data did not follow a normal distribution. Statistical significance was inferred when $p<0.05$.

Data and code availability

The transcriptomic data are deposited at the European Genome-phenome Archive (EGA), which is hosted by the EBI and the CRG, under accession number EGAS00001004244. Flow cytometry files can be found at www.flowrepository.org under FR-FCM-Z2JL. Lipidomic data and annotation are provided in Tables E6 and E7. The code for CoCena[2] is publicly deposited on GitHub (https://github.com/UlasThomas/CoCena2).

REFERENCES

1. Global Initiative for Chronic Obstructive Lung Disease (GOLD) [Internet]. [cited 2021 Jan 24].Available from: https://goldcopd.org/wp-content/uploads/2020/11/GOLD-REPORT-2021-v1.1-25Nov20_WMV.pdf.

2. Haque RA, Usmani OS, Barnes PJ. Chronic idiopathic cough: a discrete clinical entity? *Chest* [Internet] American College of Chest Physicians; 2005 [cited 2020 Mar 30]; 127: 1710–1713Available from: http://www.ncbi.nlm.nih.gov/pubmed/15888850.

3. Kardos P, Dinh QT, Fuchs K-H, Gillissen A, Klimek L, Koehler M, Sitter H, Worth H. [Guidelines of the German Respiratory Society for Diagnosis and Treatment of Adults Suffering from Acute, Subacute and Chronic Cough]. *Pneumologie* [Internet] Georg Thieme Verlag; 2019 [cited 2020 Mar 30]; 73: 143–180Available from: http://www.ncbi.nlm.nih.gov/pubmed/30776835.

4. Meyer KC, Raghu G, Baughman RP, Brown KK, Costabel U, Du Bois RM, Drent M, Haslam PL, Kim DS, Nagai S, Rottoli P, Saltini C, Selman M, Strange C, Wood B. An official American Thoracic Society clinical practice guideline: The clinical utility of bronchoalveolar lavage cellular analysis in interstitial lung disease. Am. J. Respir. Crit. Care Med. 2012. p. 1004–1014.

5. Picelli S, Björklund ÅK, Faridani OR, Sagasser S, Winberg G, Sandberg R. Smart-seq2 for sensitive full-length transcriptome profiling in single cells. *Nat. Methods* [Internet] 2013 [cited 2017 Jun 20]; 10: 1096–1098Available from: http://www.nature.com/doifinder/10.1038/nmeth.2639.

6. Love MI, Huber W, Anders S. Moderated estimation of fold change and dispersion for RNA-seq data with DESeq2. *Genome Biol.* [Internet] 2014 [cited 2018 Feb 14]; 15: 550Available from: http://www.ncbi.nlm.nih.gov/pubmed/25516281.

7. Soneson C, Love MI, Robinson MD. Differential analyses for RNA-seq: transcript-level estimates improve gene-level inferences. *F1000Research* [Internet] 2015 [cited 2018 Jul 23]; 4: 1521Available from: https://f1000research.com/articles/4-1521/v2.

8. Leek JT, Johnson WE, Parker HS, Jaffe AE, Storey JD. The SVA package for removing batch effects and other unwanted variation in high-throughput experiments. *Bioinformatics* 2012; 28: 882–883.

9. Ritchie ME, Phipson B, Wu D, Hu Y, Law CW, Shi W, Smyth GK. Limma powers differential expression analyses for RNA-sequencing and microarray studies. *Nucleic Acids Res.* Oxford University Press; 2015; 43: e47.

10. Subramanian A, Tamayo P, Mootha VK, Mukherjee S, Ebert BL, Gillette MA, Paulovich A, Pomeroy SL, Golub TR, Lander ES, Mesirov JP. Gene set enrichment analysis: a knowledge-based approach for interpreting genome-wide expression profiles. *Proc. Natl. Acad. Sci. U. S. A.* [Internet] 2005 [cited 2018 Nov 12]; 102: 15545–15550Available from: http://www.pnas.org/cgi/doi/10.1073/pnas.0506580102.

11. Newman AM, Liu CL, Green MR, Gentles AJ, Feng W, Xu Y, Hoang CD, Diehn M, Alizadeh AA. Robust enumeration of cell subsets from tissue expression profiles. *Nat. Methods* [Internet] 2015 [cited 2018 May 23]; 12: 453–457Available from: http://www.nature.com/articles/nmeth.3337.

12. Xue J, Schmidt SV, Sander J, Draffehn A, Krebs W, Quester I, De Nardo D, Gohel TD, Emde M, Schmidleithner L, Ganesan H, Nino-Castro A, Mallmann MR, Labzin L, Theis H, Kraut M, Beyer M, Latz E, Freeman TC, Ulas T, Schultze JL. Transcriptome-Based Network Analysis Reveals a Spectrum Model of Human Macrophage Activation. *Immunity* [Internet] 2014 [cited 2017 Jun 16]; 40: 274–288Available from: http://www.ncbi.nlm.nih.gov/pubmed/24530056.

13. Fulton DL, Sundararajan S, Badis G, Hughes TR, Wasserman WW, Roach JC, Sladek R. TFCat: the curated catalog of mouse and human transcription factors. *Genome Biol.* [Internet] 2009 [cited 2018 May 26]; 10: R29Available from: http://genomebiology.biomedcentral.com/articles/10.1186/gb-2009-10-3-r29.

14. The Human Protein Atlas - surfaceome [Internet]. [cited 2020 Jan 23].Available from: https://www.proteinatlas.org/search/protein_class:Predicted+membrane+proteins+AND+NOT+protein_class:Predicted+secreted+proteins.

15. The Human Protein Atas - secretome [Internet]. [cited 2020 Jan 23].Available from: https://www.proteinatlas.org/search/protein_class:Predicted+secreted+proteins+AND+NOT+protein_class:Predicted+membrane+proteins.

16. Harrell Jr FE, with contributions from Charles Dupont, many others. Hmisc: Harrell Miscellaneous [Internet]. 2019.Available from: https://cran.r-project.org/package=Hmisc.

17. Warnes GR, Bolker B, Lumley T. gtools: Various R Programming Tools [Internet]. 2018.Available from: https://cran.r-project.org/package=gtools.

18. Csardi G, Nepusz T. The igraph software package for complex network research. *InterJournal* [Internet] 2006; Complex Systems: 1695Available from: http://igraph.org.

19. Gu Z, Eils R, Schlesner M. Complex heatmaps reveal patterns and correlations in multidimensional genomic data. *Bioinformatics* Oxford University Press; 2016; 32: 2847–2849.

20. Gustavsen JA, Pai S, Isserlin R, Demchak B, Pico AR. RCy3: Network biology using Cytoscape from within R. *F1000Research* [Internet] 2019 [cited 2020 Jan 22]; 8: 1774Available from: https://f1000research.com/articles/8-1774/v3.

21. Briatte F. ggnetwork: Geometries to Plot Networks with “ggplot2” [Internet]. 2016.Available from: https://cran.r-project.org/package=ggnetwork.

22. Wickham H. ggplot2: Elegant Graphics for Data Analysis [Internet]. Springer-Verlag New York; 2016.Available from: https://ggplot2.tidyverse.org.

23. Yu G, Wang L-G, Han Y, He Q-Y. clusterProfiler: an R Package for Comparing Biological Themes Among Gene Clusters. *Omi. A J. Integr. Biol.* [Internet] Mary Ann Liebert, Inc. 140 Huguenot Street, 3rd Floor New Rochelle, NY 10801 USA ; 2012 [cited 2019 Aug 1]; 16: 284–287Available from: http://www.liebertpub.com/doi/10.1089/omi.2011.0118.

24. Kolde R. pheatmap: Pretty Heatmaps [Internet]. 2019.Available from: https://cran.r-project.org/package=pheatmap.

SUPPLEMENTARY FIGURES

Fig. S1 – Representative multi-color flow cytometry analysis of the lymphoid compartment of a control patient (a). Absolute numbers of lymphoid immune cells in the BALF of control, GOLD2 and GOLD3/4 COPD patients calculated with traditional gating. Data are from 8-23 patients per group and are represented as mean ± SD (b). Bar plot of ILC concentration in BALF of control and COPD patients calculated with flow cytometry traditional gating (c). Bar plot of ILC1 concentration in the BALF of control and COPD patients calculated with flow cytometry traditional gating (d). Mean ± SD is shown from 16-17 patients and data were analysed with an unpaired two-tailed student t-test, * $p<0.05$, BALF, bronchoalveolar lavage fluid; ILC, innate lymphoid cell

Fig. S2 - Hierarchical clustering of the 25% most variable transcripts (a). Matrix of hierarchically clustered PCCM showing the distance from 0 to 100 (blue to red) based on all present transcripts (b). Hierarchical clustering of the patient group means of the top 20 most variable transcripts filtered by a list of TFs (c), known epigenetic regulators (d), surface (e) and secreted molecules (f), PCCM, Pearson correlation coefficient matrix; TF, transcription factor

SUPPLEMENTARY TABLES

Table 1 – Detailed demographics of control and COPD patients.

Table 2 – Detailed demographics of rejected patients.

Table 4 – Detailed information for the antibodies used in the study.

Table 5 – Surface markers that were used to identify major immune cell types in BALF from control and COPD patients.

Table 6 – Raw lipidomic data generated in the study.

Table 7 - Lipidomic data annotation table.

Table E1

Patient ID	Diagnosis	BALF volume recovered	BALF recovery ratio	Cellularity (millions)	FEV1/FVC	FEV1%	GOLD grade	Group	Sex	Age	Smoking history	Packyears	LAMA	LABA	ICS	Death	Hospitalizations/year	Exacerbations/year	Flow cytometry	RNA-seq	Lipidomics
12	Chronic cough	65	0.54	5.3	72	90	NA	NA	M	61	Past	20	No	Formeterol 6 ug	Beclometason 100 ug	No	0	0	Yes	No	No
18	Chronic cough	40	0.33	5.6	86	77	NA	NA	F	66	Never	NA	Tiotropium 2.5 ug	Olodaterol 2.5 ug	No	No	0	0	Yes	No	No
21	Chronic cough	45	0.38	20.4	85	109	NA	NA	F	36	Never	NA	No	No	No	No	0	0	Yes	No	No
22	Chronic cough	35	0.29	9.8	82	101	NA	NA	F	68	Never	NA	No	No	No	No	0	0	Yes	No	No
27	Chronic cough	100	0.83	19.4	89	108	NA	NA	M	67	Past	20	No	No	No	No	0	0	Yes	No	No
35	Chronic cough	35	0.29	2.3	109	82	NA	NA	M	65	Current	75	No	No	No	No	0	0	Yes	No	No
36	Chronic cough	65	0.54	1.3	82	95	NA	NA	F	49	Past	2	No	No	No	No	0	0	Yes	No	No
39	Chronic cough	35	0.29	4.2	75	90	NA	NA	M	59	Current	45	No	No	No	No	0	0	Yes	No	No
45	Chronic cough	45	0.38	3.3	107	102	NA	NA	F	62	Current	30	No	No	No	No	0	0	Yes	No	No
51	Chronic cough	35	0.29	5.2	111	100	NA	NA	F	68	Never	NA	No	No	No	No	0	0	Yes	No	No
56	Chronic cough	45	0.38	1.1	91	91	NA	NA	F	59	Never	NA	No	No	No	No	0	0	Yes	No	No
59	Chronic cough	50	0.42	0.5	89	88	NA	NA	F	30	Past	2	No	No	No	No	0	0	Yes	No	Yes
61	Chronic cough	55	0.46	1.4	84	80	NA	NA	F	60	Never	NA	No	No	No	No	0	0	Yes	No	No
72	Chronic cough	40	0.33	0.5	81	101	NA	NA	F	74	Never	NA	No	No	No	No	0	0	Yes	No	No
74	Chronic cough	50	0.42	4	111	92	NA	NA	M	44	Past	15	No	No	No	No	0	0	Yes	No	No
77	Chronic cough	30	0.25	5.6	90	89	NA	NA	F	58	Never	NA	No	No	No	No	0	0	Yes	No	Yes
79	Chronic cough	40	0.33	21	102	102	NA	NA	F	56	Never	NA	No	No	No	No	0	0	Yes	No	No
91	Chronic cough	35	0.29	31	85	70	NA	NA	M	41	Never	NA	No	No	No	No	0	0	No	Yes	No
111	Chronic cough	45	0.38	21	78	92	NA	NA	F	27	Never	NA	No	No	No	No	0	0	Yes	No	Yes
113	Chronic cough	65	0.54	20.5	84	99	NA	NA	M	65	Never	NA	No	No	No	No	0	0	Yes	Yes	Yes
116	Chronic cough	45	0.38	25	76	96	NA	NA	M	58	Past	25	No	No	No	No	0	0	Yes	No	Yes
123	Chronic cough	50	0.42	13.9	77	96	NA	NA	F	53	Past	40	Glycopyrronium 85 ug	Indacaterol 43 ug	Budenosid 400 ug	No	0	0	Yes	No	No
128	Chronic cough	50	0.42	1.68	79	69	NA	NA	F	53	Never	NA	No	No	No	No	0	0	No	Yes	No
133	Chronic cough	40	0.33	4.8	80	111	NA	NA	F	49	Never	NA	No	No	No	No	0	0	Yes	No	No
135	Chronic cough	60	0.50	18.1	77	132	NA	NA	M	58	Never	NA	No	No	No	No	0	0	Yes	No	Yes
139	Chronic cough	50	0.42	10.5	79	88	NA	NA	F	55	Never	NA	No	No	No	No	0	0	Yes	No	No
141	Chronic cough	60	0.50	4.5	76	97	NA	NA	M	60	Never	NA	No	No	No	No	0	0	Yes	No	Yes
146	Chronic cough	80	0.67	6.3	86	89	NA	NA	F	45	Never	NA	No	No	No	No	0	0	Yes	No	No
167	Chronic cough	35	0.29	10.5	78	96	NA	NA	M	52	Current	30	Tiotropium 10 ug	No	No	No	0	0	Yes	No	No
172	Chronic cough	50	0.42	22.1	78	110	NA	NA	M	53	Never	NA	No	No	No	No	0	0	Yes	Yes	No
177	Chronic cough	45	0.38	10.5	79	63	NA	NA	F	62	Current	40	No	Formeterol 9 ug	Budenosid 320 ug	No	0	0	Yes	No	No
184	Chronic cough	70	0.58	4.2	86	99	NA	NA	M	48	Past	1	No	No	No	No	0	0	No	Yes	No
190	Chronic cough	40	0.33	46.2	76	117	NA	NA	M	60	Past	8	No	No	No	No	0	0	No	Yes	No
1	COPD	40	0.33	3.1	67	40	3	D	M	63	Past	150	Spiriva 18 ug	Formeterol 9 ug	Budenosid 320 ug	No	1	2	Yes	No	No
8	COPD	80	0.67	7.1	65	42	4	D	M	63	Past	140	Spiriva 18 ug	Formeterol 9 ug	Budenosid 320 ug	No	1	2	Yes	No	No
16	COPD	40	0.33	5.2	66	64	2	B	M	71	Current	27	Tiotropium 2.5 ug	Olodaterol 2.5 ug	No	NA	NA	NA	Yes	No	No
32	COPD	60	0.50	8.1	67	26	4	D	M	64	Past	150	Spiriva 18 ug	Formeterol 9 ug	Budenosid 320 ug	No	1	2	Yes	No	No
40	COPD	45	0.38	8.2	59	45	3	B	F	80	Past	35	Umeclidinium 55 ug	Vilanterol 22 ug	No	Yes	3	3	Yes	No	No
44	COPD	40	0.33	6.8	48	56	2	B	M	74	Past	40	No	No	No	Yes	0	0	Yes	No	No
47	COPD	40	0.33	7.8	55	41	3	B	M	67	Past	80	Glycopyrronium 43 ug	Indacaterol 85 ug	No	No	0	2	Yes	No	No
48	COPD	35	0.29	9.4	55	48	3	B	F	81	Past	25	No	No	No	No	0	0	Yes	No	No
52	COPD	60	0.50	4	52	46	3	B	F	81	Past	25	No	No	No	No	0	0	Yes	No	No
54	COPD	60	0.50	24.3	61	38	3	D	M	72	Past	50	Glycopyrronium 50 ug	Indacaterol 110 ug	No	No	0	1	Yes	No	No
80	COPD	50	0.42	6	44	32	3	D	F	59	Past	50	Tiotropium 2.5 ug	Olodaterol 2.5 ug	No	No	0	0	Yes	No	Yes
83	COPD	50	0.42	31	68	79	2	B	M	64	Past	135	Tiotropium 2.5 ug	Formeterol 6 ug	Beclometason 200 ug	No	1	2	Yes	Yes	Yes
94	COPD	40	0.33	1.35	62	60	2	D	F	57	Current	40	Tiotropium 2.5 ug	Olodaterol 2.5 ug	No	No	1	1	Yes	Yes	No
103	COPD	50	0.42	10.2	67	47	3	D	F	64	Past	62	Tiotropium 2.5 ug	Olodaterol 2.5 ug	No	No	0	1	Yes	No	Yes
105	COPD	50	0.42	32	66	34	3	B	M	60	Current	35	Tiotropium 2.5 ug	Olodaterol 2.5 ug	No	No	0	0	Yes	No	Yes
115	COPD	50	0.42	24	69	69	2	B	M	80	Past	10	No	No	No	No	1	1	Yes	Yes	No
120	COPD	40	0.33	8.4	69	68	2	B	M	62	Never	NA	No	No	No	No	0	0	No	Yes	No
122	COPD	40	0.33	6.9	69	64	2	B	M	48	Current	30	Tiotropium 2.5 ug	Olodaterol 2.5 ug	No	No	0	0	No	Yes	No
130	COPD	35	0.29	6.8	69	67	2	B	M	68	Past	60	No	No	No	No	1	2	Yes	No	No
137	COPD	45	0.38	5.2	65	68	2	D	M	59	Past	70	Tiotropium 2.5 ug	Olodaterol 2.5 ug	No	No	0	0	Yes	No	Yes
142	COPD	65	0.54	11	68	63	2	B	M	68	Past	20	Tiotropium 18 ug	Salmeterol 50 ug	Fluticason 100 ug	No	0	0	Yes	No	No
145	COPD	50	0.42	10.1	67	57	2	D	F	46	Current	40	Tiotropium 2.5 ug	Olodaterol 2.5 ug	No	No	0	1	Yes	No	Yes
152	COPD	35	0.29	11.4	61	67	2	B	M	58	Current	60	Glycopyrronium 85 ug	Indacaterol 43 ug	No	No	0	1	Yes	No	No
155	COPD	40	0.33	4.8	68	80	2	B	M	54	Current	100	Tiotropium 18 ug	Formeterol 6 ug	Beclometason 100 ug	No	0	0	Yes	No	Yes
157	COPD	70	0.58	15	60	71	2	B	M	52	Past	30	Tiotropium 2.5 ug	Olodaterol 2.5 ug	No	No	0	0	Yes	No	No
160	COPD	35	0.29	46	66	70	2	B	M	77	Past	45	Tiotropium 2.5 ug	Olodaterol 2.5 ug	No	No	0	0	Yes	No	No
161	COPD	35	0.29	11	65	29	4	D	F	67	Past	20	Tiotropium 18 ug	Formeterol 9 ug	Budenosid 320 ug	No	0	1	Yes	No	No
162	COPD	35	0.29	10.1	55	73	2	D	F	53	Past	15	Tiotropium 2.5 ug	Formeterol 6 ug	No	No	0	0	Yes	No	No
164	COPD	40	0.33	11.4	56	50	2	D	M	63	Current	50	Tiotropium 2.5 ug	Olodaterol 2.5 ug	No	No	1	1	Yes	No	No
173	COPD	50	0.42	4.8	55	59	2	B	M	74	Current	50	Glycopyrronium 85 ug	Indacaterol 43 ug	No	Yes	1	1	Yes	No	No
175	COPD	40	0.33	15	66	50	2	D	M	55	Past	70	Glycopyrronium 44 ug	Formeterol 4.5 ug	Budenosid 160 ug	No	1	1	Yes	No	No
176	COPD	50	0.42	1.5	65	33	3	D	M	67	Past	60	Tiotropium 2.5 ug	Olodaterol 2.5 ug	No	No	1	1	Yes	No	Yes
185	COPD	50	0.42	21.5	66	49	3	B	M	63	Current	50	Tiotropium 2.5 ug	Olodaterol 2.5 ug	No	No	0	2	No	Yes	No
194	COPD	35	0.29	7.5	65	47	3	A	M	68	Current	30	No	Formeterol 6 ug	Beclometason 100 ug	No	0	0	No	Yes	No
200	COPD	25	0.21	3.2	53	29	4	D	M	63	Current	40	Glycopyrronium 85 ug	Indacaterol 43 ug	No	No	0	2	No	Yes	No
202	COPD	35	0.29	30	51	27	4	B	M	67	Past	70	Tiotropium 2.5 ug	Olodaterol 2.5 ug	No	No	0	2	No	Yes	No

Table E2

Patient ID	Diagnosis	BALF volume recovered	BALF recovery ratio	Reason for rejection	Cellularity (millions)
13	ACOS	30	0.25	diagnosis	1.35
26	ACOS	15	0.13	diagnosis	4.1
28	ACOS	25	0.21	diagnosis	22.4
107	ACOS	20	0.17	diagnosis	1
132	ACOS	40	0.33	diagnosis	2
147	ACOS	40	0.33	diagnosis	3
169	ACOS	50	0.42	diagnosis	4.8
5	Asthma	15	0.13	diagnosis	not calculated
6	Asthma	10	0.08	diagnosis	not calculated
30	Asthma	35	0.29	diagnosis	11.3
33	Asthma	25	0.21	diagnosis	15.6
37	Asthma	45	0.38	diagnosis	4.2
38	Asthma	45	0.38	diagnosis	3.1
46	Asthma	40	0.33	diagnosis	4.5
58	Asthma	20	0.17	diagnosis	0.8
65	Asthma	45	0.38	diagnosis	46
96	Asthma	50	0.42	diagnosis	5.5
98	Asthma	20	0.17	diagnosis	22.3
110	Asthma	50	0.42	diagnosis	19.5
117	Asthma	50	0.42	diagnosis	0.67
124	Asthma	50	0.42	diagnosis	18
134	Asthma	45	0.38	diagnosis	11.6
150	Asthma	45	0.38	diagnosis	0.8
153	Asthma	32	0.27	diagnosis	63
171	Asthma	25	0.21	diagnosis	30
70	Atelectasis	35	0.29	diagnosis	14.8
9	Cancer	20	0.17	diagnosis	not calculated
11	Cancer	25	0.21	diagnosis	not calculated
24	Cancer	40	0.33	diagnosis	6.5
62	Cancer	75	0.63	diagnosis	2.1
81	Cancer	30	0.25	diagnosis	3.3
88	Cancer	50	0.42	diagnosis	22
73	Chronic cough	40	0.33	bloody sample	18
76	Chronic cough	42	0.35	bloody sample	13.2
90	Chronic cough	42	0.35	bloody sample	0.8
106	Chronic cough	30	0.25	bloody sample	15.8
127	Chronic cough	45	0.38	low recovery ratio (less than 30%)	3.6
138	Chronic cough	27	0.23	low recovery ratio (less than 30%)	1
2	COPD	35	0.29	low recovery ratio (less than 30%)	11.8
3	COPD	5	0.04	bronchial lavage	9.2
4	COPD	5	0.04	low recovery ratio (less than 30%)	11.6
7	COPD	10	0.08	low recovery ratio (less than 30%)	not calculated
10	COPD	5	0.04	low recovery ratio (less than 30%)	not calculated
14	COPD	25	0.21	low recovery ratio (less than 30%)	1.56
15	COPD	15	0.13	low recovery ratio (less than 30%)	not calculated
17	COPD	20	0.17	low recovery ratio (less than 30%)	1.4
20	COPD	75	0.63	bloody sample	120
23	COPD	42	0.35	bloody sample	8.4
25	COPD	15	0.13	low recovery ratio (less than 30%)	2
29	COPD	40	0.33	presence of mucus	not calculated
31	COPD	15	0.13	low recovery ratio (less than 30%)	5.6
34	COPD	20	0.17	low recovery ratio (less than 30%)	not calculated
41	COPD	15	0.13	low recovery ratio (less than 30%)	2.1
42	COPD	35	0.29	low recovery ratio (less than 30%)	26
43	COPD	30	0.25	low recovery ratio (less than 30%)	4.8
49	COPD	35	0.29	low recovery ratio (less than 30%)	not calculated
50	COPD	40	0.33	bloody sample/presence of mucus	not calculated
53	COPD	10	0.08	low recovery ratio (less than 30%)	not calculated
55	COPD	35	0.29	presence of mucus	20.4
57	COPD	25	0.21	low recovery ratio (less than 30%)	1
60	COPD	28	0.23	bloody sample	68.4
66	COPD	20	0.17	low recovery ratio (less than 30%)	not calculated
67	COPD	15	0.13	low recovery ratio (less than 30%)	not calculated
68	COPD	35	0.29	bloody sample	7
69	COPD	32	0.27	bloody sample	12.6
71	COPD	40	0.33	presence of mucus	not calculated
75	COPD	30	0.25	low recovery ratio (less than 30%)	0.7
84	COPD	35	0.29	bloody sample	21
85	COPD	45	0.38	presence of mucus	0.5
86	COPD	0	0.00	low recovery ratio (less than 30%)	not calculated
89	COPD	25	0.21	low recovery ratio (less than 30%)	0.2
92	COPD	25	0.21	low recovery ratio (less than 30%)	1
93	COPD	15	0.13	low recovery ratio (less than 30%)	1.1
95	COPD	17	0.14	bloody sample/presence of mucus	13.9
97	COPD	22	0.18	bloody sample	16.5
99	COPD	25	0.21	bloody sample/presence of mucus	13.6
100	COPD	60	0.50	bloody sample	10.2
101	COPD	30	0.25	presence of mucus	0.72
102	COPD	27	0.23	bloody	56.4
104	COPD	45	0.38	bloody sample/presence of mucus	14.4
108	COPD	20	0.17	presence of mucus	1
109	COPD	20	0.17	bloody sample	1
119	COPD	22	0.18	presence of mucus	0.2
125	COPD	40	0.33	low recovery ratio (less than 30%)	20.3
126	COPD	20	0.17	presence of mucus	0.09
129	COPD	10	0.08	low recovery ratio (less than 30%)	not calculated
136	COPD	15	0.13	low recovery ratio (less than 30%)	0.2
140	COPD	37	0.31	bloody sample	30
143	COPD	30	0.25	presence of mucus	not calculated
144	COPD	35	0.29	presence of mucus	0.3
151	COPD	12.5	0.10	low recovery ratio (less than 30%)	not calculated
154	COPD	30	0.25	presence of mucus	not calculated
156	COPD	40	0.33	presence of mucus	3.3
158	COPD	32	0.27	low recovery ratio (less than 30%)	3.5
163	COPD	20	0.17	presence of mucus	4.2
165	COPD	30	0.25	bloody sample/presence of mucus	54
166	COPD	25	0.21	low recovery ratio (less than 30%)	not calculated
168	COPD	10	0.08	low recovery ratio (less than 30%)	10.1
170	COPD	50	0.42	bloody sample	not calculated
174	COPD	25	0.21	low recovery ratio (less than 30%)	2.2
131	Fibrosis	20	0.17	diagnosis	not calculated
87	Idiopathic immunodeficiency	50	0.42	diagnosis	0.5
148	NSIP	40	0.33	diagnosis	not calculated
19	Pneumonia	30	0.25	diagnosis	12.3
118	Sarcoidosis	45	0.38	diagnosis	4.44
159	Sarcoidosis	40	0.33	diagnosis	not calculated

Table E4

RRID	Antigen	Fluorochrome	Clone	Volume (ul)	Laser	Detector	Catalog number	Company
AB_439781	CD3	PE/Cy7	UCHT1	3	488 nm	780/60	300420	Biolegend
AB_396815	CD3	Alexa Fluor 647	UCHT1	5	633 nm	660/20	557706	BD Biosciences
AB_893322	CD4	PerCP/Cy5.5	RPA-T4	3	488 nm	695/40	300530	Biolegend
AB_2564510	CD8	BV650	SK1	3	405 nm	655/15	344730	Biolegend
AB_314174	CD11c	FITC	3.9	5	488 nm	530/30	301604	Biolegend
AB_830693	CD14	APC/Cy7	HCD14	3	633 nm	780/60	325620	Biolegend
AB_395798	CD14	FITC	M5E2	5	488 nm	530/30	555397	BD Biosciences
AB_2561354	CD16	BV605	3G8	2	405 nm	610/20	302039	Biolegend
AB_314248	CD19	APC/Cy7	HIB19	5	633 nm	780/60	302218	Biolegend
AB_314242	CD19	APC	HIB19	5	633 nm	660/20	302212	Biolegend
AB_395992	CD33	FITC	HIM3-4	3	488 nm	530/30	555626	BD Biosciences
AB_2563466	CD45	BV711	HI30	3	405 nm	785/60	304050	Biolegend
AB_396820	CD56	Alexa Fluor 647	B159	5	633 nm	660/20	557711	BD Biosciences
AB_2732786	CD56	BV510	NCAM16.2	5	405 nm	510/50	563041	BD Biosciences
AB_314496	CD66b	FITC	G10F5	3	488 nm	530/30	305104	Biolegend
AB_2572566	CD66b	PE	G10F5	2	488 nm	585/42	12-0666-41	Thermo Fisher Scientific
AB_11154222	CD117	BV421	YB5.B8	5	405 nm	450/40	562434	BD Biosciences
AB_314580	CD123	FITC	6H6	5	488 nm	530/30	306006	Biolegend
AB_2296056	CD127	PE	HIL-7R-M21	5	488 nm	585/42	557938	BD Biosciences
AB_2566234	CD203c	PE/Dazzle	NP4D6	5	488 nm	616/23	324623	Biolegend
AB_11203707	CD294	APC	BM16	7	633 nm	660/20	350110	Biolegend
AB_2571902	FcεRI	Alexa Fluor 700	AER-37	5	633 nm	730/45	334630	Biolegend
AB_2629719	Siglec-8	PE/Cy7	7C9	6.5	488 nm	780/60	347111	Biolegend
AB_893567	HLA-DR	PerCP/Cy5.5	L243	3	488 nm	695/40	307630	Biolegend

Cell type	Expressed markers
AMs	$CD45^{+}HLA\text{-}DR^{+}CD66b^{-}Autofluoresence^{+}$
Neutrophils	$CD45^{+}HLA\text{-}DR^{-}CD66b^{+}CD16^{+}Siglec\text{-}8^{-}$
Monocytes	$CD45^{+}HLA\text{-}DR^{+}CD66b^{-}CD14^{+}Autofluorescence^{lo}$
DCs	$CD45^{+}HLA\text{-}DR^{+}CD66b^{-}CD14^{-}Autofluorescence^{lo}CD117^{-}$
Eosinophils	$CD45^{+}HLA\text{-}DR^{-}CD66b^{+}CD16^{-}Siglec\text{-}8^{+}$
Mast cells	$CD45^{+}HLA\text{-}DR^{+}CD66b^{-}CD14^{-}$ $Autofluorescence^{lo}Fc\varepsilon RI^{+}CD117^{+}CD203c^{+}$
$CD4^{+}$ T cells	$CD45^{+}CD3^{+}CD4^{+}CD8^{-}$
$CD8^{+}$ T cells	$CD45^{+}CD3^{+}CD4^{-}CD8^{+}$
Double positive T cells	$CD45^{+}CD3^{+}CD4^{+}CD8^{+}$
Double negative T cells	$CD45^{+}CD3^{+}CD4^{-}CD8^{-}$
B cells	$CD45^{+}CD19^{+}$
NK cells	$CD45^{+}CD3^{-}CD19^{-}CD56^{+}$
ILC1s	$CD45^{+}CD56^{-}CD127^{+}CD117^{-}CRTH2^{-}$
ILC2s	$CD45^{+}CD56^{-}CD127^{+}CD117^{-}CRTH2^{+}$
ILC3s	$CD45^{+}CD56^{-}CD127^{+}CD117^{+}CRTH2^{-}$

Table E5

Table E6

Name	Class	Sample	Internal Standard	chemsc	C	db	mass	error	ISpmol	INT:Blank.mzML	INT:C079.mzML	INT:C080.mzML	INT:C081.mzML	INT:C083.mzML	INT:C084.mzML	INT:C103.mzML	INT:C105.mzML	INT:C123.mzML	INT:C135.mzML	INT:C137.mzML	INT:C141.mzML	INT:C145.mzML	INT:C149.mzML	INT:C155.mzML	INT:C176.mzML
###	CE																								
CE(16:1)	CE	1	0	H78 C43 O2 N1	16	1	640.6029	0.36 ppm	111.6	43726.1	61038.2	24052.7	30729.8	47575.5	77292.9	62075.6	229237.3	27220.4	105033.6	442100.2	73326.7	133971.1	51790	106263	103030.4
CE(16:0)	CE	1	0	H80 C43 O2 N1	16	0	642.6184	0.14 ppm	111.6	13514	86151.4	27509.2	1560334.1	60952.3	69716	97584.8	369087.5	37803.2	169222.9	727968.3	90248.8	255521	90381.9	174262.6	142101
CE(18:3)	CE	1	0	H78 C45 O2 N1	18	3	664.602	-1.01 ppm	111.6	2072	12270.2	4817.3	3259.2	11647.1	10585.5	10223.3	12241.9	4409	15846.2	82857.2	7931.7	22633.4	9461	14979.6	13473
CE(18:2)	CE	1	0	H80 C45 O2 N1	18	2	666.6181	-0.46 ppm	111.6	44555.6	99338.8	42048	34804.3	99512	98842.2	88811.6	191723.6	43051.7	186654.6	720152.8	101974.3	236647.9	116769	153555.1	136597.8
CE(18:1)	CE	1	0	H82 C45 O2 N1	18	1	668.6338	-0.38 ppm	111.6	75248.1	267185	105359	164901	259533.6	356149.8	238967.1	1497166.6	120531.1	811245.1	1758113.8	248652.4	671958.6	224559.9	435726	530888
CE(18:0)	CE	1	0	H84 C45 O2 N1	18	0	670.65	0.53 ppm	111.6	9506	19732.1	7498.2	8731.4	14684.5	17440.4	22067.6	89058.3	8416.2	52988.1	172110.8	21402.5	65886.2	20962.4	47674.4	30077.8
CE(20:4)	CE	1	0	H80 C47 O2 N1	20	4	690.6169	-2.18 ppm	111.6	0	99688	55835.9	54748.8	176588.8	141685.6	59924.7	411413.9	97487	162371.6	638114	62329.5	212519.1	59485.3	163119	149480.2
CE(20:3)	CE	1	0	H82 C47 O2 N1	20	3	692.633	-1.43 ppm	111.6	1998.1	25063.3	17490.3	24729.2	51363.8	55971.5	14742.2	215606.3	51132.8	94473.7	158255.2	14857.4	73806.3	13468.1	48181.5	74849.8
CE(20:2)	CE	1	0	H84 C47 O2 N1	20	2	694.6489	-1.06 ppm	111.6	3520.2	5270.3	3314.6	6173.4	10876.7	11127.8	3871.7	60024.1	9126.6	35725.1	23170	4250.5	10566.7	2561.3	8438.7	18279.2
CE(20:1)	CE	1	0	H86 C47 O2 N1	20	1	696.6638	-2.21 ppm	111.6	6351.6	9594.4	5489.4	7020.1	8631.7	10501.1	7347.3	63589.8	9384.8	45824.6	38168.4	10164	13252.1	8605.1	12141.2	16281
CE(22:2)	CE	1	0	H88 C49 O2 N1	22	2	722.6792	-2.49 ppm	111.6	0	3775.1	1519.3	0	5455.8	1899.5	2203	10771.1	2665.4	5318	8842.1	2155.9	3450.2	1303.1	2085.6	2679.4
CE(22:1)	CE	1	0	H90 C49 O2 N1	22	1	724.6959	-1.03 ppm	111.6	1345.4	1813.9	2183.3	3674.9	5178.8	7079.8	2378.6	22954.5	3656.3	12409.1	7444	3486.4	4247.2	1424.2	4005.8	7615.1
CE(22:0)	CE	1	0	H92 C49 O2 N1	22	0	726.7125	0.38 ppm	111.6	3163.3	1245.6	0	4959.5	3428	2777.1	2153.2	7344.8	3747.4	6567.7	8611.3	4815.2	5428.4	2922.1	5686.9	6822.4
CE(24:1)	CE	1	0	H94 C51 O2 N1	24	1	752.7271	-1.03 ppm	111.6	2993.9	1584.7	3133.6	4996.4	4923.8	7746	2554.8	53098	6403	16774.5	9592.8	4897.3	6919.9	3458.6	6039.4	13562
###	CE_IS																								
CE(17:1)	CE_IS	0	1	H80 C44 O2 N1	17	1	654.6188	0.62 ppm	111.6	87997.9	353031.5	328772.6	407443.2	243978.2	320113.9	779278.1	996635.6	1452203.1	1237946.4	1607094.1	1349853.7	1598662	1524180.2	1182471.4	1097669.5
###	Cer																								
Cer(d18:1/14:0)	Cer	1	0	H64 C32 O3 N1	14	0	510.4883	0.55 ppm	32.2	0	0	906.5	877.3	830.4	750.2	1963.6	1434.3	2465.2	1488.7	1200.5	0	1528.6	1917.7	2146.4	1669.7
Cer(d18:1/16:0)	Cer	1	0	H68 C34 O3 N1	16	0	538.5197	0.58 ppm	32.2	2242.3	57103.6	64601.7	47708.6	75301.1	38865.1	68467.1	98356.6	108482.9	106530.9	55254.4	49514.2	65101.4	103322.7	90835.6	84620.7
Cer(d18:1/18:1)	Cer	1	0	H70 C36 O3 N1	18	1	564.5348	-0.39 ppm	32.2	0	1718.4	1400.8	1579.6	0	0	0	1142	2021.1	3784.7	1150.1	1533.2	1480	2911.1	2168.2	1651.4
Cer(d18:1/18:0)	Cer	1	0	H72 C36 O3 N1	18	0	566.5507	-0.01 ppm	32.2	1178.8	3144.3	2680.6	2929.5	1434.7	1072.6	1914.5	3374.9	3084.1	5652.7	3084.9	3319.8	2855.2	3865	3821.1	4173.1
Cer(d18:1/20:0)	Cer	1	0	H76 C38 O3 N1	20	0	594.5813	-1.09 ppm	32.2	0	0	1184.7	1160.4	0	0	1362.3	1615.5	2534.6	1772	1209.4	1447.8	1824.1	2166.2	1785.8	1464.6
Cer(d18:1/22:0)	Cer	1	0	H80 C40 O3 N1	22	0	622.6133	0.01 ppm	32.2	0	7995.9	10308.4	13517.1	8609.5	5042.2	11067.4	13706	18524.9	16057.1	9246.5	10563.6	10734.9	19506.2	12434.5	13082.7
Cer(d18:1/24:1)	Cer	1	0	H82 C42 O3 N1	24	1	648.6287	-0.36 ppm	32.2	1506.7	46922	38529.8	61946.3	59130.5	29084.9	43434.9	99207.4	87117.8	82444	68085.9	60780.3	37469.8	114286.5	87044.4	90046.3
Cer(d18:1/24:0)	Cer	1	0	H84 C42 O3 N1	24	0	650.6448	0.41 ppm	32.2	3815.3	47787.7	50451.4	81550.8	51144.8	30673.4	43816.8	63007.8	131248.1	87136	77897.2	70957.3	70390.1	166490.6	66736.3	85563.4
###	Cer_IS																								
Cer(d18:1/17:0)	Cer_IS	0	1	H70 C35 O3 N1	17	0	552.5357	1.21 ppm	32.2	822089	530232.7	482047.4	589318.6	386563.1	397177.4	690326.2	761366.9	949451.2	946663.6	908744.7	809667.8	985108.3	906907.1	850775.8	768277.5
###	DAG																								
DAG(32:0)	DAG	1	0	H72 C35 O5 N1	32	0	586.5405	-0.05 ppm	64.3	56674.2	38695.3	28745.2	41416.6	26423.7	339412.6	382215.9	132837	107069.7	183158.6	213357.9	96360.3	128103.8	68855.6	52110	104667.3
DAG(34:0)	DAG	1	0	H76 C37 O5 N1	34	0	614.5721	0.54 ppm	64.3	62508	41792.6	28644.7	66727.2	25758.2	756432.6	774322.4	242361.5	180545.7	270318.8	380505.9	131702	178200.8	111297.9	60854.9	198866.5
DAG(36:0)	DAG	1	0	H80 C39 O5 N1	36	0	642.6035	0.56 ppm	64.3	46697.5	20024.3	14375.5	52357.3	17071.7	435750.9	496457.1	147854	95554.8	135185.2	214718.8	66411.8	113023.2	64366.7	39476	129753.2
###	DAG_IS																								
DAG-IS(31:1)	DAG_IS	0	1	H68 C34 O5 N1	31	1	570.5098	1.09 ppm	64.3	1183199.8	640651.7	691703.3	784398.2	516612.9	533265.4	754573.9	1143552.2	1445576.7	1434441.9	1566849.5	1295282.8	1392331.5	1333812.5	1299625.4	960829.8
###	DiHexCer																								
DiHexCer(d18:1/16	DiHexCer	1	0	H88 C46 O13 N1	16	0	862.6231	-2.17 ppm	55.2	0	10001.1	9665.8	4971.2	5355.2	10115.3	8886.8	9122.3	14685.6	22674.6	10328.4	15022.2	18736.2	22278.9	17238.1	31041
DiHexCer(d18:1/24	DiHexCer	1	0	H102 C54 O13 N	24	1	972.7349	0.29 ppm	55.2	0	10742.6	7996.5	7485	3903.8	13269.6	8844.2	11312.9	24024.7	37217.1	12044.8	16905.1	14760.3	30949.6	16383.1	35282.6
DiHexCer(d18:1/24	DiHexCer	1	0	H104 C54 O13 N	24	0	974.751	0.77 ppm	55.2	0	8402.5	8595	8942.6	4483.5	10094	8886.4	6995.2	23967.8	35455.5	10799.4	14508.9	20837.9	34995	13228	27055.5
###	DiHexCer_IS																								
HexCer(d18:1/12:0	DiHexCer_IS	0	1	H70 C36 O8 N1	12	0	644.51	0.66 ppm	55.2	1103774	703291.6	731974.9	784093.3	586460.4	546273.1	915868.3	1075647.9	1208610.7	1199692.3	1365235.7	1260860.2	1220099.9	1303375.1	1093301.2	915034.7
###	HexCer																								
HexCer(d18:1/16:0	HexCer	1	0	H78 C40 O8 N1	16	0	700.5724	0.24 ppm	55.2	0	38811.1	20926.2	20982	13392.7	24599.7	42873.8	30403.6	40182	100231.6	15880.7	23314.4	26697.9	28157.2	30244.8	27605.3
HexCer(d18:1/18:0	HexCer	1	0	H82 C42 O8 N1	18	0	728.602	-2.05 ppm	55.2	0	5576.4	1696.7	1269.4	1152.5	1165.7	1738.9	3224.9	2146.2	3228.2	1793.2	1470.8	0	7813.9	3645.8	3787.1
HexCer(d18:1/22:0	HexCer	1	0	H90 C46 O8 N1	22	0	784.6642	-2.46 ppm	55.2	0	36131.5	20754	21554.5	9352.6	9269.7	28803.5	18243	25435.2	54658.6	12759.2	17071.1	17251.4	16790.1	15950	17453.9
HexCer(d18:1/24:1	HexCer	1	0	H92 C48 O8 N1	24	1	810.6791	-3.29 ppm	55.2	0	54065.7	29801.8	40937	15144	28100.6	61493.5	53628.3	56029.1	123733.6	30648.5	32636.9	22699.7	36391.1	40253.4	48468.7
HexCer(d18:1/24:0	HexCer	1	0	H94 C48 O8 N1	24	0	812.6961	-1.59 ppm	55.2	0	64327.9	37351.6	52082.9	25654.7	34987.2	86369.2	39657.3	69019.2	120865.8	35026	40058.3	63005.7	55652.7	39827.4	47410.4
###	HexCer_IS																								
HexCer(d18:1/12:0	HexCer_IS	0	1	H70 C36 O8 N1	12	0	644.51	0.66 ppm	55.2	1103774	703291.6	731974.9	784093.3	586460.4	546273.1	915868.3	1075647.9	1208610.7	1199692.3	1365235.7	1260860.2	1220099.9	1303375.1	1093301.2	915034.7
###	LPC																								
LPC(16:2)	LPC	1	0	H47 C24 N1 O7	16	2	492.3076	-1.79 ppm	35	2133.4	3635.1	2464.4	3689.9	2304.8	2126.2	5764.1	4884.3	5142.6	8441.7	3856	6606.7	5879.2	7238.5	5243.3	20578.8
LPC(16:1)	LPC	1	0	H49 C24 N1 O7	16	1	494.3243	0.42 ppm	35	2826.1	47797.3	19908.6	15230.7	31498.5	25657.4	28307.9	47407.7	16859.6	27940	33415	27626.1	48305.4	23490.5	33259.3	38817
LPC(16:0)	LPC	1	0	H51 C24 N1 O7	16	0	496.3402	0.82 ppm	35	37034.3	1442717.4	219689.6	270701.6	559598.2	560068.3	282424.2	316597	237591.4	665129.2	348976.2	340218.8	507978.5	250089.5	320354.1	1474576.4
LPC(18:3)	LPC	1	0	H49 C26 N1 O7	18	3	518.3227	-2.80 ppm	35	1208.5	4439.9	1848.8	2484.2	2635	1416.8	6264.9	5138.2	4429.8	2647.3	3334.4	2120.1	3507.5	3203.6	3915.7	16935.5
LPC(18:1)	LPC	1	0	H53 C26 N1 O7	18	1	522.3527	-5.27 ppm	35	7749.3	223636.6	90917.7	92028.1	184651	112549.5	161365.5	176376.5	87708.3	136861.4	304374.6	188045	295463.9	104579.9	134917.6	100651.6
LPC(18:0)	LPC	1	0	H55 C26 N1 O7	18	0	524.3718	1.35 ppm	35	12053.2	234481.7	81396.2	125492.4	165272	99370	141177.8	108471.6	135911.4	176304.6	261187.3	137565.5	216162	90061.3	105271.1	486526.8
LPC(20:6)	LPC	1	0	H47 C28 N1 O7	20	6	540.3063	-3.95 ppm	35	0	2327.8	0	0	0	0	3680.3	3131.3	3264.2	3471.6	1741.5	1505.4	2689.4	4352	5738.4	39283.6
LPC(20:5)	LPC	1	0	H49 C28 N1 O7	20	5	542.3232	-1.75 ppm	35	1302.8	6224.7	5115.6	4912.6	6677.2	4393	9056	10671.9	3294.2	7967.3	13839.9	7318.8	12133.4	9444.1	7923.7	23130.5
LPC(20:4)	LPC	1	0	H51 C28 N1 O7	20	4	544.3385	-2.24 ppm	35	7046.1	91548.2	93943.7	82579.9	102967.8	54044.5	96462.1	149367.6	70498.5	60858	108264.5	61914.5	122043.3	71056.3	45705.9	57584.8
LPC(20:3)	LPC	1	0	H53 C28 N1 O7	20	3	546.353	-4.34 ppm	35	1980.8	21732.5	12814.4	11390.4	23072.5	13367.6	23283.1	20147.9	17998.6	18689.3	41118.5	21899.3	44154.4	19422.1	16326.5	28136.4
LPC(20:1)	LPC	1	0	H57 C28 N1 O7	20	1	550.3865	-0.35 ppm	35	1489.7	26170.1	25020.9	26346.8	13722.4	9235.3	33722.2	50009.8	14114.8	25163.1	25523.8	15097.7	18570.2	15521.4	14267.3	41082.2
LPC(20:0)	LPC	1	0	H59 C28 N1 O7	20	0	552.4022	-0.37 ppm	35	1104	6133.6	3053.3	3781	4378.8	1954	7581.4	7697	3979	8193	7880.5	3465	5175.4	5068.7	10895.7	41644.5
LPC(22:6)	LPC	1	0	H51 C30 N1 O7	22	6	568.3406	1.55 ppm	35	1783.9	15226.7	12755.2	9883.7	31914	14608.5	24332.7	21812	4438.1	22541.6	61105.8	25315.7	63199.5	18031.2	28670.5	45444.9
LPC(22:5)	LPC	1	0	H53 C30 N1 O7	22	5	570.3554	0.03 ppm	35	2343.8	22885.5	21207.9	17246.7	37035.8	18244.2	28679.5	26751	9978.2	28649.8	65066.7	24705.3	67432.7	23336.6	26271.9	34490.8
LPC(22:4)	LPC	1	0	H55 C30 N1 O7	22	4	572.3692	-3.31 ppm	35	2858.4	94348.5	134009.3	155688.9	132233.2	52001.3	108509.9	171358.6	124120.4	106894.9	75001	58208	69520.2	91652.8	56925.6	106457.3
LPC(22:3)	LPC	1	0	H57 C30 N1 O7	22	3	574.3837	-5.31 ppm	35	1370.9	12543	11513.2	12346.8	9474.8	6331.6	14625.4	15580.8	13879.9	11386.5	9769.8	7250.7	10082.1	13978.3	9813.5	30362.5
LPC(22:1)	LPC	1	0	H61 C30 N1 O7	22	1	578.4175	-0.90 ppm	35	6961.1	14023.1	7992.7	8379.3	7061.2	5714.8	15136.3	17430.6	7732.4	8577.8	6300.3	4583.4	7031.2	10624.7	8265.8	24325.7
LPC(22:0)	LPC	1	0	H63 C30 N1 O7	22	0	580.433	-1.20 ppm	35	5127.1	20945.5	6990.3	14004.1	11129.4	6617.6	25108	27686.7	9781.9	13335.9	10758.7	7967.7	11283.6	13232.1	11820.5	48786.7
###	LPC_IS																								
LPC(17:1)	LPC_IS	0	1	H51 C25 P1 O7	17	1	508.3409	2.23 ppm	35	443106.1	779957.4	798291.1	967816.9	664500.4	648805.8	898014.6	1048180.1	1135345.1	1148737.1	1315640.3	1181621.3	1150478.3	1266295.7	1170403	1125285.8
###	LPCO																								
LPC-O(14:0)	LPCO	1	0	H47 C22 N1 O6	14	0	452.3131	-1.08 ppm	35	0	2472.5	897.6	1041	0	0	8958.7	2881.8	3083.9	4114.4	1463.3	1571.6	2953.5	4538.6	4786.8	16940.8
LPC-O(16:1)	LPCO	1	0	H49 C24 N1 O6	16	1	478.3293	0.11 ppm	35	0	4711.6	1136.9	1400.2	710.6	0	4177.7	2479.2	4537.9	7195.9	2992.1	3798.6	3446.2	9432.8	3634.7	19493.1
LPC-O(16:0)	LPCO	1	0	H51 C24 N1 O6	16	0	480.3449	0.10 ppm	35	3274.1	23121.5	13792.4	9012.4	6223.5	4999.1	15536.5	16502.2	20572	29009.9	7890.2	5647.3	11413.8	21398.4	10653.6	40050.5
LPC-O(18:1)	LPCO	1	0	H53 C26 N1 O6	18	1	506.3613	1.56 ppm	35	0	3428.9	1815.1	2063.5	1283.5	871.4	4397.8	4816.3	5975.6	6394.1	3260.7	3264.9	3059.1	6890.5	5235.3	22283.5
###	LPCO_IS																								
LPC(17:1) b	LPCO_IS	0	1	H51 C25 P1 O7	17	1	508.3409	2.23 ppm	35	443106.1	779957.4	798291.1	967816.9	664500.4	648805.8	898014.6	1048180.1	1135345.1	1148737.1	1315640.3	1181621.3	1150478.3	1266295.7	1170403	1125285.8
###	MAG																								
MAG(16:0)	MAG	1	0	H42 C19 O4 N1	16	0	348.3105	-0.94 ppm	104	184647.6	400425.6	471172.2	67181.2	41194.3	576562.9	939762.1	364846.6	231333.5	389699.7	428767.2	297037.8	222838.7	153544.7	103449.1	189346.4
MAG(18:0)	MAG	1	0	H46 C21 O4 N1	18	0	376.3418	-0.96 ppm	104	143635.6	292036.2	377460.3	64276.2	35676.1	790141.9	1167658.9	404981.4	293925.1	391451.9	503878.3	352575.9	278358.4	166838.1	92137.4	216731.7
###	MAG_IS																								
MAG(17:1)	MAG_IS	0	1	H42 C20 O4 N1	17	1	360.3104	-1.10 ppm	104	187213.7	108589.4	102518.1	111698.6	85784.8	89018.3	173165.7	196859.5	521201.9	457387.5	521081.8	429901.6	463270.7	495939.5	430409.2	374256.1
###	PC																								
PC(30:1)	PC	1	0	H75 C38 N1 O8	30	1	704.5225	0.07 ppm	396.2	94763	58195.9	62333	107142.1	84112.7	37966.7	79398.2	59930.1	47099.3	45499.8	21610.3	25574	28676.1	63035.8	31658	32989.9
PC(30:0)	PC	1	0	H77 C38 N1 O8	30	0	706.5381	-0.06 ppm	396.2	59203.9	2995482.8	1180492.3	1718916.8	2453130.5	1347287.7	889366.8	858883.5	768737.6	1937905.8	504276.5	604352.7	376359.1	810864.5	725599.5	693045.2
PC(32:3)	PC	1	0	H75 C40 N1 O8	32	3	728.5189	-4.91 ppm	396.2	11971.7	225418.4	60246.8	90756.2	121694.8	96637.9	161408.8	105819	95661.2	92731	37136.4	34683.6	17477.8	68181.7	81736.4	169998.1
PC(32:2)	PC	1	0	H77 C40 N1 O8	32	2	730.537	-1.52 ppm	396.2	23913.1	103473.2	106323.1	142599.3	126670.6	66127.5	100558.4	127769.8	111377.3	89343.1	68576.1	58172.9	52762.7	135916.6	116786.7	83917.1
PC(32:1)	PC	1	0	H79 C40 N1 O8	32	1	732.5529	-1.23 ppm	396.2	126910.7	3054471.3	1815699.2	2374054.7	2382761.7	1886606.2	930016.2	1589414.2	954982.9	1235899.4	733059.7	1254173.1	510529.4	1772269.4	1166360	837946
PC(32:0)	PC	1	0	H81 C40 N1 O8	32	0	734.5682	-1.65 ppm	396.2	382935	20200598.2	7537844.9	6243347.6	18176313.8	7061428.1	3873032.6	3965045.2	3267678.9	7160417.1	3532169.1	3223184.5	1920585	3818184	3671580	4495011.1
PC(34:4)	PC	1	0	H77 C42 N1 O8	34	4	754.5351	-3.97 ppm	396.2	26831.2	223735.1	107868.9	161748.5	136576.7	140976.1	183169.5	312327.3	136192	88358.1	59630.8	95424.8	44123.5	157590.8	111600.1	204110.5
PC(34:3)	PC	1	0	H79 C42 N1 O8	34	3	756.5505	-4.32 ppm	396.2	39426	1621372.8	482271.4	560307.4	779317.4	718506.8	835100.8	777967.9	505764.2	600540.1	300855.6	255180.3	214425.2	455903.6	357658.8	939379.9
PC(34:2)	PC	1	0	H81 C42 N1 O8	34	2	758.5682	-1.58 ppm	396.2	123171.2	3792175.3	2389498.6	3825474.1	3206579.5	1748870	1264920.9	1240462.5	1510854.7	2550213.7	1353868.6	1167600.5	612907.1	1685723.2	1204831.5	1465554.6
PC(34:1)	PC	1	0	H83 C42 N1 O8	34	1	760.5835	-2.05 ppm	396.2	210409.9	8377264.1	7994422.3	10795843.4	6372420.8	5709126.9	3966469.9	5620289.3	3836807.3	6032471.3	4137171.7	3270706.1	1604220.8	5245712.5	4081377.3	2975422.3
PC(36:5)	PC	1	0	H79 C44 N1 O8	36	5	780.5511	-3.46 ppm	396.2	14950.9	416517.3	287950.4	422748.2	443620.4	290262.8	251816	357499.9	341059.4	327444.8	193080.6	151285.1	96920.8	405701.1	168364.7	396696.8
PC(36:4)	PC	1	0	H81 C44 N1 O8	36	4	782.5672	-2.83 ppm	396.2	52235.1	3131507.9	2488642.5	4372170.6	5503179.9	2935413.4	1177718.3	1787921.8	2054615	1823286	1291281.9	1280611.2	684967.1	2532112.6	1412675.2	1738095.6
PC(36:3)	PC	1	0	H83 C44 N1 O8	36	3	784.5831	-2.56 ppm	396.2	31184.8	1531928.2	1100035	1772026.4	2080323.5	1112153.1	624518.9	723607.6	964456.5	1045916	761350.7	600373.8	390082.9	1268254.2	831060.8	771191.2
PC(36:2)	PC	1	0	H85 C44 N1 O8	36	2	786.5991	-2.10 ppm	396.2	56660.8	2163868	1975878.4	2220701.4	1639472.2	1351784.5	1075028.5	1360594.5	1111428.6	1442150	1115602.5	716009.3	585250.5	1733160.3	1325999.1	806209.9
PC(36:1)	PC	1	0	H87 C44 N1 O8	36	1	788.6144	-2.52 ppm	396.2	1024125.1	1593886.9	1168584.4	1471065.7	1174253.6	878054.7	659694.3	494660	615921.9	956971.4	633107.9	575888.7	403731	842964.7	724909	423173.7
PC(38:7)	PC	1	0	H79 C46 N1 O8	38	7	804.5519	-2.37 ppm	396.2	12126.7	151774.7	98960.4	173572.1	184205.9	101057.6	80068.7	115633.1	244887.3	56028.8	0	42426.6	0	131062.5	64481.7	181798.5
PC(38:6)	PC	1	0	H81 C46 N1 O8	38	6	806.5696	0.23 ppm	396.2	15342.2	322790.2	218734.6	292058.8	395925.4	221485.4	147530.5	88875.5	196707.6	214496.5	227763.9	91956.7	70889.2	249785.1	124356.8	199509
PC(38:5)	PC	1	0	H83 C46 N1 O8	38	5	808.5873	2.77 ppm	396.2	21031.1	660085.6	492368.3	927441.7	1102396.6	679720.9	437672.8	498860.6	587805	540116	469595.6	250725.7	207825.8	668908.2	467857.6	392527
PC(38:4)	PC	1	0	H85 C46 N1 O8	38	4	810.6002	-0.67 ppm	396.2	20501.2	1058612.9	749101.5	1317524.8	1967854.5	642374.5	372565.9	405138.9	712436.1	611518.2	588028.8	331034.4	263615.5	839380.2	558389.2	450253.2
PC(38:3)	PC	1	0	H87 C46 N1 O8	38	3	812.6157	-0.87 ppm	396.2	15213.1	306336.5	260393.3	263292.3	440302	212695.1	100259.9	122915.2	187357.4	217627.4	316323	119017.4	118420.5	275341.9	214835.4	131650.7
PC(38:2)	PC	1	0	H89 C46 N1 O8	38	2	814.6318	-0.33 ppm	396.2	48541.3	121070.6	96154.2	77629.2	113895.5	83323.1	54093.5	65900.6	0	127250.3	72939.7	41892.9	31477.8	71098.5	106632.1	55087.4
PC(38:1)	PC	1	0	H91 C46 N1 O8	38	1	816.6475	-0.22 ppm	396.2	33745.7	96908.4	71781.1	61393	73114.3	94448.4	44013.2	28111.5	61596.6	68531.9	32794.8	57586.6	39140.7	26862.8	25114	12419.2
PC(40:6)	PC	1	0	H85 C48 N1 O8	40	6	834.5998	-1.14 ppm	396.2	25878.4	198514.5	127163	99971.9	282199.1	165023.5	63652.5	32930.8	288965.5	87496.1	246786.5	82174	107406.4	83359.3	56213.2	43215.6
PC(40:5)	PC	1	0	H87 C48 N1 O8	40	5	836.6155	-1.04 ppm	396.2	13209	214444.9	131296	105460.4	262537.4	154619.9	74609.6	76359.6	86264.3	102720	260422.3	62723.7	83326.5	90159.7	122694.4	58194.6
PC(40:4)	PC	1	0	H89 C48 N1 O8	40	4	838.6313	-0.90 ppm	396.2	11929.5	75535.1	64411.8	66159.3	108539.9	53747.7	50228.5	45103.7	61302	51137.1	76733.8	31703.3	40374	61318.8	75658.4	32181.7
PC(40:3)	PC	1	0	H91 C48 N1 O8	40	3	840.6468	-1.02 ppm	396.2	12666.9	18197.4	16953.8	17044.1	21824	16707.2	25332.6	22635.8	19704.3	14725.5	16586.7	12982.6	12685.8	23909.1	30902.3	9494.2
PC(40:2)	PC	1	0	H93 C48 N1 O8	40	2	842.6619	-1.71 ppm	396.2	7960.6	8037	5689	9709.1	7714.9	10500.7	16752.5	14332.1	3120.8	10654.8	6628.6	7394.7	6994.3	6762.4	9383.7	2614.1
PC(40:1)	PC	1	0	H95 C48 N1 O8	40	1	844.6778	-1.44 ppm	396.2	8752.2	10244.5	5372.8	7973.3	11974.9	8773.5	25318.6	25493.5	10374.6	13644.2	11802.9	11389.4	15166	11390.3	11593.3	6424.8
PC(40:0)	PC	1	0	H97 C48 N1 O8	40	0	846.6936	-1.24 ppm	396.2	21621.5	5356.3	2089.3	2061	3389.9	1411.9	14210.3	12596	2036	3758	4378.9	3983	10485.3	3414.7	5463.5	2478.3
PC(42:4)	PC	1	0	H93 C50 N1 O8	42	4	866.6623	-1.22 ppm	396.2	4749.6	4228.1	3885.7	0	7533.7	4916.2	10607.4	4389.6	0	4674.2	0	0	3704.2	4857	9031.7	0
PC(42:3)	PC	1	0	H95 C50 N1 O8	42	3	868.6784	-0.62 ppm	396.2	5197.5	4406.4	0	3534	4563.5	6208.5	9204.6	8119.5	5989.5	2487.5	2180.7	4121.7	5923.8	7321.6	12501.8	5879.6
PC(42:2)	PC	1	0	H97 C50 N1 O8	42	2	870.6926	-2.28 ppm	396.2	5869	5120.7	3593.1	5007.4	5568.6	6405.7	27166.7	24638.1	6370.8	6820.3	10484.9	8751.4	16406.5	11381.7	10554.3	5294.2
PC(42:1)	PC	1	0	H99 C50 N1 O8	42	1	872.7089	-1.58 ppm	396.2	5151.1	10202.8	10195	14827.3	13833	13736.9	25749.4	36959	8884.9	9615.5	15281.9	9425.9	13976.8	9764.1	11270.4	4242.4
PC(42:0)	PC	1	0	H101 C50 N1 O8	42	0	874.7253	-0.69 ppm	396.2	6513.4	7074.4	4906.7	4904.8	7006.5	2490.8	20739.1	10121.8	1891.7	2005.7	0	2156.5	6357.5	4065.7	0	2161.1
###	PC_IS																								
PC(31:1)	PS_IS	0	1	H77 C39 O8 P1	31	1			396.2	29792986.6	14423523.2	18421237.5	17889448.4	15095197.3	12711736.3	13044554.5	14292859.5	9863335	10707260.7	7768271.2	10017635.1	8329867.8	10790115	8251220.2	6331385.5
###	PC-O																								
PC-O(32:1)	PC-O	1	0	H79 C40 N1 O7	32	1	716.5588	-0.07 ppm	396.2	25359.8	112161.7	116348.5	179280.9	111194.5	81988.5	75408.6	117139.8	127925.5	95086.1	72701.8	75420.3	68718.4	100200.1	59753.1	74894.3
PC-O(34:2)	PC-O	1	0	H81 C42 N1 O7	34	2	742.5728	-2.30 ppm	396.2		187258.1	239426.9	222533.6	163944.6	107293.7	249601.8	232032.8	283248.8	217370.8	124609.2	77994	156216.9	194655.4	150223.2	191399.6
PC-O(34:1)	PC-O	1	0	H83 C42 N1 O7	34	1	744.5887	-2.02 ppm	396.2	15679.3	591692.2	750283.8	846031.3	366435.8	403323.8	555780.5	609271.5	440833.6	589337.7	308741.5	305725.7	346234	308325.8	394999.7	397878.8
PC-O(34:0)	PC-O	1	0	H85 C42 N1 O7	34	0	746.6044	-1.93 ppm	396.2	54478.5	667819	549799.2	818337.8	358447.3	417039.3	614607.7	688564.8	500886.4	510102.9	377450.3	208273.4	468767.7	426989.8	543434.8	371975.2
PC-O(36:3)	PC-O	1	0	H83 C44 N1 O7	36	3	768.588	-2.77 ppm	396.2	83497.8	2996535.5	2868320.8	4671808.9	3049363.7	2421021.3	1323243.8	2443304.4	3211716.9	1733744.8	1234699.7	1001945.2	1965531.1	1534204.4	1694413	1096181.8
PC-O(36:2)	PC-O	1	0	H85 C44 N1 O7	36	2	770.6039	-2.44 ppm	396.2	60891.5	515733.9	456111.9	866112.5	516127.4	394120.4	289281.2	443870.4	581662	398053.5	236495.7	182854.2	468432.4	330183.5	461260	265337.8
PC-O(36:1)	PC-O	1	0	H87 C44 N1 O7	36	1	772.62	-1.96 ppm	396.2	28055	259677.2	251185.2	357038.1	132188.1	167268.5	188070.3	213797.2	186865.6	205363	140665.4	160403.1	123932	185002.1	136821.1	112471.3
PC-O(36:0)	PC-O	1	0	H89 C44 N1 O7	36	0	774.6355	-2.06 ppm	396.2	17864.6	59950.3	85746.8	92143.1	24122.2	27261.7	39876.4	55114.4	66660.6	57755.5	33959.2	32454.8	39356.9	47307.7	44608.4	24733.6
PC-O(38:4)	PC-O	1	0	H85 C46 N1 O7	38	4	794.6036	-2.76 ppm	396.2	43464.4	2449054.5	2701468.2	4453422.7	2679447.2	2017824.2	927745	1736834.9	2648942.7	1698936.4	1134451.2	1117248.7	1208850	2154499.1	1775520.7	1327298.5
PC-O(38:3)	PC-O	1	0	H87 C46 N1 O7	38	3	796.619	-3.06 ppm	396.2	29847.4	1075589.7	1712419.5	2221444	1388054.9	660794.5	501469.4	810409.8	1478276.5	843546.1	536356.1	515592.9	842909.6	1097169.3	975277.5	431359
PC-O(40:5)	PC-O	1	0	H87 C48 N1 O7	40	5	820.6202	-1.50 ppm	396.2	11746.3	134684.3	214114.2	222799.1	142347.8	111974.9	93833.1	180358	185149.9	154486.4	115972.7	66107.6	106517.3	132320.6	176882.3	83916.8
PC-O(40:4)	PC-O	1	0	H89 C48 N1 O7	40	4	822.6357	-1.73 ppm	396.2	8931.7	190529.7	346844.7	300196.9	201835.9	136951	153856.2	237245.7	324424.4	192674	173131.1	68899.4	205166.9	186945	264641.9	90644.5
PC-O(40:3)	PC-O	1	0	H91 C48 N1 O7	40	3	824.6519	-1.00 ppm	396.2	10885.3	81526.8	209737.1	180179.3	100605.2	58976.6	73822.5	111223.9	243975.6	87819.6	86724	47770.7	114681.4	128839.5	192745.8	41037.8
PC-O(42:6)	PC-O	1	0	H89 C50 N1 O7	42	6	846.6354	-2.00 ppm	396.2	21621.5	20137.8	21312.2	12691	13124.1	8182.5	35219.9	39943.2	61416.5	10508.4	18469.6	1486	14461.8	16467.4	14215.6	13968
PC-O(42:4)	PC-O	1	0	H93 C50 N1 O7	42	4	850.6683	-0.12 ppm	396.2	11708.7	55552.3	82139.4	64595.5	48958.7	47735.9	42974.1	75336.4	96414.9	45274.4	57873.1	26936.4	42482.7	72806.4	105431.8	52782.6
PC-O(42:3)	PC-O	1	0	H95 C50 N1 O7	42	3	852.6833	-0.87 ppm	396.2	7867.2	40243	81520.9	59512.1	41305.4	33330.6	51081.3	40191.2	189897.1	43038.8	46105.5	21461.4	56374.6	63351.3	115717.1	42487.8
PC-O(42:2)	PC-O	1	0	H97 C50 N1 O7	42	2	854.6992	-0.62 ppm	396.2	11366.3	14076.6	18379.9	15450.3	11077.4	10084.1	15659.8	4705.2	27052	8418.8	0	0	13773.9	8983.9	22240.9	6544.3
###	PC-O_IS																								
PC(31:1) b	PC-O_IS	0	1	H77 C39 O8 P1	31	1			396.2		14423523.2	18421237.5	17889448.4	15095197.3	12711736.3	13044554.5	14292859.5	9863335	10707260.7	7768271.2	10017635.1	8329867.8	10790115	8251220.2	6331385.5
###	PE																								
PE(34:3)	PE	1	0	H73 C39 N1 O8	34	3	714.5046	-3.12 ppm	210.4	0	3829.8	1302.3	1454.8	1414.8	0	4647.7	4395.4	2874.8	2424.9	2027	1311.8	2187.7	2387.3	3162.3	1908.7
PE(34:2)	PE	1	0	H75 C39 N1 O8	34	2	716.5225	0.02 ppm	210.4	7889.1	51435.2	33816.3	33960.4	25860.5	31612.1	59068	53523	33632.7	36317.1	31720.8	26602.5	33471.2	52562.4	48583.5	32397.6
PE(34:1)	PE	1	0	H77 C39 N1 O8	34	1	718.538	-0.20 ppm	210.4	3249.5	155926.8	215536.4	124574.2	73171.9	114717.5	287056.2	195194.5	121230.6	188047.9	82951.5	88282.6	156182.7	176978.1	206546.5	92581.4
PE(34:0)	PE	1	0	H79 C39 N1 O8	34	0	720.5515	-3.17 ppm	210.4	0	10783.3	12473.2	10071	7634.3	7854.7	36579.7	14874.1	13936	13990.3	9563.5	9538.7	29748.6	14312.4	28148.7	6771.1
PE(36:5)	PE	1	0	H73 C41 N1 O8	36	5	738.5042	-3.50 ppm	210.4	1215.2	7629.6	5297.5	7366.2	4832.5	5318.5	11291.6	13273	5863.1	5940.5	3387.2	2081.9	4491.4	7152.4	6443.4	4199
PE(36:4)	PE	1	0	H75 C41 N1 O8	36	4	740.5191	-4.51 ppm	210.4	1857.9	67885.1	57806.6	79309.2	63109	58356	48571.6	67953.3	80259.1	77810.5	53217.8	39230.6	65912.2	97904.1	76487.9	50601.9
PE(36:3)	PE	1	0	H77 C41 N1 O8	36	3	742.5354	-3.61 ppm	210.4	0	52783.3	22842.7	29834	30456	27244.2	46606.6	36272.2	34221.2	48990.3	30339.8	22236.7	32250.2	43687.5	55023.9	32252.2
PE(36:2)	PE	1	0	H79 C41 N1 O8	36	2	744.5525	-1.66 ppm	210.4	4151	195723.5	118441.3	156174	89020.7	93588.3	242159.8	199203	133906.9	243759.1	130398.7	114144.6	117945.2	149067.9	283478.1	126655.6
PE(36:1)	PE	1	0	H81 C41 N1 O8	36	1	746.5682	-1.62 ppm	210.4	9638.7	480419.5	477803.1	451580.1	264176.2	276900.7	508033.3	530392.8	619953	607211.7	444867.1	422801.8	284712.8	676105.1	747021.6	383623.9

PE(38:7)	PE	1	0	H73 C43 N1 O8	38	7	762.5022	-6.02 ppm	210.4	0	5420.5	4463.9	4643.9	3985.3	5443.3	5632	13332	7482.5	2628.9	1894.2	1608.5	2110.3	3778.4	3288.6	6795.1
PE(38:6)	PE	1	0	H75 C43 N1 O8	38	6	764.5182	-5.65 ppm	210.4	1244.7	19842.8	17129.4	22730.3	19247.3	21723	15848.9	25849.4	15418.4	26354.1	25450.8	12740.5	10977.9	21463.9	21296.6	20865.5
PE(38:5)	PE	1	0	H77 C43 N1 O8	38	5	766.5372	-1.18 ppm	210.4	1408.8	82581.1	59129.5	92587	90289.3	70240.6	65686	78850.8	73967.3	72322.5	63589.5	47920.1	43226.2	99150.9	75822.4	51708.5
PE(38:4)	PE	1	0	H79 C43 N1 O8	38	4	768.5525	-1.69 ppm	210.4	9459.4	485642.9	542265.3	606636.1	562147.4	415879.8	272095.1	503727.2	664652.5	540783.5	474265.9	290831.3	268531.7	487159.1	338052.9	297002.1
PE(38:3)	PE	1	0	H81 C43 N1 O8	38	3	770.5674	-2.67 ppm	210.4	0	61465.1	58028.4	77334.9	60873.5	47079.9	37246.7	66787.2	78720.2	77803.7	63965.9	54044.1	59712.9	86054.4	81292.8	54017.8
PE(38:2)	PE	1	0	H83 C43 N1 O8	38	2	772.5836	-1.85 ppm	210.4	0	11819.8	7237.7	7075.5	6066.3	8718.3	10897.5	13194.2	10236.5	17474	9668.2	12095.5	7499	13673.1	17867.7	9306
PE(38:1)	PE	1	0	H85 C43 N1 O8	38	1	774.5992	-2.04 ppm	210.4	0	9737.1	6507.6	8148.9	5544.3	6406.1	6218.9	10320.5	0	14093.6	8159.4	10013.5	7183.3	11043.6	10171.8	7506.2
PE(40:7)	PE	1	0	H77 C45 N1 O8	40	7	790.5342	-5.02 ppm	210.4	2348.7	39940.8	33627.4	46929.5	28850.2	24903.2	41280.3	73621	67528.9	27541.6	22420	11612.7	20456.2	47691.8	43157.9	61738.3
PE(40:6)	PE	1	0	H79 C45 N1 O8	40	6	792.5519	-2.41 ppm	210.4	0	21451	21860.8	24603.2	20158.4	21577.6	19827.5	30565.1	17712.9	31365.2	20752.8	16572.5	12714.6	28905.6	33292.8	25088.3
PE(40:5)	PE	1	0	H81 C45 N1 O8	40	5	794.5678	-2.06 ppm	210.4	0	31265.1	30193.5	27049.8	24112.9	29606.6	22374.5	44247.8	29098.2	28373.6	19561.6	19920.1	19776.3	34683.8	42426.8	20705.9
PE(40:4)	PE	1	0	H83 C45 N1 O8	40	4	796.5826	-3.08 ppm	210.4	0	22186.3	32021.7	22967.9	22555.3	19666.1	24791	46677.7	37721.6	32724.1	29735.8	17370.2	26482.9	29225.4	65787.6	20952.8
PE(40:3)	PE	1	0	H85 C45 N1 O8	40	3	798.5983	-3.04 ppm	210.4	0	2602.4	3593	2559.9	3268.9	3232.1	4673.7	6737.1	7086.5	5904.6	4874.2	2626.5	5198	6601.5	9124.1	2928.2
PE(40:2)	PE	1	0	H87 C45 N1 O8	40	2	800.6167	0.43 ppm	210.4	0	2837.6	0	2958.4	2217.6	2405.1	3256.2	4650.8	4338.4	5850.4	3493.3	2414	2921.2	2911.2	4982.6	2495.1
PE(40:1)	PE	1	0	H89 C45 N1 O8	40	1	802.6273	-5.91 ppm	210.4	0	4920.1	4078.3	5762.5	3830.6	4256	5117	6861	6017.6	8574.5	4760.8	4595.3	10038.5	6880.3	5595	3892.7
###	**PE_IS**																								
PE(31:1)	PE_IS	0	1	H71 C36 P1 O8 N	31	1	676.4911	-0.08 ppm	210.4	4578149.5	3216799.1	3135672.2	3797116.5	3271578	3256309.6	3877345	4450069.3	3622721.8	3151096.2	4165842.2	3867889.5	3978094.4	3793131.1	2934740.2	2779934.8
###	**PE-O**																								
PE-O(36:4)	PE-O	1	0	H75 C41 N1 O7	36	4	724.5265	-1.46 ppm	250	1348.6	96784.8	105419.9	99807.7	73029.2	101103	61769.6	134117.3	129553	147084.4	96632.8	83404.1	59585	129978.4	128469.6	87372.2
PE-O(36:2)	PE-O	1	0	H79 C41 N1 O7	36	2	728.5578	-1.51 ppm	250	0	9395.5	7043.7	9937.4	3103	6409.5	3451.1	7267.4	8634.9	16247.9	7057.8	8270.6	3125.5	8601	6767.3	9708.5
PE-O(36:1)	PE-O	1	0	H81 C41 N1 O7	36	1	730.5735	-1.38 ppm	250	0	13514.2	17634.2	19506.9	4132.3	10227.5	6885.2	15966.6	18374.7	28745	13425.1	14890.3	4067.5	17326	10925.2	14063.1
PE-O(36:0)	PE-O	1	0	H83 C41 N1 O7	36	0	732.5889	-1.75 ppm	250	0	8364.6	13315.6	8707.8	3567	5092.2	3083.9	7953.3	9188.6	14147.9	8925.6	9104.6	3997.8	7389.4	5258.5	6199.2
PE-O(38:7)	PE-O	1	0	H73 C43 N1 O7	38	7	746.5085	-4.61 ppm	250	0	24757.6	16889.1	24750	13306.3	18872.5	30722.2	57440.8	40001	16119.9	9835.8	9638	7451.1	19221.3	19310.3	46946.7
PE-O(38:6)	PE-O	1	0	H75 C43 N1 O7	38	6	748.5265	-1.43 ppm	250	0	10912.1	9134.1	14379.6	6821.7	12023	7584.5	16845.6	13187.7	18396.3	15086.4	9885.3	7303.9	13420.1	15196.5	15406.8
PE-O(38:5)	PE-O	1	0	H77 C43 N1 O7	38	5	750.5424	-1.10 ppm	250	0	66036.7	43897.6	82537.8	48659.8	54472.7	29388.1	72831.4	76785	104168.1	73645.7	61643.5	26419.5	92200.6	66333.5	60810.9
PE-O(38:4)	PE-O	1	0	H79 C43 N1 O7	38	4	752.5577	-1.53 ppm	250	1706.2	162792.3	187661.2	249040.4	128528.4	119499.2	62760.7	133057.4	196734.4	203143.1	147501.9	153218.5	57418.4	249602.3	113573.5	117061.6
PE-O(38:3)	PE-O	1	0	H81 C43 N1 O7	38	3	754.5733	-1.67 ppm	250	0	64633.8	99702.7	123784.9	48113.3	51126.9	25238.5	72379.5	84617.8	103669.5	65136	61156.5	29768.5	87520.4	54655.5	57682.7
PE-O(40:8)	PE-O	1	0	H75 C45 N1 O7	40	8	772.5239	-4.80 ppm	250	0	13716.6	9163.1	18001	7726	14757.5	16722.5	36298.2	29676.3	12798.3	9587.5	8455.7	5600.5	16817.3	13600.5	28433.9
PE-O(40:6)	PE-O	1	0	H79 C45 N1 O7	40	6	776.5571	-2.25 ppm	250	0	12712.3	13814.5	15025.1	8703.9	11001.7	6283	14822.5	17323.4	17364	10482.6	9900.3	4027.3	15287.7	9097.3	11056.4
PE-O(40:5)	PE-O	1	0	H81 C45 N1 O7	40	5	778.5732	-1.74 ppm	250	0	16306	19830	22406.1	10440.8	13443.9	9641.6	21453.1	22614.6	20398.4	22296.6	14083.3	8034.7	24567.7	15503.4	13937.7
PE-O(40:4)	PE-O	1	0	H83 C45 N1 O7	40	4	780.5884	-2.31 ppm	250	0	19565.5	32203.4	30464.5	17588	12672.8	14847.5	26617.5	43040.5	30943.2	27161.9	23086.4	11896.4	37244.7	19105.8	16366.5
###	**PE-O_IS**																								
PE-O(31:1)	PE-O_IS	0	1	H71 C36 P1 O8 N	31	1	676.4911	-0.08 ppm	210.4	4578149.5	3216799.1	3135672.2	3797116.5	3271578	3256309.6	3877345	4450069.3	3622721.8	3151096.2	4165842.2	3867889.5	3978094.4	3793131.1	2934740.2	2779934.8
###	**PI**																								
PI(32:2)	PI	1	0	H79 C41 N1 O13	32	2	824.5287	0.47 ppm	80.6	2200.1	0	0	1289.9	0	1271.8	1712.8	2802.1	11139.1	4559.8	4673.7	2997.9	2047.7	4879.8	1945.3	2153.6
PI(32:1)	PI	1	0	H81 C41 N1 O13	32	1	826.5442	0.26 ppm	80.6	1487.6	8603.3	5009.8	2547.4	1536.6	3430.1	2137.1	2256.2	9358	10211.5	5832	5918.7	7119.8	8228	11672.2	5131.9
PI(34:2)	PI	1	0	H83 C43 N1 O13	34	2	852.5552	-5.18 ppm	80.6	2068.3	33593.7	23263.6	11812.3	11731.1	11259.4	5688.6	8385.5	26850.1	25479.2	16930.6	15366.6	27432.5	26270.3	42893.7	57485.7
PI(34:1)	PI	1	0	H85 C43 N1 O13	34	1	854.5732	-2.47 ppm	80.6	1823.8	383261	96380.7	84161.3	51718.4	68555.1	12895.7	21788.4	71617.4	157389.8	61124.5	115381.9	102182.9	80468.2	156205.3	126464.5
PI(36:4)	PI	1	0	H83 C45 N1 O13	36	4	876.5592	-0.53 ppm	80.6	2017	82004	51730.5	45680.1	32809.1	33231.5	9149.5	14930	72186.6	83805.6	38152.2	52195.3	46391	121361.6	76722.5	76968.8
PI(36:3)	PI	1	0	H85 C45 N1 O13	36	3	878.5745	-0.92 ppm	80.6	0	49789.3	27680.1	19546	24498.2	15801	7663.2	6523.4	49995.6	50510.8	29864.8	30724.8	43925.5	81503.4	61666.1	78270.8
PI(36:2)	PI	1	0	H87 C45 N1 O13	36	2	880.5901	-0.98 ppm	80.6	4216	446382.1	151210.5	125636	99655	83770.1	31091.1	29978.2	140777.7	267301.8	134645	221096.3	189457.1	278849	389114.9	304276.4
PI(36:1)	PI	1	0	H89 C45 N1 O13	36	1	882.6061	-0.60 ppm	80.6	2870.1	715074.6	160208.2	161529.4	122776.2	87568.9	26345.5	31581.1	121964.6	378085.5	171448.4	330994.8	224880.6	273476.1	297750.7	268075.1
PI(38:6)	PI	1	0	H83 C47 N1 O13	38	6	900.561	1.44 ppm	80.6	0	26404.7	15580.4	12074.4	12550.8	11836.9	1914.2	2555.5	9891.5	23216.5	10641.6	11370.6	12956.7	20575.3	10844.9	17303.4
PI(38:5)	PI	1	0	H85 C47 N1 O13	38	5	902.5779	2.88 ppm	80.6	0	72092.9	54081.6	38601.5	29573.8	28123	8861.7	12409.6	63756.2	103100.7	48604.2	49006.1	46423.6	229384.9	77708.9	78211.8
PI(38:4)	PI	1	0	H87 C47 N1 O13	38	4	904.5942	3.56 ppm	80.6	19462.7	1102262.7	902657.1	601157.3	438282.4	293033.1	97494.5	185096.4	891684.1	1377984.6	587834.7	967524.9	516834	2040080.5	1054040.8	972984.3
PI(38:3)	PI	1	0	H89 C47 N1 O13	38	3	906.6098	3.51 ppm	80.6	5943.7	188755.3	143993.7	102251.7	60894.7	61500.4	24295.2	31407.8	210069.4	280063.5	127387.7	225424.2	167362	587801.9	252611.9	219080
PI(40:6)	PI	1	0	H87 C49 N1 O13	40	6	928.5904	-0.62 ppm	80.6	0	64436.6	52872.7	47482.1	37650.9	33792.4	4692.1	10480	50009.6	95350.5	55100.5	52059.8	56571.4	122403.4	51785.7	51560.5
PI(40:5)	PI	1	0	H89 C49 N1 O13	40	5	930.6075	0.93 ppm	80.6	0	44992.5	38573.4	23786.1	25691.7	20407.8	5161.2	9449.7	48706.4	73724.2	32412.2	30474.3	41964.5	93796.5	43133.5	33097.4
###	**PI_IS**																								
PI-IS(34:0)	PI_IS	0	1	H87 C43 O13 P1	None	0	856.5899	-1.19 ppm	80.6	611400	838167	745756.3	371282.6	296228	235804.2	82615.3	91773	448512.8	916402.1	564048.3	703722.6	794006.9	853765	942684	851253.2
###	**SM**																								
SM(16:0)	SM	1	0	H80 C39 N2 O6	16	0	703.5749	0.03 ppm	99.2	218764.9	3314423.6	2789465.8	4176216.2	2951049.9	2536419.9	2303893.3	3188830.1	3570026.6	4394662.1	1857994.9	1914139.1	1479938.6	4141290.9	2978048.3	1345265
SM(18:0)	SM	1	0	H84 C41 N2 O6	18	0	731.6046	-2.15 ppm	99.2	12987	80332.4	69196.2	76812.5	76443.3	43247.1	44055.3	51619.3	36343.1	41324.4	96837.1	35379.9	29050.5	49669.8	51340.8	26232.1
SM(22:1)	SM	1	0	H90 C45 N2 O6	22	1	785.6517	-1.78 ppm	99.2	20042.4	91001.5	105814.2	121329.9	95055.1	78123.6	55553.8	62153.8	52499.5	45975.7	90241.9	38444.1	37236.4	67472.1	69185.5	33951.4
SM(22:0)	SM	1	0	H92 C45 N2 O6	22	0	787.667	-2.19 ppm	99.2	48702.4	381108.3	437358.6	525158	296677.2	225331.9	201260.9	203367.3	230375.6	290472.4	248105.9	172647.5	154308.4	270461.2	216999.1	143342.2
SM(24:2)	SM	1	0	H92 C47 N2 O6	24	2	811.6682	-0.71 ppm	99.2	19937	187167.3	151591.6	230120.4	140265.6	149072.6	139452.4	163727	190214.6	158446.2	177621.6	79318.4	60266.9	162743.3	181640.5	106278.1
SM(24:0)	SM	1	0	H96 C47 N2 O6	24	0	815.6995	-0.72 ppm	99.2	58005.1	1211690.4	1374632.2	1695652.3	1232971	985760.1	1067572.2	1156323.7	1487883.8	930105.2	996172.8	684613.8	724605.7	1423697.9	905609.6	1121741.5
SM(26:1)	SM	1	0	H98 C49 N2 O6	26	1	841.7153	-0.52 ppm	99.2	6892.7	23415.4	19046.2	24414.6	18590.7	24799	34082	38992.8	34496.3	20598.6	29644.9	25492.8	19149.2	21519.6	19056.9	34388.3
SM(26:0)	SM	1	0	H100 C49 N2 O6	26	0	843.7303	-1.27 ppm	99.2	7480.2	11349.2	8982.4	10136.9	10953.6	9765.7	11834.3	9608.6	8652.3	4939.3	11845.7	7237.2	6548.2	12823.2	8027.7	11353.4
###	**SM_IS**																								
SM(17:0)	SM_IS	0	1	H82 C40 P1 O6 N	17	0			99.2	2970275.7	2045022	2414172.3	2531138.7	2482307	2183832.5	1761943.2	1984316.2	2045916.4	2183271.6	2040929.7	1923360.3	1646603.6	1955169.4	1195672.1	1391604.4
###	**PS**																								
PS(32:0)	PS	1	0	H75 C38 N1 O10	32	0	736.5117	-0.77 ppm	98.8	1166.2	2908.7	3078.5	3359	3205.3	5017.8	7713.3	4110.6	1748.3	1632.6	2498.5	2669.9	3115.9	9911.1	8821.7	9100.5
PS(34:2)	PS	1	0	H75 C40 N1 O10	34	2	760.5112	-1.41 ppm	98.8	1637.3	3901.3	12586.6	10280.9	3597.8	7932.6	3943.2	2805.6	2460.4	7310.3	2493.1	5444.9	4339	7022.9	2388.2	3885.4
PS(34:1)	PS	1	0	H77 C40 N1 O10	34	1	762.5275	-0.63 ppm	98.8	11450.2	48055.7	52812.1	76261.5	48836	69658.6	29061.6	47661.2	56058.7	66616.9	74982	65485.8	49774.8	66346.5	54323	52880.4
PS(34:0)	PS	1	0	H79 C40 N1 O10	34	0	764.5426	-1.28 ppm	98.8	3464.6	6135.4	4578.6	8678.7	8585.6	7251	14700	9037.8	4451.1	7616	8500.1	5509.1	8711.3	19725.2	24034.6	20787.1
PS(36:4)	PS	1	0	H75 C42 N1 O10	36	4	784.5098	-3.21 ppm	98.8	4136.7	5482.7	6160.8	7055.5	7086.8	7261.2	9716.7	10145.9	7288.4	6301.5	4921.5	4893.6	6017.9	9905.8	7863.5	10824.1
PS(36:3)	PS	1	0	H77 C42 N1 O10	36	3	786.5264	-1.98 ppm	98.8	1373.8	8463.2	4766.5	12485.1	5444.8	5528.5	3887.3	3102	4934.4	3822.9	5047.4	3956.8	4191.1	7771.8	6294.9	5383.5
PS(36:2)	PS	1	0	H79 C42 N1 O10	36	2	788.5422	-1.83 ppm	98.8	21827.2	91856.9	61932.1	142646.4	79309.7	72979.4	35149.6	26378.1	29562.2	35912.8	38960.9	33985.9	39062.6	48909.8	60384.9	55064.7
PS(36:1)	PS	1	0	H81 C42 N1 O10	36	1	790.5577	-1.92 ppm	98.8	143495.5	662058.4	679952.2	1061043.8	584970.3	637620.4	169225.3	236899.5	161137.5	292326.8	324986.1	263834.9	303188.3	365689.9	398445.2	395259.4
PS(38:5)	PS	1	0	H77 C44 N1 O10	38	5	810.525	-3.70 ppm	98.8	2822.5	6228.9	5280.6	12988.9	9294.9	7264.7	6010.4	6359.4	9421.7	10489.6	8202.1	4996.3	5345	8141.6	6807.2	6938.2
PS(38:4)	PS	1	0	H79 C44 N1 O10	38	4	812.5423	-1.63 ppm	98.8	29400.2	44986.8	46518	79643	66597.1	60863.7	38498.2	50591.8	32818	43231.9	46477.9	29729.6	31947.6	55541.7	49563.3	43726.9
PS(38:3)	PS	1	0	H81 C44 N1 O10	38	3	814.5589	-0.48 ppm	98.8	8169.7	30011.8	28789.3	39041.4	30243.2	37757.5	8232.5	16531.7	21154.9	30508.5	28779.7	20659.9	23474.6	25139.7	25857.9	20071.4
PS(38:2)	PS	1	0	H83 C44 N1 O10	38	2	816.5748	-0.18 ppm	98.8	2338.6	13135.6	12091.6	14445.1	10400.8	14267.7	2168.4	5442.1	3549.7	8779	6468.8	6650.7	6584.9	7920.5	6865.1	6397.7
PS(38:1)	PS	1	0	H85 C44 N1 O10	38	1	818.5882	-2.94 ppm	98.8	4438.4	18695.2	17938.2	23087.3	13879.7	18927.7	4074.9	8348.3	1619	6721.7	7276	6872.9	6004.3	6389.1	6846.7	7013.4
PS(40:5)	PS	1	0	H81 C46 N1 O10	40	5	838.5582	-1.27 ppm	98.8	5815.4	13575.3	13455.6	13776.7	13360.7	21652.9	8543.9	14961.5	54586.2	74149.2	56295.9	40030.7	33159.4	26369.3	25459.7	22171.4
PS(40:4)	PS	1	0	H83 C46 N1 O10	40	4	840.5744	-0.64 ppm	98.8	5870	14633.9	17463.5	19831	17754.4	21416.7	6276.5	19590.2	29224.1	34977.5	36775.3	26403.9	26364.8	19913.3	24818.8	23076.6
PS(40:2)	PS	1	0	H87 C46 N1 O10	40	2	844.6063	0.11 ppm	98.8	1970.8	7990.1	5243.1	4651.5	6047.5	7660.9	2900.2	3625.2	2142.2	3160.7	2867.5	2566.9	2920.3	2800.7	2341.3	2150.6
###	**PS_IS**																								
PS(31:1)	PS_IS	0	1	H71 C37 P1 O10	31	1	720.4805	-0.67 ppm	98.8	293088.7	316077.4	336419.6	464264.1	397662.1	382876.2	132608.9	189063.9	59360.6	146018.2	168650.4	181091.2	191187	242008.1	297576.3	261273.9
###	**CL**																								
CL(64:0)	CL	1	0	H141 C73 O17 P	64	0	1351.9675	1.91 ppm	28.6	1681.4	3365.9	3232.3	1571.8	2642	3464.8	0	2967.6	3031	0	4064.7	1439.1	0	7706.6	3072.9	0
CL(66:4)	CL	1	0	H135 C75 O17 P	66	4	1369.9172	-0.61 ppm	28.6	0	0	0	0	0	0	0	2704.8	1514.9	1569.6	0	3811.9	0	13958.9	5873.6	4118.7
CL(68:5)	CL	1	0	H137 C77 O17 P	68	5	1395.9315	-1.53 ppm	28.6	0	9167.7	14791.1	6626.1	3362	8899.5	3304.8	9663.8	8841.1	7527.3	4385.1	9718.2	7915.8	37919.9	20561.9	21347
CL(68:4)	CL	1	0	H139 C77 O17 P	68	4	1397.947	-1.68 ppm	28.6	0	16826.3	21882.4	10290	4478.1	12650.6	4382.2	16445.2	8875.9	5536.2	6583.8	12522.5	12720.4	35182.3	24782.2	15423.1
CL(68:1)	CL	1	0	H145 C77 O17 P	68	1	1404.0019	4.06 ppm	28.6	3383.2	8172.2	14999.8	6377.9	0	0	5646	0	26730.4	18876.4	11943.7	11412.2	12769	11894.1	7235.2	8808
CL(70:6)	CL	1	0	H139 C79 O17 P	70	6	1421.9578	5.95 ppm	28.6	1845.9	61110.2	57666.1	40147.2	19207	24987.3	18909.4	28086.5	46583.4	30969.1	34048.2	32397.8	24769.5	117721	78058	61161.1
CL(70:5)	CL	1	0	H141 C79 O17 P	70	5	1423.9731	5.71 ppm	28.6	0	64945.2	102897.9	44490.3	23732.9	36707.2	24980.2	38019.1	47599.3	46723.7	28958.7	59175.8	42574	133088.7	126132.8	59405.4
CL(70:4)	CL	1	0	H143 C79 O17 P	70	4	1425.9878	5.03 ppm	28.6	4272.6	39882.7	85007.1	34358.4	18981.8	21433.1	21467.9	39382.2	37922.9	33277.2	22848.5	38403.7	51721.1	81086.5	87951	40994.8
CL(70:3)	CL	1	0	H145 C79 O17 P	70	3	1428.0025	4.35 ppm	28.6	0	18750	46574.1	18101.6	6948.2	5978.5	8008.9	14003.7	27380.4	20364.9	15914.1	14799.8	27967.7	25366.2	37729.4	16429.3
CL(70:0)	CL	1	0	H153 C79 O17 P	70	0	1436.0701	7.85 ppm	28.6	0	27940	24719.2	30748.2	13088.3	11436.6	8327.2	15969.8	1990.1	13346.3	11338	11060.5	12554.6	17702.5	19252.3	7691.3
CL(72:8)	CL	1	0	H139 C81 O17 P	72	8	1445.9559	4.55 ppm	28.6	0	32576	38400.2	0	5822.4	5149.6	13803.9	15239.6	20968.4	10875.6	8073.4	10577.3	6110.7	33737.8	27338.1	30486.7
CL(72:7)	CL	1	0	H141 C81 O17 P	72	7	1447.9721	4.91 ppm	28.6	7237.6	133037.3	152598.3	60710.7	48309.6	35246.3	41160.4	36411.4	109103.4	105547.8	89960.2	55589.6	38360.2	233080.9	4515.1	117019
CL(72:6)	CL	1	0	H143 C81 O17 P	72	6	1449.988	5.08 ppm	28.6	12077.4	185062.5	223667.1	126112.6	76019.8	49290.3	62827.8	46979	140241.4	146621	103661.4	81239.4	84332.4	280979	226001.2	174007.3
CL(72:5)	CL	1	0	H145 C81 O17 P	72	5	1452.0031	4.72 ppm	28.6	4813.3	138455.1	248104.2	113346.3	50889	36764.3	49094.1	43483.4	116851.3	96452.5	75514.2	89925.8	82661.6	193638.6	191536.2	128384.2
CL(72:4)	CL	1	0	H147 C81 O17 P	72	4	1454.0136	1.14 ppm	28.6	3756.5	38771.5	91529.7	42215.8	16212.5	0	16250.1	14259.6	41137.8	37171.2	26545.7	36244.3	43219.4	68572.7	87135.1	41886.6
CL(74:10)	CL	1	0	H139 C83 O17 P	74	10	1469.9546	3.58 ppm	28.6	2340.3	36784.7	31833.3	13682.2	11000.1	8824.2	14022.8	9508.9	28293.8	9353.4	6887.6	7713.9	6090.4	37591	14272.9	47579.2
CL(74:9)	CL	1	0	H141 C83 O17 P	74	9	1471.9713	4.29 ppm	28.6	0	57623.5	63162.6	29653.8	16447.1	13699.2	22905.8	17562.6	35104.3	21233.3	10097.7	11192.7	16582.3	69071.8	25403.4	74543.5
CL(74:8)	CL	1	0	H143 C83 O17 P	74	8	1473.9879	4.92 ppm	28.6	4774.1	77063.6	100265	40472.6	21241.2	12283.2	21902.9	20138.1	55914.7	32074.9	19179.5	28250.3	30342.9	89159.2	50005.8	83327.6
CL(74:7)	CL	1	0	H145 C83 O17 P	74	7	1476.0025	4.21 ppm	28.6	3578	48712.8	64489.2	39608.7	20396.9	12915.8	14337.4	17098.8	36276.4	24173.5	18164.5	25162	33147	62745.5	45149.3	51456.6
CL(74:2)	CL	1	0	H155 C83 O17 P	74	2	1486.0708	-2.48 ppm	28.6	0	35674.9	18060.5	28833.9	26857.9	3257.7	1461.6	2549.9	5773.5	19824.8	8815	7738.6	7503.3	19169.1	13042.8	7104
###	**CL_IS**																								
CL(56:0)	CL_IS	0	1	H125 C65 O17 P	None	0	1239.8311	-7.01 ppm	28.6	549745.5	426503.3	480285.2	295187.1	163895.2	152437.4	74980	109841.9	220121.2	323307.5	200591.7	476498.4	478842.8	607743.8	495028.4	444405.6

Table E7

sample	date_quartile	type	cells	diagnosis	stage	sex	age	BMI	fixed	smoking	ex_smoking	pack-years	asthma	medication	group	disease
INT:C079.mzML	3_17	AM	5*10~4	chronic cough		F	58	22.8	N	NA	NA	NA	NA	Y	ctrl	ctrl
INT:C080.mzML	3_17	AM	5*10~4	COPD	3/D	F	59	32	N	N	Y	50	N	Y	3_4	COPD
INT:C081.mzML	3_17	AM	4.7*10~4	COPD	2	M	70	20.2	N	N	Y	15	N	N	2	COPD
INT:C083.mzML	3_17	AM	5*10~4	COPD	2	M	64	36.3	N	N	Y	2925	N	Y	2	COPD
INT:C084.mzML	3_17	AM	5*10~4	COPD	4/D	M	61	18.9	N	N	Y	100	N	Y	3_4	COPD
INT:C103.mzML	4_17	AM	5*10~4	COPD	3	F	64	19.5	N	Y	N	62	N	Y	3_4	COPD
INT:C105.mzML	4_17	AM	5*10~4	COPD	3	M	60	29.3	N	N	Y	35	N	Y	3_4	COPD
INT:C123.mzML	1_18	AM	5*10~4	smoker		M	58	32.4	N	N	Y	40	NA	Y	ctrl	ctrl
INT:C135.mzML	1_18	AM	5*10~4	chronic cough		M	58	22.4	N	N	N	0	NA	N	ctrl	ctrl
INT:C137.mzML	1_18	AM	5*10~4	COPD	2	M	59	35.8	N	N	Y	10	N	Y	2	COPD
INT:C141.mzML	2_18	AM	5*10~4	chronic cough		M	60	29	N	N	N	0	NA	N	ctrl	ctrl
INT:C145.mzML	2_18	AM	5*10~4	COPD	2	F	46	37.5	N	Y	N	40	N	Y	2	COPD
INT:C149.mzML	2_18	AM	1*10~5	COPD	2	F	66	19.5	N	Y	N	40	N	Y	2	COPD
INT:C155.mzML	2_18	AM	5*10~4	COPD	2	M	54	26.2	N	Y	N	100	N	Y	2	COPD
INT:C176.mzML	3_18	AM	5*10~4	COPD	4	M	67	26.3	N	N	Y	60	N	Y	3_4	COPD